STABILITY OF COHESIVE SEDIMENTS SUBJECT TO PORE WATER AND GAS EBULLITION FLUXES AND EFFECTIVENESS OF SAND AND AQUABLOK® CAPS IN REDUCING THE RESUSPENSION RATES

by

Pinar Cakir Kavcar

A dissertation submitted in partial fulfillment
of the requirements for the degree of
Doctor of Philosophy
(Civil Engineering)
in The University of Michigan
2008

Doctoral Committee:

Professor Steven J. Wright, Chair
Professor Peter Adriaens
Professor Guy A. Meadows
Associate Professor Aline J. Cotel

To my family

ACKNOWLEDGEMENTS

First and foremost, I would like to express my sincere gratitude to my dissertation committee chair and advisor, Prof. Steven J. Wright who has been an excellent mentor over the years. I have been privileged to have his direction, guidance, and help on everything from working in the hydraulics laboratory to writing my dissertation. His enthusiasm and dedication to research, to help young people in becoming wiser through a proper education and through continuous support has always been a source of motivation and admiration for me. I will definitely miss working with him. I am very thankful to my master's thesis advisor, Prof. A. Metin Ger for being an inspirational mentor and for supporting me during my efforts leading up to the University of Michigan. Thanks to Assoc. Prof. Aline J. Cotel, Prof. Peter Adriaens, and Prof. Guy A. Meadows for serving on my committee and for their generous guidance.

I would like to thank my colleagues Rong Wu for sharing the pressure of our common course work and Hans Tritico for his day-saver practical ideas in the lab and outside the lab. Many thanks are also due to our lab technicians for their help around the lab. Thanks to all the undergraduate and graduate students who have in some way or another contributed to the research reported in this dissertation.

Words can not be enough to express my gratitude to my husband, Osman Kavcar. He is the source of my life. My humble success is a result of his continuous support and love. I am extremely grateful to my wonderful parents; my mother Raife Cakir and my father Ibade Cakir, for their unconditional love, support and encouragement to achieve my goals all my life. Many thanks to my brother, Deniz Cakir and my sister-in-law, Cansu Cakir who have always offered me their support and admiration.

Finally, support for this research is gratefully acknowledged. This research was conducted under a project sponsored by the Strategic Environmental Research and Development Program. Further support was provided by the Department of Civil and Environmental Engineering and the Program of Environmental and Water Resources Engineering at the University of Michigan.

TABLE OF CONTENTS

LIST OF FIGURES

LIST OF TABLES

LIST OF APPENDICES

CHAPTER 1

INTRODUCTION

Many pollutants released to the environment from industrial-municipal discharges, runoff or ship waste settle and accumulate in the silts and muds (sediments) on the bottoms of rivers, lakes, estuaries, and oceans. Important sediment contaminants include: polynuclear aromatic hydrocarbons (PAHs), polychlorinated biphenyls (PCBs), mercury, dioxins and metals which are hazardous and persist in the sediment for a long time even after their sources have been removed. The contaminated sediment poses ecological and human health risks in many watersheds throughout the United States. All but one of the 43 Areas of Concern (AOCs) designated for the Great Lakes contain contaminated sediments. Nationwide, the U.S. Environmental Protection Agency has identified over 19000 contaminated sediment sites, with 8000 "probably associated with harmful effects on aquatic life or human health" (U.S. EPA, 2004). At the same time, the cost of remediating these sites is staggering with estimates for cleanup costs at the AOCs ranging from 1.7-4.4 billion dollars. There is considerable interest in in-situ management of the risks from contaminated sediments with prospects for considerable reduction in remediation costs.

A relatively recently developed management technique involves sediment being left in place but covered with a cap that is resistant to erosion and has a relatively low permeability to minimize contaminant migration through the cap. This technology has the potential to significantly reduce remediation costs dominated by dredging and subsequent disposal of contaminated sediments. However, since the contamination remains in-situ, it is critical to ensure that capped systems behave as anticipated. Concern about uncertainties in predicting cap performance as well as the long-term viability of caps

currently limits the application of capping solutions for remediating contaminated sediment sites.

Capping manages contaminated sediment without creating additional exposure associated with dredging, e.g., sediment resuspension, and potential direct human exposure during disposal of dredged material. Caps are typically composed of clean sand or gravel. A more complex cap design can include geo-textiles, and other permeable or impermeable elements in multiple layers that may include additions of material to lower the flux of some contaminants (e.g., carbon-based materials). Although capping is potentially a good alternative to other remediation techniques such as dredging, there have been some notable failures of capping systems that have been implemented to date. For example, PCB-contaminated sediments in Manistique Harbor of Lake Michigan were covered with a cap that included a diffusion barrier of crushed limestone sand, a geo-membrane, and an armor layer to prevent erosion by storm waves. Unfortunately, methane gas that was microbially generated in the sediments accumulated beneath the geo-membrane and ultimately floated the armor layer. Therefore, it is essential to develop a good understanding of fundamental processes within the sediments and fill the knowledge gaps in order to be able to apply the capping alternative.

Mass transfer between the sediment bed and the overlying surface water can depend on a wide range of processes. Since hydrophobic contaminants adsorb easily to sediment solids, resuspension can account for much of the contaminant sediment-water column mass transfer that occurs under ambient conditions. In order to prevent resuspension and consequently re-introduction of contaminants into the water column, capping might be utilized which involves covering the contaminated sediment with clean material to isolate the contaminated sediment physically from the water column. There are several possible cap configurations but the caps considered within the scope of this study are sand caps and caps constructed with AquaBlok® material which is a patented technology consisting of small sized aggregates covered with bentonite that hydrates under water creating a relatively low permeability layer. The major objective of this research study is to quantify the sediment resuspension rates into the water column and investigate the stability of

capped and uncapped sediment beds under the influence of shear stresses due to advective flow (waves and currents), pore water fluxes (groundwater seepage) and gas ebullition fluxes due to microbial activity. The effect of advective flow is commonly addressed in studies investigating bed stability or resuspension rates. However the effects of ebullition and seepage are not included in these types of studies mostly because of the lack of knowledge on fundamentals regarding these processes. As a result of hydrologic processes in river, estuarine, marine or tidal systems, the resultant pressure head differentials could create seepage fluxes which result in some degree of destabilization of the beds or increase resuspension rates. In addition, ebullition, in which excess gases are generated in the sediment beds by micro-organisms from organic matter, could potentially contribute to the destabilizing effects and resuspension rates. In this study, the potential significance of these selected processes in destabilizing the beds and/or increasing the resuspension rates was determined. The effectiveness of two capping approaches in controlling resuspension rates due to the applied shear stresses, pore water and gas ebullition fluxes was investigated by a comparison to the resuspension rates measured for beds without caps.

This investigation was conducted as a part of a research project entitled “Integrating Uncertainty Analysis in the Risk Characterization of In-Place Remedial Strategies for Contaminated Sediments” which was led by the University of Michigan and involving additional organizations. The overall project aim was to develop process understanding of seepage and ebullition on PAH fluxes, and integrate these parameters in an uncertainty-based remedial assessment framework for capping strategies. One of the subtasks of the project involves two scales of sediment analysis that were performed separately to (i) evaluate the effectiveness of capping in reducing the resuspension rates and in increasing the stability of contaminated sediment beds which are subject to advective flow induced shear stresses, ebullition and seepage fluxes (flume-scale experiments which are the subjects of this dissertation), (ii) evaluate the effectiveness of capping in reducing contaminant fluxes from the contaminated sediment beds to the water column when the beds are subject to ebullition and seepage fluxes (flux chamber experiments).

The laboratory experiments performed in this study were conducted on actual sediment transported to the laboratory from the project demonstration site, the Anacostia River in Washington DC. The Anacostia River is a freshwater tidal system draining an urban watershed enclosing 176 square miles in Maryland and the District of Columbia, has been identified as one of the most contaminated rivers in the Chesapeake Bay watershed by EPA in 1990s (U.S. EPA, 2004). The sediments on the bottom of this river are contaminated with high levels of PCBs, PAHs, heavy metals and other chemicals. Several pilot cap configurations including sand cap and AquaBlok® cap implemented in the Anacostia River have been monitored to evaluate long-term feasibility in the presence of external forcings. The sand caps for the laboratory investigations in this study were created with sand blends of different grain sizes and with locally available sand meeting the size specifications of a demonstration cap placed in the Anacostia River, while the materials to construct the AquaBlok® cap were obtained from the product manufacturer.

In an effort to present the findings of this investigation, Chapter 2 begins with a brief review of studies in the literature. Chapter 3 introduces the specific objectives of the experimental investigations and continues with the description of experimental apparatus used and procedures followed. Chapter 4 presents the experimental results for the non-cohesive sediment beds. Chapter 5 presents the experimental results for the uncapped and capped cohesive sediment beds. Finally, Chapter 6 presents a summary of the conclusions and recommendations for future research.

CHAPTER 2

BACKGROUND

Re-introduction of sediment-bound contaminants back into the water column can occur through a wide variety of processes. These processes can be categorized as resuspension related processes and non-resuspension related processes. Non-resuspension processes include direct desorption from surface sediments to the water column, gas ebullition (3-phase partitioning, solid-gas-liquid), groundwater flow (2-phase partitioning, solid-liquid) and diffusive mass transport enhanced by bioturbation (mixing processes by benthic organisms in the sediment bed). It is presumed that the major fraction of contaminants is associated with fine-grained cohesive sediments although this may not be universally true. This research considers only the physical process of resuspension, which allows for direct contact of contaminants and the overlying water, facilitating mass transfer processes. Fine-grained particles should be more impacted by resuspension effects since their very low settling velocities once introduced into the water column ensure a relatively long residence time before deposition occurs. The importance of resuspension in contaminant transfer processes has been emphasized in previous studies. For example, Achman et al. (1996) reported that sediment resuspension dominates the sediment-water exchange of PCBs in the Hudson River estuary. Over time, sediment resuspension together with advective flow can transport a significant portion of contaminated sediment from one site to another. For example, Eganhouse et al. (2000) estimated that 50% of contaminated sediments on the Palos Verde Shelf, CA, were lost over 10-12 years because of sediment resuspension and advective transport. During the time sediment particles are suspended, sorbed contaminants are subject to phase partitioning including transfer to dissolved and vapor phases increasing the risk of exposure by humans and the aquatic life.

One of the primary functions of a sediment cap which is a technique for contaminated sediment management is to prevent resuspension of cohesive sediments and consequently re-introduction of contaminants into the water column. This technique involves covering the contaminated sediment with clean material to isolate the contaminated sediment physically from the water column while providing adequate stability to a bed subject to various conditions leading to resuspension. In order to examine the effectiveness of capping strategies, it is first important to understand what processes and factors can potentially influence the resuspension of cohesive sediments. Then, the impact of various capping strategies must be considered to determine their effectiveness. A review of the reported studies in the literature related to these topics is presented in this chapter, indicating that the extent of the available knowledge related to various aspects of resuspension processes is limited. In addition, little is known about the effectiveness of various capping technologies in limiting sediment resuspension.

This chapter is organized along three major topics. First, a general discussion of capping strategies and methods is presented. Then, since some sediment caps are simply a clean sand layer placed over contaminated sediments, the stability of non-cohesive sediments is reviewed especially in relation to the pore water flux through it. This is followed by a related review associated with cohesive sediments focusing on the processes of seepage and ebullition together with advective flow induced shear stresses. This is particularly relevant as it is necessary to understand how effective different capping strategies might be in influencing different types of resuspension processes. The chapter concludes with an identification of research needs that forms the basis for the research pursued in this investigation.

2.1. Capping as a Remedial Alternative

U.S. EPA (2005) categorizes major remedial alternatives for managing risks associated with contaminated sediments as in-situ and ex-situ alternatives. In-situ approaches include: (1) Capping (either reactive or not); (2) Monitored natural recovery through naturally occurring processes such as sediment deposition or biodegradation by microorganisms; (3) Hybrid approaches (a thin cap placement to enhance recovery via

natural deposition); (4) Institutional controls (e.g., waterway or land use restrictions). Ex-situ approaches include: (1) Dredging (hydraulic or mechanical dredging of sediment and transportation to shore for treatment and disposal); (2) Excavation (similar to dredging except for the initial dewatering or water diversion at the site). Selection of an alternative or a combination of different alternatives to be implemented involves investigation of several factors ranging from site characterization information related to many physical, chemical and biological properties of the site to risk and cost assessments. Advantages and disadvantages of each remedial technique should be clearly understood before implementation.

Capping can be conducted by applying a clean layer of sand or gravel which is a low cost solution with an ease of placement. The goal of an effective cap design is to reduce exposure of aquatic organisms to sediment contaminants and providing appropriate protection of human health and the environment. A capping design should address remediation through three primary functions: (1) Physical isolation of the contaminated sediment from the aquatic environment; (2) Stabilization of contaminated sediment by preventing resuspension; (3) Reduction of contaminant fluxes into the water column (Palermo et al., 2002). In order to ensure that hydraulic forces do not erode the cap and resuspend the underlying contaminated sediment, sometimes cobble or stone may be added to the top of the cap to provide additional armoring (e.g., see Wright et al., 2001) even though often a sand layer alone is sufficient. The level of protection could also be raised by increasing the cap thickness. Geo-membrane material may be used beneath the cap in soft sediments to support the cap. However, microbially generated gas build-up under the geo-membrane could cause stability problems. It is also possible to include another cap layer in the cap design with some additives to encourage degradation or sequestration of contaminants which involves enhancement of adsorption of contaminants to solids reducing the bioavailability (Wolfe, 2004). Active capping as a remediation technique is being tested on the Anacostia River demonstration site. In addition to a cell with sand cap (30 cm thick) alone, the demonstration project includes a cell with apatite for sequestration of metals and a cell with coke mats for sequestration of organics. All active layers are separated from native sediment by a layer of fine sand and

topped with layers of medium sand (8 cm) and fine gravel (16 cm) for protection against advective flow induced shear. In this type of application, only contamination that penetrates into the active layer receives treatment. Another test cell includes AquaBlok® material (10 cm after hydration with an additional cover of 20 cm sand) which is a very low permeability layer of gravels covered with bentonite. This material stabilizes the bed once it is hydrated under water and minimizes the contaminant fluxes due to its low permeability but it is not an active cap. Figure 2.1 shows the cap study design layout for the demonstration area and the location from which the contaminated sediment used in this research study was collected.

Many contaminated beds are composed of soft cohesive sediments that can easily be disturbed. Uncontrolled placement of the capping material can result in the resuspension of contaminated sediments into the water column (U.S. EPA, 2005). Uniform and slow application that ensures the cap to be formed in layers is often necessary to avoid resuspension or mixing with the underlying contaminated sediment. Additional uncertainty is associated with the increase of short-term contaminant fluxes as a result of the consolidation of the native sediment by the weight of the cap. One of the major challenges is to achieve a uniform cap thickness. Various types of equipment and placement methods can be used for capping projects. Granular cap material such as sand or gravel can be handled in a dry state until released into the water over the contaminated site. It is also possible to mix the cap material with water to form a slurry and discharge it by pipe into the water column either at the water surface or at depth. Armor layer materials can be placed from barges or from the shoreline using conventional equipment, such as clamshells. Placement of geo-membranes could require different types of equipment. In the Anacostia demonstration site, a conventional clamshell bucket with a digital GPS for bucket location was used to place sand and AquaBlok®.

One of the important advantages of capping to other remedial alternatives is that it can quickly reduce the exposure to contaminants. If a cap is properly designed and placed, it can prevent bioaccumulation by providing long term isolation of aquatic organisms from contaminated sediments and it can reduce the contaminant fluxes into the

water column. Dredging requires more infrastructure for treatment and disposal which can be more expensive compared to a capping project conducted using locally available materials and equipment (Palermo et al., 2002). Another major advantage of capping is that the potential of contaminated sediment resuspension during the implementation of capping is relatively low compared to removal operations. However, since the contaminated sediment is left in place, if the cap is disturbed contaminants could become exposed. Processes leading to destabilization of the cap should be carefully investigated considering site specific information. It may also be necessary to develop institutional controls to protect caps from disturbances such as boat anchoring (U.S. EPA, 2005).

2.2. Stability of Non-Cohesive Sediment Beds Subject to Advective Flow Induced Shear Stress and Pore Water Flux

Coarse-grained sediments composed of particles greater than 62 μm are called non-cohesive sediments and they resist erosion mainly through gravitational forces. When the stream flow velocity increases gradually over a non-cohesive sediment bed, the motion of sediment can be observed if the bed shear stress induced by the flow exceeds a certain critical value. The critical condition, that is the shear stress just less than that necessary to initiate sediment motion, is called “threshold”. For applications of interest where the flows are turbulent and the bed materials are at least slightly irregular, this threshold condition is not constant in space or time, making its definition somewhat arbitrary. A slight increase in bed shear stress above the critical value causes a small degree of sediment motion, which is known as “incipient motion”. The threshold of sediment motion forms an essential part of the understanding of sediment bed stability. In addition to the hydrodynamic forces, a potentially significant process that could lead to sediment destabilization is vertical pore water pressure gradients due to groundwater discharge through the stream bed for example or possibly induced by tidal fluctuations in estuaries. In order to examine the stability of non-cohesive sediment beds under conditions of pore water flux, previous studies on non-cohesive sediments are reviewed.

Shields has been the recognized pioneer to define the incipient motion with his experimental work on sediment beds composed of nearly uniform particles under

unidirectional flows. Although many people refer to Shields' findings, the original work was published in German and the experimental methodology was not clearly specified (e.g., see Yalin and Karahan, 1979; Buffington, 1999). It is assumed that incipient motion can be detected visually or determined by extrapolating the bed-load transport curve to a shear stress level that bed-load movement ceases. Shields reported these two different methods to define incipient motion criteria (Buffington, 1999). According to Buffington, Shields suggested these two definitions without explicitly indicating which method was employed during his experimental studies. However, throughout his dissertation he discussed the results being representative of uniform grains implying that he used the bed-load extrapolation method. Shields also added that in case of a bed consisting of different grain sizes, bed-load extrapolation method can not be used because of the possible movement of only the smaller grain sizes. For this case, he suggested using a weak motion criteria defined by Kramer (1935) who defined the weak movement of sediment as the condition where only a few of the smallest particles are in motion at isolated zones. However, Kramer also indicated three other bed shear conditions for the sediment bed as: (1) no particles are in motion (no transport); (2) many particles of mean size are in motion, (medium transport); and (3) particles of all sizes are in motion at all points and at all times, (general transport). Furthermore, he indicated the difficulty of defining clear limits between these regimes. Yalin (1976) proposed that some difficulties could be eliminated if the observation area and time, number of particles in motion and particle size are incorporated into a non-dimensional number for an experiment when any motion is observed. At incipient motion, this number needs to be maintained as a constant finite number close to zero. Thus, a variety of concepts of sediment threshold have been put forward and are variously used by researchers following up on Shields' original work. The inconsistency of these different concepts leads to varying results.

In general, most studies in the literature have addressed the initiation of motion conventionally expressed by the Shields curve (e.g., Vanoni, 1975) which does not include the effect of pore water movement through the sediment bed due to vertical pressure gradients. A review of the literature indicates that relatively few studies have been conducted to examine the effect of bed seepage on incipient motion. The review of

the extant literature about the effects of seepage on bed stability contains some apparently contradictory findings; while most investigations indicate that vertically upward flow through the bed sediment decreases the sediment stability, some studies have reported the opposite conclusion. In the following discussion, the situation where pore water flows through the sediment bed upwards into the main flow is referred to as *injection* while downward flow into the sediment bed is referred to as *suction*.

Simons and Richardson (1966) qualitatively pointed out that seepage of water into the bed would presumably increase the effective weight of the bed particles and, therefore, increase the stability of the bed. Conversely, for a stream with groundwater flow into the channel, the effective weight of the bed particles decreases and thus decreases the bed stability. The majority of experimental measurements have tended to back up this conclusion. For example, as a result of their experimental work on test beds with median grain sizes ranging from 0.13 mm to 0.57 mm, Oldenziel and Brink (1974) concluded that suction always decreases the rate of sand transport whereas injection does the reverse. In discussing implications of their research, it is mentioned that as the flow velocity near bed and the bed shear stress is reduced with injection, there might be a possibility of a decreased rate of transport. Cheng and Chiew (1999) also noted a tendency for lowered critical shear velocity as injection velocities are increased for the test beds with median grain sizes ranging from 0.63 mm to 1.95 mm. On the other hand, Martin (1970) reported that inflow seepage does not enhance incipient motion of the sediment particles even up to a quick bed condition. He also suggested that suction may delay incipient motion for a turbid water flow if finer particles settle in the bed filling the porous medium, resulting in a more resistant bed. Likewise, Harrison and Clayton (1970) did not observe any significant increase in erosion when inflow seepage occurred.

Watters and Rao (1971) studied the effects of seepage on the hydrodynamic drag and lift forces acting on a non-cohesive sediment particle to determine whether or not seepage has a role in initiation of sediment motion. In their experiments, the flume bed consisted of plastic spheres configured in four different ways. The results of the study indicated that the effects of the seepage are to modify sublayer thickness of the channel bed, the

particle boundary layer, the wake pattern behind the sediment particles and the velocity profile near the channel bed. According to their conclusions, injection increases the sublayer thickness and intensity of the turbulent fluctuations, and decreases the near bed velocity. They indicated that an exposed particle on the bed would be subjected to lower lift and drag forces under conditions of injection and presumably this would result in increased sediment stability.

In the study conducted by Rao et al. (1994) it was stated that the change in average bed shear stress depends on the relative magnitudes of the bed shear stress and the critical shear stress of the particles under the no-seepage condition, sediment concentration, and the seepage rate. Sands with grain sizes ranging from 0.34 mm to 0.80 mm were used in the study with different initial conditions either transporting or non-transporting and applying seepage as suction or injection. Experimental results showed that seepage could cause increase or decrease in bed shear stress and this change depends on the initial flow condition and the rate of seepage applied. The work presented by Rao and Sitaram (1999) investigated bed stability using seven different sizes of sand (0.32-3.0 mm) under the effect of injection or suction. . In this study, the criterion for incipient motion defined by Yalin (1976) was utilized. They concluded that suction reduces the stability of the bed particles and increases their mobility whereas injection does the opposite.

In general, the direct effect of seepage is considered to produce a seepage force in the direction of the seepage flow; this would produce a destabilizing effect with injection and the opposite effect with suction. Nevertheless, in the context of a boundary layer flow with a given free stream velocity, it is known that injection through a porous boundary alters the boundary layer and thus the wall-shear stress (e.g., Turcotte, 1960). Specifically injection increases the thickness of the boundary layer and therefore decreases the magnitude of the wall shear stress since the skin friction is reduced relative to a condition without injection at the same free stream velocity. A consistent conclusion has been drawn by Cheng and Chiew (1998a) from their experimental study indicating that with increased injection velocity, the bed shear stress is decreased. This is directly related to the issues discussed by Watters and Rao. However, Cheng and Chiew also reported that

rms values of the velocity fluctuations and the Reynolds shear stress increase rapidly near a bed subject to injection relative to a condition without injection at the same free stream velocity. Furthermore, if only the alterations on the velocity profile were to be considered to examine the effect of seepage on the critical sediment motion, the results may be contradictory. For example, Maclean (1991) noted that as suction draws faster moving flow into contact with bed, boundary shear stress is increased. On the other hand, it may be presumed that as injection increases the Reynolds shear stress near the bed, suction would decrease the turbulence, thereby decreasing the bed shear stress.

It appears that discussions in the literature related to changes in stability of non-cohesive sediment beds subject to suction or injection are obscured by a lack of precision. There have been several explanations of the effects of injection or suction from a limited perspective that does not consider every phenomenon involved in the process. Bed stability should be examined by evaluating the critical bed shear stress in a way that all the different effects of seepage either on the flow or on the sediment bed particles are considered together. First of all, injection or suction can be characterized in terms of the seepage velocity or in terms of the pressure gradient. Overall in the literature, seepage velocity seems to be used most often but if it is considered that displacement of particles is due to the interaction of elementary particle forces, then pressure gradient is likely to be more relevant. Seepage velocity and pressure gradient will be related through additional parameters such as bed porosity and grain size, making it difficult to provide definitive statements regarding the influence of seepage velocity on particle stability. The second effect is related to the modification of the boundary layer by the presence of injection or suction.

The Shields curve has been developed over a range of grain sizes that covers hydrodynamically smooth boundary surfaces (small grain size) to hydraulically rough (large grain size) presumably explaining the complex shape of the Shields curve. Injection or suction velocities will alter the nature of the boundary layer near the bed surface and this effect should be correlated with seepage velocities rather than pressure gradient. It is easy to reason qualitatively that injection decreases the local velocity near

the bed surface while suction has the opposite effect. Thinking only in terms of velocity, this could lead to a conclusion that suction decreases bed stability while injection increases it. However, this line of reasoning does not account for the fact that Shields criteria are based on bed shear stress and thus do not directly address how the shear stress-based Shields curve should be modified by injection or suction. Regardless, if it is considered that the external factor controlling bed seepage in natural systems is an applied piezometric head gradient, then larger grain sizes would be subject to larger injection or suction velocities and thus more boundary layer modification. Therefore, it is reasonable to consider that with respect to elementary particle forces, smaller grain sizes could be more influenced by pressure gradients due to groundwater or tidal flows while the boundary layer modification would be more pronounced for large grain sizes. It may be difficult to make general statements regarding effects of injection or suction on bed stability. More importantly, it is necessary to communicate with precision whether changes in bed stability are due to changes in seepage rates vs. bed pressure gradients, mean external flow velocity or bed shear stress, etc.

If a criterion is developed for how Shields curve is modified by injection or suction, this does not totally resolve the issue of how to apply the result in a practical application. Generally bed shear stress is computed by one of several approaches, either by applying a uniform flow equation such as Manning's equation where the bed shear stress can be related to mean velocity and depth or by using the uniform flow relation where the bed shear stress is related to the product of slope and hydraulic radius. Neither one of these approaches are applicable due to the modification of the boundary layer if there is significant seepage through the bed. A need to relate the bed shear stress modified by bed seepage to that determined by more conventional means remains to be resolved in order to apply any research findings to practical applications.

Careful consideration is required to predict the effect of seepage on bed stability from experimental results as many potentially conflicting factors are involved in the analysis. It is important to also note that several of the previous studies involved flows with relatively small depths, on the order of a few centimeters, apparently in an attempt to

increase the effects of seepage on the flow or to ensure the formation of a fully developed turbulent boundary layer (e.g. Rao and Sitaram, 1999). The low bulk flow Reynolds numbers associated with these flow conditions leads to the possibility that the results cannot be generalized to more typical flow conditions. One more major issue is related to the bed shear stress determination as some of the studies show indications of possible errors involved in the computation of the bed shear stress. Bed shear stress cannot be measured directly unless a load cell on a discrete bed segment is used and this approach cannot feasibly be integrated into an experiment with bed seepage. Therefore, the common approach is to use an integral momentum balance to use measured changes in local water depth and momentum fluxes to compute the bed shear stress as the residual in the momentum balance (e.g., see Oldenziel and Brink, 1974; Rao and Sitaram, 1999). This approach is complicated by a variety of experimental issues but ultimately the bed shear stress is estimated as the difference between several large numbers and therefore difficult to determine with precision. There is some indication that some of the conflicting results on the effect of seepage on bed stability may be simply due to differences in the protocol to compute bed shear stress.

2.3. Stability of Capped and Uncapped Cohesive Sediment Beds Subject to Advective Flow Induced Shear Stress, Pore Water Flux and Gas Ebullition

2.3.1. Nature of Cohesive Sediment Beds

In contrast to non-cohesive sediments, cohesive sediments contain significant amounts of clay minerals and resist erosion by forces related to the electro-chemical bonds between individual particles. These forces can be much larger than the weight forces of individual particles (Raudkivi, 1998). The erodibility of cohesive sediments is highly influenced by the layered structure of the clay minerals. The forces between particles may be covalent bonds, electrostatic interactions, hydrogen bonds, van der Waals forces and hydration forces (Simon and Collison, 2001). Erosion of cohesive materials was described by Mehta (1991) as breaking the bonds between particles or detaching cohesive aggregates as the first mode, detachment of a plane as the second mode and fluidized bed flow as the last mode.

The grain size is the most important factor affecting the erodibility of coarse-grained sediments. However, because of larger grain size and lesser inter-particle forces, the erosion of coarse sediments is qualitatively quite different than erosion of cohesive sediments. It is also much better understood and more widely investigated. Comprehensive relationships predicting cohesive sediment erosion and resuspension have not yet been developed. In addition to the difficulty in defining the driving and resisting forces on cohesive streambeds, prediction of incipient motion criteria and erosion rates are dependent on various parameters of the cohesive sediment media. Soil characteristics such as particle size, clay percentage, clay mineralogy, surface and pore water chemistry and pH are likely to be important for determining resistance to erosion. A comprehensive list of 28 parameters to characterize cohesive sediments was developed by Berlamont et al. (1993) (see Table 2.1). All of these parameters can potentially affect the bed stability. The extent of consolidation and thus the bulk density is another significant factor influencing the erosion rates in addition to the properties of the bed and the eroding fluid (Hunt and Mehta, 1985). Erosion rates for a sediment bed depend significantly on the bulk density and decrease rapidly as the bulk density increases (Jepsen et al., 1997). Since most cohesive sediment beds are formed by the processes of settling and consolidation, the consolidation degree of the sediment beds should be taken into account carefully during experimental studies conducted to measure erosion rates. In the study by Parchure and Mehta (1985), erosion behavior of sediment deposits was investigated in laboratory experiments representative of the top active layer of estuarine beds. With reference to experimental results of their study, relatively thin bed deposits stabilize in a period on the order of a week. While a deep column of sediment consolidates, the bulk density of the sediment generally increases with depth and time as the pore water moves up and out of the solid-water matrix. It is noted that laboratory measurements that prepare an entire bed with a total thickness of 10 cm, for example, at once may not be representative of the conditions in typical depositional environments that may deposit only a few cm per year in a gradual and somewhat continuous manner.

Floc formation in cohesive sediments may also be an important phenomenon with regards to the erosion resistance of the sediment surface. Flocs are formed due to

interparticle forces in the cohesive sediments during the process of resuspension-settling-deposition and are more likely to be formed in water with higher ionic strength. This process may be influenced by particle composition, particle sizes, particle densities and turbulence levels in the flow. The flocs can be larger or smaller depending on the resulting differential settling rates. In a study by Lau and Droppo (1999), the critical shear stresses were measured under different conditions of bed formation. It was observed that beds deposited under quiescent conditions and beds deposited under flowing conditions (under shear) had different strengths to erosion. The critical shear stress for the latter was up to eight times larger than that of the former. Under flowing conditions, stronger bed particle bonds and flocs are developed resulting in more resistance to erosion. In a series of sequential erosion-deposition experiments, Lau et al. (2001) demonstrated the effects of depositional history on erosion and showed how the rate of erosion reflected the structure of the bed. This research showed that layers of sediment deposited under different conditions would not have the same shear strength.

2.3.2. Effect of Advective Flow

Hydrophobic contaminants absorb strongly onto fine-grained organic containing sediments, and thus fate of these contaminants is dependent on the fate of the sediments. Sediments are in contact with the water column through any resuspension process. Therefore, the conditions leading to resuspension may be critical to concentrations of contaminants within the water column where they can more readily result in environmental exposure to humans and aquatic organisms. Erosion of cohesive sediment beds is assumed to occur largely as a result of hydraulic shear stress; yet, there is no well-established general theory for calculating the rate of erosion of cohesive sediment beds.

At present, measurement of erosion characteristics of sediments are available at two scales: (1) laboratory investigations with sediment samples from a site and, (2) in-situ observations and measurements. Various types of devices have been deployed for these investigations using different methods to introduce stress and measure erosion. An annular lab or in-situ flume is one of the devices commonly used (e.g., Fukuda and Lick, 1980; Maa et al., 1998; Amos et al., 2003). This apparatus generates flow at the water

surface by the rotation of the cover just in contact with the surface and shear is exerted on the bed in a closed circular system. The bed shear stress is not uniform across the bed but increases from the inner wall towards the outer wall due to secondary currents formed by the centripetal acceleration in the flow. Sediment accumulation along the walls of the annulus is possible which may cause underestimation of the resuspension rates. Particle concentrations in suspension are usually measured by optical backscatter sensors in terms of turbidity. It is easier to minimize secondary current effects by conducting experiments in a straight flume. However, unless the flume is long or the depth is low, the flow will involve a developing boundary layer and will not be totally spatially uniform. Many researchers used straight flumes especially for in-situ erosion measurements (e.g., Ravens and Gschwend, 1999; Houwing, 1999; Aberle et al., 2003). These flumes generally have a rectangular sediment test section on which straight flow at a known velocity is applied over the bed surface, and the resulting erosion rate is estimated by measuring the mass of sediment suspended exiting the flume. A specific type of straight flume, commonly referred to as Sedflume is also widely used (McNeil et al., 1996; Jepsen et al., 1997). This flume has a test section with an open bottom through which a core tube can be inserted. The coring tube can be filled with either reconstructed or undisturbed sediment although keeping the sediment undisturbed during this process would be difficult. Then, the core sediment is pushed upwards into the flow manually keeping it flush with the flume floor at all times. As the sediment in the core erodes, the rate of continuous core movement is recorded which in turn provides the erosion rate. The validity of Sedflume measurements depends in part on the operator's ability to keep the top of the eroding sample core flush with the bottom of the channel as the experiment proceeds, which may be complicated by erosion of the core into an irregular surface.

The erosion of cohesive materials has been described as occurring by one of three mechanisms by Mehta et al. (1989): (1) floc by floc detachment under low excess shear stress conditions, (2) erosion of masses of bed material below the bed surface under high values of excess shear, or by (3) fluidization of the mud–water interface. In the literature, bed shear stress is the main parameter that is used to characterize erosion rates. Both laboratory and in-situ measurements of cohesive sediment erosion are generally based on

a procedure in which a series of bed shear stress levels are applied stepwise over time steps of a fixed duration (e.g., Parchure and Mehta, 1985; Ravens and Gschwend, 1999; Aberle et al., 2006). Measurements are performed to compute the erosion rate which is the amount of sediment eroded per unit time per unit area. The erosion rate is usually calculated using measured fluxes of suspended sediment concentration although the potential importance of bed load transport as a part of cohesive sediment erosion was indicated by several researchers (e.g., Debnath et al., 2007; Aberle, 2004). Erosion rates are typically high at the beginning of an experimental shear stress step and then decrease with time (e.g., see Parchure and Mehta, 1985; Lick et al., 1995; Piedra-Cueva and Mory, 2001; Amos et al., 2003; Ravens, 2007). Therefore, determination of time dependent erosion rates led to different approaches. For example, Ravens and Gschwend (1999) defined rate in two ways; either including the effect of the initial peak or excluding it and examining only the "plateaus" after the initial response passed. They assume that the initial higher erosion rate is associated with flow disturbances associated with increasing the flow rate and that the erosion relatively quickly decreases to a constant rate. Tolhurst et al. (2000) averaged the resuspension rates over each shear stress step whereas Houwing (1999) assumed that the erosion rate for an applied bed shear stress level was the initial peak value. Determination of critical shear stress has also involved some different interpretations. In some studies critical shear stress, τ_c is determined by extrapolating erosion rate versus shear stress values to zero erosion (e.g., Ravens and Gschwend, 1999) and some researchers define τ_c as a shear stress level at which significant erosion occurs (e.g., Maa et al., 1998). Parchure and Mehta (1985), on the other hand, define critical shear stress as a depth dependent parameter. Unfortunately, there has been little firm agreement about the conclusions of these investigations and the most appropriate mathematical formulation to compute erosion rate from measurements.

Beds considered in experimental investigations can be divided into two categories: (1) Beds in the form of a slurry or remolded/compacted with uniform properties over the bed and, (2) Beds which are allowed to consolidate while suspended sediment deposits on the bed over time. The bed bulk density and shear strength increase with time and depth.

Erosion studies with these types of beds have led to different erosion rate-shear stress formulations. A power relationship has been commonly used in the general form of

$$E = K(z_0)(\tau - \tau_c(z_0))^m \tag{2.1}$$

where E is the erosion rate per unit area of bed surface [$ML^{-2}T^{-1}$], $K(z_0)$ is an empirical erosion coefficient with its dimension depending on the exponent m, τ is the applied bed shear stress [FL^{-2}], $\tau_c(z_0)$ is the critical bed shear stress for erosion, and z_0 is the depth of erosion [L] (e.g., Maa et al., 1998; Ravens and Gschwend, 1999). The exponent, m is assumed to be 1 in some studies (e.g., Ravens and Gschwend, 1999) and the depth dependence of the parameters is omitted by some researchers. The other type of erosion function for deposited beds is suggested by Parchure and Mehta (1985) in the form of

$$\ln\frac{E}{\varepsilon_f} = \alpha(\tau - \tau_c)^{0.5} \tag{2.2}$$

where ε_f is the floc erosion rate when $\tau = \tau_c$ [$ML^{-2}T^{-1}$] and α is a model constant [$(FL^{-2})^{-0.5}$]. Equation 2.2 is significantly different than Equation 2.1 as erosion is finite at $\tau = \tau_c$. Parchure and Mehta suggested this equation for modeling the rate of erosion of the top, active layer of an estuarial bed which has a non-uniform shear strength with depth.

Sanford and Maa (2001) more recently derived an expression which describes the time-dependency of the erosion rate over a shear stress step as described above. A modification to Equation 2.1 with $m = 1$ was performed by differentiating it with respect to time and the resultant function is

$$E = \rho_d(z_0)\beta(\tau - \tau_{c0})e^{-\varphi\beta(t-t_0)} \tag{2.3}$$

where $\rho_d(z_0)$ is the dry bulk density at sediment depth z_0, β is a local parameter, τ_{c0} is critical bed shear stress when τ is first applied at $t = t_0$, t is time, t_0 is time at which a new shear stress is applied, and $\varphi = d\tau_c / dz_0$. For a uniform bed ($\varphi = 0$), Equation 2.3 reduces to $E = K(\tau - \tau_c)$ with $K = \rho_d \beta$. For a non-uniform bed ($\varphi \neq 0$), Equation 2.3 describes an exponential decay of erosion rate with time.

The effect of consolidation degree on the erosion rates related to the bulk density was formulated with a different expression by Jepsen et al. (1997) as

$$E = B\tau^{\lambda}\rho_w^{\eta} \tag{2.4}$$

where B, λ, and η are constants that depend on the type of sediment, and ρ_w is the bulk density. Consolidation times were varied from 1 to 60 days. It was reported that bulk density of the sediments generally increase with depth and time, consequently shear strength increases but water trapped in the sediment can cause a local decrease in density.

2.3.3. Effect of Pore Water Flux

Not much is known about the effects on fine-grained sediments due to the interaction of groundwater seepage with streams and the limitations such interactions may create on contaminated cohesive sediment remediation by capping. Pore water flow through the sediments is presumably driven by piezometric head gradients that vary in time due to hydrologic processes. In estuaries, the effects may exhibit shorter time responses due to tidal fluctuations which can create short term variations in the head differences. The highest groundwater discharge corresponds with periods of low tide and could potentially even reverse direction during high tide. In the Anacostia River, reported measurements of seepage rates range between -0.049-5 cm/d and the high rate corresponds to a period approximately two hours after a high tide (Horne Engineering Services, Inc., 2003).

The groundwater seepage phenomenon can indirectly affect the stability of sediments by altering the consolidation rates in the sediment and changing the bulk density, and

thus the erosion resistance. Although the effects of bulk density on erosion rates have been studied by many researchers (e.g., Hunt and Mehta, 1985; Jepsen et al., 1997), the effect of a continuous seepage and therefore a change in the consolidation process has not been studied to the knowledge of the author. One expected result suggested by Simon and Collision (2001) is that in addition to the advective flow induced shear stresses on cohesive stream beds, another mechanism contributing to the detachment of cohesive aggregates is upward-directed seepage forces.

Determination of seepage rates generally requires in-situ measurements. Methods for estimation of local groundwater seepage typically involve placement of bags to collect flow crossing the sediment-water interface to estimate a net volumetric inflow across the sediment bed over relatively short periods of time (e.g., Cable et al, 1997). More recently, seepage meters were placed in the narrow section of an inverted funnel placed at the sediment-water interface allowing precise measurements of inflows and outflows (Chadwick, 2002). The range of groundwater fluxes reported in the literature varies significantly depending on the sediment type of the bed and other characteristics of the site. Spatial and seasonal variations in the sites where seepage measurements are collected also affect the ranges. Methods that integrate seepage estimates over a larger scale tend to show median seepage rates that are lower than those obtained by point measurements, possibly due to the effect of averaging out localized high seepage fluxes. An extensive review of coastal seepage studies can be found in Cable et al. (1997), Taniguchi et al. (2002) and Burnett et al. (2001). These reviews indicate that measured seepage rates at different sites span from 0.01 cm/d to 124 cm/d. The higher rates reported generally correspond to sand or coarse sand beds. If only silty sand or mud beds are considered, this range is narrower due to the lower permeability relative to sand beds and highest flux for these types of beds was reported as 12 cm/d. However, there are some interesting implications of the measured seepage rates reported for sites with low permeability sediments. It is plausible that the hydraulic conductivity of fine-grained sediments could be on the order of 10^{-4} cm/s or less (e.g., see Charbeneau, 2000). Assuming that Darcy's law describing the flow through a porous medium applies and considering, for example a 10 cm/d seepage flux reported in the literature for a silty sand

bed, the required hydraulic gradient would be 1.16 to support this seepage flux. Since a vertical upwards gradient of greater than one implies a *quick* condition, the bed should not be stable due only to seepage effects. One possible explanation for this is that non-Darcian flow through channels may be responsible for the primary transport of pore water through the sediments. This preferred flow would change many aspects of sediment resuspension and mass transfer of contaminants and should be carefully considered for relevance at a particular site. Experimental investigations studying seepage effects should be performed considering the possibility of channel formation.

2.3.4. Effect of Gas Ebullition

Although ebullition is accepted as a potentially important mechanism for the fate of contaminants, no comprehensive studies have been reported in the literature related to the effect of ebullition on bed stability or on resuspension rates which facilitates the bioavailability of the contaminants to aquatic organisms. Although ebullition may be insignificant at some sites, there is evidence that ebullition can have a significant impact on stability of sediments, and in some cases with geo-textile caps, uplift of the cap has been observed (EPA/Manistique and the Oxbow, WI sites- Palermo et al., 2002) due to excessive gas build-up beneath the geo-textile.

Ebullition is the result of a series of processes in which excess gases are generated by micro-organisms from organic matter. The gases contain methane (46-95%), nitrogen (3-50%), and trace amounts of hydrogen, carbon dioxide, ammonia, and hydrogen sulfide (Fendinger et al., 1992). In cohesive sediment beds under organic rich conditions, ebullition leads to accumulation of gas dissolved in pore water and in bubbles. Gas bubbles are produced (see Figure 2.2) when the sum of the partial pressures of dissolved gases exceeds the ambient pressure (Fendinger et al., 1992). Methane gas dominates in the composition of the bubbles in many environments although this depends on predominant microbial ecology and nutrient availability. Most of these bubbles originate from the upper 10-20 cm of the sediment column (Joyce and Jewell, 2003). Martens and Klump (1980) reported a range of bubble sizes between 0.062 cm and 0.37 cm with a mean volume of 0.104 ml at a water depth of 7.5 m. Richardson (1998) reported bubble

sizes between 0.04 cm and 0.50 cm within soft, marine sediments. Bubbles grow until a pressure threshold is reached as they have to build up a certain amount of buoyancy to overcome the cohesive strength of the sediment and migrate upward. Ebullition generally occurs episodically due to changes in shear stress or pressure which influence the sediment matrix and thus affect the gas bubble release (Joyce and Jewell, 2003). Increased hydraulic shear stresses, atmospheric pressure changes, or tidal hydrostatic pressure changes will lead to a sudden release of gas bubbles which ceases after the excess pressure is relieved. This is followed by a period in which continued microbial activity increases the amount of gas to levels leading to new bubble formation. In the case of coarse grained non-cohesive sediments, the sediment layer could force these bubbles to migrate through the available pores, thus breaking up larger bubbles into many small ones. On the other hand, in fine-grained sediments, the growing bubbles fracture the sediment rather than move around the grains. These fractures combine and form channels reaching to the surface (Huls et al., 2003a-b). The size of the bubbles and thus the sizes of the channels in the sediment layer would depend on the amount of gas in them, ambient temperature and pressure.

Temperature strongly affects both microbial activity rates and the saturation concentration of the gas. As a result, ebullition is highly seasonal (Joyce and Jewell, 2003). Martens and Klump (1980) found that in the winter, bubbles were completely absent from the sediment matrix. Ebullition was observed to occur within a sediment temperature range of 17 °C to 27 °C.

One effect of the gas bubbles in the sediment is to increase sediment porosity and reduce bulk density, thus potentially decreasing the critical shear stress for resuspension (Joyce and Jewell, 2003; Jepsen et al., 2000). Because gas generation and bubble formation are temperature dependent, erosion rates may also be affected by changes in temperature. Jepsen et al. (2000) found that at 20 °C, gas bubbles decreased sediment densities by up to 10%, increased erosion rates by up to a factor of sixty, and decreased the critical shear stress by up to a factor of twenty when compared to the sediments with no gas. At lower temperatures, these effects decreased significantly.

Bubbles rising through the sediment matrix exert an erosive force along their path, and as a result have the potential to mix buried sediments and move them to the surface, similar to bioturbation (Liikanen et al., 2002). The entrained particles are released into the water column upon the bubble's exit from the channel, and settle near the channel exit or are advected depending on the strength of the advective flow (Martens and Klump, 1980). Huls et al (2003a-b) trapped such particles in glass wool suspended in water just above the sediment-water interface in experiments involving undisturbed cores of sediments with high ebullition rates. They measured PAH flux, and found that increasing bubble production increased the amount of PAH gathered on the glass wool. Other than such observations, however, the mechanism and rates of this physical process remain completely unknown.

The combined effects of ebullition and groundwater seepage have been observed in Stryker Bay (Huls et al., 2003a-b). Observations showed an interaction between ebullition and pore water movement such that they can suppress or enhance each other's rates. Ebullition may increase the permeability of the sediment matrix, thereby facilitating pore water flow and resuspension of sediments and/or contaminants. On the other hand, if seepage is high enough, dissolved methane will be removed from the system, thus decreasing the potential for bubble formation. The balance between these two processes may vary seasonally, for example; an initial stronger groundwater seepage followed by higher ebullition rates due to higher summer temperatures, and a final phase in which pore water may flow more freely through channels in the sediment. The combined effects of pore water movement and ebullition on the stability of cohesive sediment beds are unknown. Furthermore, observations reported in the same study on the impact of caps on ebullition combined with seepage showed that the coarse-grained cap material filled existing gas channels in the fine grained sediment. Within the coarse grained cap itself, ebullition channels were not formed since the gas forced to break up into much smaller bubbles. The weight of the cap also compressed the underlying fine sediment, providing increased pressures and thus a higher threshold pressure for bubble formation.

Due to the potentially complex interactions among the above mentioned factors, ebullition fluxes vary both temporally and spatially. The range of ebullition fluxes reported in the literature varies significantly. A wide range of ebullition fluxes spanning from 0.01 cm/d to 48 cm/d was reported by Chanton and Martens (1988). These measurements were obtained from several sites under different temperature, pressure, salinity levels, water depths and sediment characteristics having variable organic contents.

2.4. Summary

As addressed in the literature review above, there are many factors that might impact the stability of cohesive sediments which makes it practically impossible to conduct a research study including effects of all the relevant parameters at once. Therefore, in previous studies, researchers typically chose to examine the influence of at most only a few of the potentially relevant factors. Deriving general conclusions from these studies which did not include some of the major processes leading to destabilization of the beds or high resuspension rates would underestimate the potential risks involved in remedial strategies, specifically capping for the purposes of this study. It is concluded from the literature that the effects of pore water fluxes and gas fluxes may potentially be important since they can contribute in a variety of ways to the contaminant fluxes from the sediment bed into the water column. The scope of this investigation is limited to the physical process of resuspension and the relevant parameters affecting the resuspension rates of the cohesive sediments which have been identified as advective flow induced shear stresses, pore water fluxes and gas ebullition. In a parallel investigation as a part of the overall research project, the rate of contaminant transfer from the sediment to the overlying water column in the presence of pore water fluxes and ebullition is examined (flux chamber experiments). It is intended to gain a better understanding of the physical processes that may control the movement of contamination from the sediments to the water column by combining the results of the two studies.

Caps could be effective in limiting resuspension due to advective flow induced shear stresses, pore water flux or gas ebullition effects. However, currently there are no

systematic investigations on the use of sediment caps in controlling resuspension; hence this aspect has not been commonly included into remediation decision making for contaminated sites. Although there are various capping materials that can be used, it is useful to consider some limiting cases in terms of functional properties. At one limit is a sand cap which doesn't provide a significant limit to water or gas migration but simply acts as a physical barrier to resuspension. At the other extreme is AquaBlok®, which is intended to basically provide an impermeable seal to the sediment surface blocking contaminant, seepage and ebullition fluxes. By studying these two cases, it will be possible to make some general conclusions regarding effectiveness of capping strategies in reducing the resuspension rates. In addition, since there is confusion in the literature regarding the effects of pore water seepage on the stability of non-cohesive sediments, it is necessary to investigate this issue in more detail since it will be potentially relevant to the effectiveness of sand caps.

Assessment of the effectiveness of caps as a remedial technology requires an understanding of contaminant fluxes from sediments both in the presence and absence of caps in order to understand the potential for contaminant transfer to the water column. Predictive models can potentially be applied to evaluate the performance of proposed caps. The application of models requires two key aspects; first of all, the model framework should be adequate to represent all relevant processes and secondly, values for key model parameters must be estimated. At present, it is unclear that adequate support is available to meet either of these needs with regards to several key processes such as the effects of pore water flux and gas ebullition on contaminant mass transfer. In addition, key uncertainties exist with regards to cap behavior.

The objectives of this research study are to provide a better understanding of pore water transport and ebullition processes on cap effectiveness or bed stability in addition to the effects of erosive shear stresses. Furthermore, the observations and/or quantification of the effects of the seepage and ebullition processes could potentially be used to identify the key issues involved in a modeling framework and the long-term effects of these processes together with the relative importance of each process in site risk

reduction on a larger scale. It is understood from the ranges of seepage and ebullition fluxes reported in the literature spanning 2-4 order of magnitudes that modeling studies should be supported by data to reduce the uncertainty. Within this research study, as the experimental investigations evolve the findings will provide necessary boundary conditions for the reported ranges, narrowing down the ranges of seepage and ebullition fluxes that should be considered in a conceptual framework.

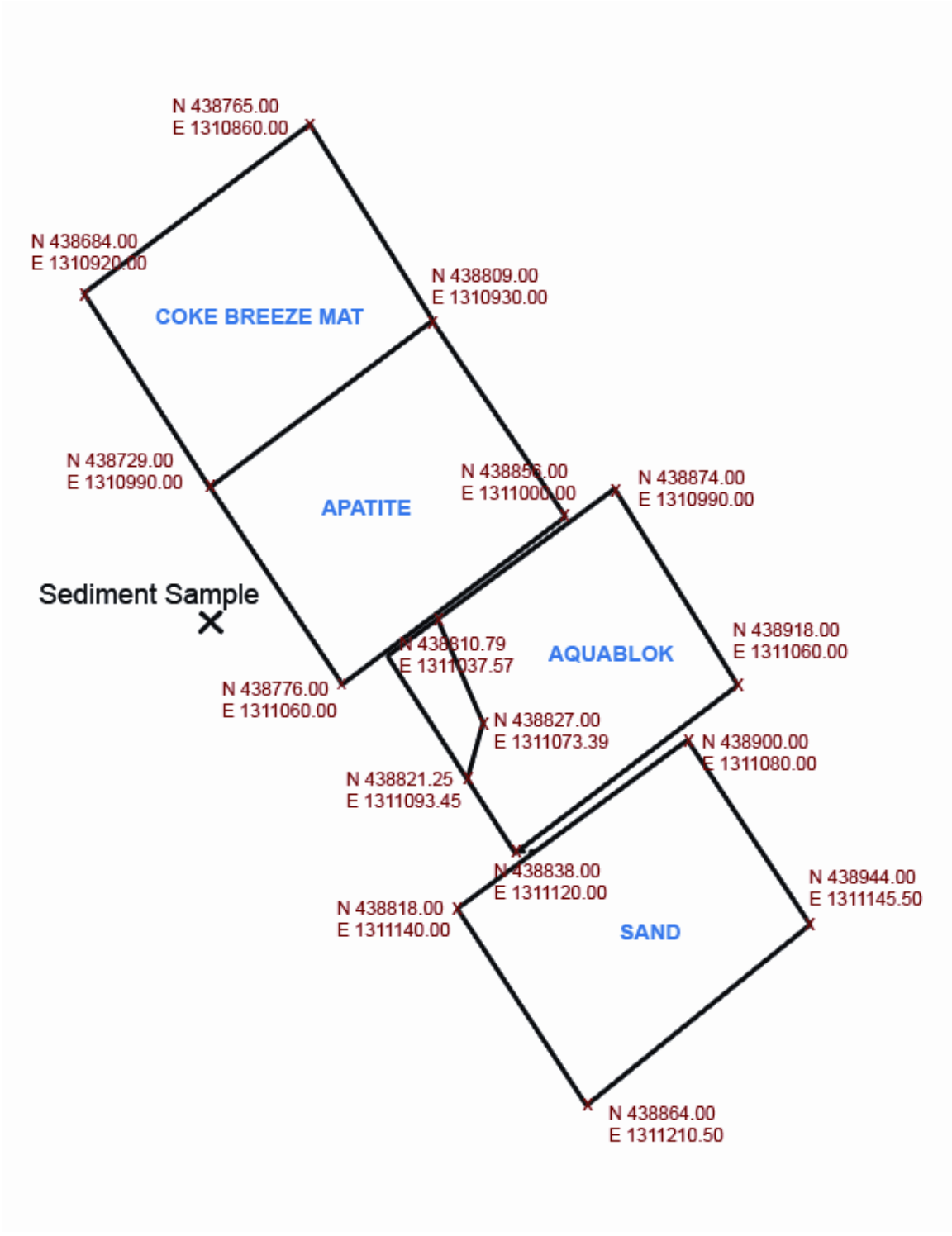

Figure 2.1: The cap study design layout for the Anacostia River demonstration area and the sediment extraction location for sediment used in this research study.

Physico-chemical properties of the overflowing fluid	
1	chlorinity
2	temperature
3	oxygen content
4	redox potential
5	pH
6	Na-, K-, Mg-, Ca-, Fe-, Al-ions
7	sodium adsorption ratio
8	suspended sediment concentration
Physico-chemical properties of the sediment	
9	chlorinity
10	temperature
11	oxygen content
12	redox potential
13	pH
14	gas content
15	organic content
16	Na-, K-, Mg-, Ca-, Fe-, Al-ions
17	cation exchange capacity
18	bulk density (density profile)
19	specific surface area
20	mineralogical composition
21	grain size distribution and sand content
Characteristics of bed structure	
22	consolidation:
	(a) consolidation curve and density profile
	(b) permeability
	(c) pore pressure and effective stress
23	rheological parameters:
	(a) upper and lower yield stress
	(b) Bingham viscosity
	(c) equilibrium slope of sediment deposits
24	Atterberg limits (liquid and plastic limit)
Water-bed exchange processes	
25	settling velocity (in laboratory and field):
	(a) as a function of sediment concentration and floc density
	(b) as a function of salinity
26	critical shear stress for deposition
27	critical shear stress for erosion
28	erosion rate

Table 2.1: A comprehensive list of parameters characterizing the cohesive sediments (Berlamont et. al, 1993).

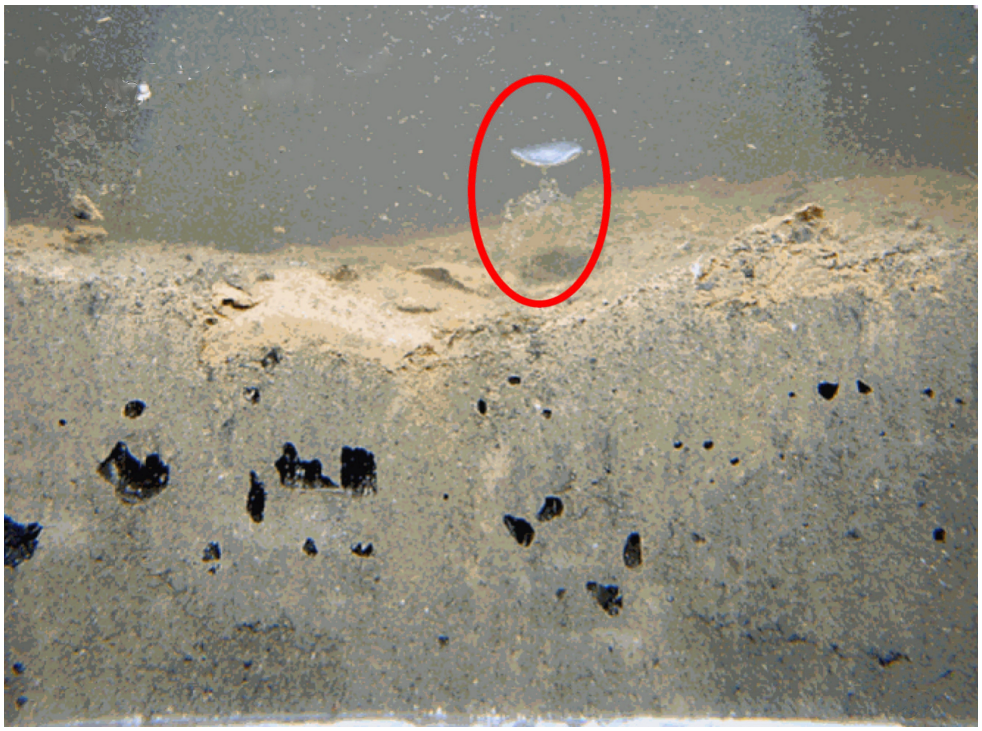

Figure 2.2: Bubble formation due to release of excess gases in the Anacostia River sediment bed.

CHAPTER 3

EXPERIMENTAL SETUP AND PROCEDURE

3.1. Experimental Objectives

Many different types of contaminants adsorb to cohesive sediments and any resuspension event could increase contaminant concentrations in water if the residence time in the water column is sufficiently long that mass transfer between the suspended sediment and the water phase is significant. In addition to the hydraulic forces eroding the cap, gas ebullition due to microbial activity and pore water movement in the sediment matrix may cause destabilization and resuspension. While many contaminants persist in sediment beds for a long time, significant natural recovery of a body of water can be achieved by placement of a clean sediment layer, which is called a cap, over the contaminated layers isolating the contaminated sediment physically from the water column. A cap should be designed considering its long-term effectiveness and stability and at the same time, it should stabilize the contaminated sediment layer providing erosion protection sufficient to reduce resuspension and transport to other sites.

The factors affecting the resuspension rates of fine-grained sediments other than hydraulic forces in the absence and presence of cap layers have not been studied widely. There is limited amount of discussion in the literature on processes related to ebullition and pore water transport leading to resuspension and consequently, some methodology needs to be developed to quantify the effects of these parameters on resuspension rates. The ultimate objective of this research study is to provide an understanding and quantification of the impacts of advective flow, groundwater seepage and gas ebullition on the physical stability of sediments and resuspension rates with or without caps. In

order to achieve this goal, laboratory experiments were conducted using the natural contaminated bed sediment from the Anacostia River which is a freshwater tidal system. The caps considered within the scope of this research project are sand caps and AquaBlok® caps. Although sand provides many of the basic protective features of a cap, additional cap effectiveness could be achieved through the use of alternate materials such as AquaBlok®, a clay mineral-based capping material which is suggested to be effective in controlling permeability while increasing the bed stability. In a report published by EPA (2005), AquaBlok® was described as an example for an engineered clay aggregate material that may enhance the chemical isolation capacity or otherwise decrease the thickness of caps, compared to sand caps.

The experimental investigations constituting this research study can be grouped into three categories excluding the preliminary exploratory investigations. In the first group, incipient motion was observed to determine the critical shear stresses on sand beds for a range of particle sizes. Thus, stability of sand caps is investigated by developing an initiation of motion criterion, particularly in the presence of pore water fluxes. A supplemental study using sand similar to the sand cap placed at Anacostia site was also performed. The experimental results are examined in the framework of a proposed modification to the basic Shields' criterion for initiation of motion that includes the effect of either positive or negative pore water flux. In the second group, the Anacostia River sediment bed experiments, suspended sediment concentrations are measured to calculate resuspension rates under different conditions of gas ebullition, pore water flux and advective flow. These sets of experiments provide the baseline data for comparison purposes in the investigation assessing the effectiveness of the sand and AquaBlok® caps to reduce resuspension, which constitutes the last group of experiments.

For the majority of this experimental work, there are no standard methods described in the literature to guide the experimental methodology. Especially with regards to the experiments with cohesive Anacostia River sediment, performing the experiments or interpreting the results was challenging. Therefore, at early stages of the investigations, some decisions had to be made related to the procedures to be followed and the setup to

be constructed. The decisions related to the pore water transport and ebullition experiments were particularly important as some of the reported seepage or ebullition rates (Limno-Tech, Inc., 2006) seem to only be explainable by the occurrence of channeling through the sediment bed. The details of the exploratory investigations leading to the final experimental setup and protocols developed for the different types of experiments are discussed in the following sections.

3.2. Preliminary Experiments and Development of Experimental Protocols

Four 55-gallon drums filled with sediment from the Anacostia River were acquired in order to perform two particular sets of laboratory experiments. These sets of experiments are referred to in the subsequent discussion as the *flume experiments* and the *flux chamber experiments*. Although the objectives of the two sets of experiments were different, there was a requirement for some commonalities in various aspects of the experimental setup. Therefore, an exploratory investigation was performed to observe various aspects of the sediment behavior and to devise experimental procedures that could be used in both set of experiments. The flume experiments refer to those performed as part of this dissertation and thus were ones in which an erosive force was applied to the surface of the sediment or the cap material by creating a flow over the relevant test surface in the laboratory flume. The flux chamber experiments were performed with no such flow but were conducted in glass aquaria that had a horizontal cross-section of approximately 45 cm by 90 cm. The purpose of these experiments was to examine the migration of selected contaminants from the sediments into the overlying water column and they were conducted for a duration of 8-10 weeks. Rates of contaminant mass transfer from the sediments into the water column due to processes such as pore water flux through the sediments and/or gas ebullition were measured in these experiments. This section describes various tests and observations that were performed on the sediment, primarily with respect to pore water flux and ebullition processes or related to cap behavior that dictated the subsequent decisions on laboratory procedures for both the flume and the flux chamber experiments.

As mentioned previously, four 55-gallon drums filled with sediment were collected from near the test cap sites in the Anacostia River (see Figure 2.1). This material was removed from the river bottom with a clam-shell dredge and placed in drums lined with plastic and delivered to the University of Michigan at an early stage of the research project. Consequently, the drums were stored in an un-refrigerated state for several months prior to the conduct of any experiments. When the drums were opened, attempts to stir the sediment yielded a hydrogen sulfide smell and the bubbling of gas through the liquids above the consolidated sediment. One of the drums was sealed sufficiently well that when the cover was removed, the relief of pressure resulted in a considerable amount of gas bubbling with the liquid spilling out the top of the drum due to the bubbling action.

An initial sample of sediment from one of the drums was removed for the purpose of a permeability test and samples were taken from two of the drums for grain size analyses. Results of those tests are presented in Section 3.5.1. Visually, the contents of all of the drums appeared to be quite similar, a very fine-grained, organic rich sediment with a dark brown color. If the sediment sat for a period of time with exposure to oxygen, the sediment color changed to a tan color. The sediment had a fair amount of foreign materials present such as plastic debris, clam shells, twigs, and other miscellaneous items. These items were removed prior to the sediment being used in any experiment.

The permeability test was performed by pushing an 8-cm diameter acrylic tube into the sediment in one of the drums and collecting an approximately 20-cm long sample within the tube. The initial experiment was performed for a 28-day duration and involved a situation where a column of water stood over the sediment for the duration of the experiment. After the completion of the falling head permeability experiment, the water level was slowly lowered by siphoning off the water. When sufficient water had been removed, the lowering of overlying pressure resulted in several small (approximately 1-cm diameter) gas bubbles to break through the sediment surface and rise through the water column. A video camera recorded these events, and a sample bubble image is shown in Figure 3.1. Upon closer observation, it was noted that the bubbles originated along the wall of the cylinder and all bubbles came from the same spot. This raised some

concern about whether it would be possible to generate pore water flow or gas ebullition without the influence of wall effects and a series of tests were conducted to devise experimental procedures to avoid water or gas migration along the test section walls.

Additional concerns were with respect to sample preparation for the conduct of the basic experiments. Since the samples were already disturbed by the sample collection process, and because of the large sediment volume required in the experiments, it was not possible to use undisturbed sediment in the experimental program. The sediments would also need to be re-used in order to perform the number of planned experiments. Therefore, it was decided to clean and thoroughly mix fairly large batches of the sediment to provide a significant sample of homogeneous sediment. Another issue was sample placement. Initial observations indicated that it was hard to place the sediment uniformly without some compaction effort if the sediment was too dry. Therefore the sediment was mixed with liquid from the drums and additional water from the laboratory tap if there was a need to increase the water content. The Anacostia River is not impacted by the ocean salinity at the sample collection site so fresh water conditions were maintained in all experiments. Test conditions in terms of bulk density and moisture content are described in Section 3.5.1. It would have been possible to let the sediment consolidate for a period of many days or weeks following placement, but this would have posed scheduling problems in conducting the number of planned experiments. In addition, there were issues of how to treat the pore water flux and/or gas ebullition during this consolidation phase. It is presumed that these processes are ongoing in a more or less continuous fashion at the field site. It would have made little sense to let the sediment consolidate for many days or weeks and then initiate these processes. Ultimately, it was decided to perform the experiments by placing the sediment and allowing it to settle for approximately 12-15 hours prior to starting any experiment. Regardless of whether the experiments were performed in this time frame or whether the sediment was allowed to stand for a few days, there was not any observable settling occurring in which the sediment separated from the water. If the same sediment was held in a large container for a week or two, then separation of the sediment from the water was observed.

Initial attempts were made in small containers to create and observe upward flow of water through the sediment. The sediment was homogenized to achieve a consistency where the sediment could slowly flow if poured from the mixing vessel. The sediment was placed in a small container approximately 20 cm in diameter which had a false floor constructed with a permeable geo-textile fabric separating the sediment and the underlying water to which pressure could be applied. The sediment was typically placed and allowed to settle overnight before conducting any experiment. Initial experiments were performed by slowly increasing the pressure until flow could be observed through the sediment. This flow typically started at a pressure head differential of about 10 cm. At this pressure head, one would see a small sediment jet erupt from the sediment surface. The jets were about 0.5 cm in diameter and a considerable amount of water with entrained sediment would flow through the channel that formed in the sediment. Even following reduction of the pressure head driving the jet, flow would continue to occur through that same channel until the pressure head driving the flow was reduced to effectively zero. In the initial experiments, these jets invariably formed at the container walls. Preliminary attempts such as artificially roughening the container wall failed to alleviate this problem. With considerable effort, it was possible to force the channels to form away from the container walls, but it was discovered that a simple way to allow this to happen was to apply the water directly into the bottom of the sediment layer away from the walls. This led to separate methods for creating injection systems that could meet this objective for the two sets of experiments. For the flume experiments, the injection system consisted of a set of parallel *soaker hoses* that are described elsewhere in this dissertation. These soaker hoses, used for yard irrigation purposes, are composed of hydrocarbon materials with small openings in the hose walls. There was concern that they might contaminate the chemical analyses performed in the flux chamber experiments. For the flux chamber experiments, the distribution system was through a set of *bubble bars* which are devices used to provide aeration in fish aquaria. The bubble bars are basically blocks of fused sand contained in a plastic housing and the air is applied below the sand and allowed to flow up through the pores between the sand grains. Both of these two setups were used for application of both air and water to the experiments. Under water, both injection systems generated very small bubbles on the order of one mm diameter.

Experimentation with air injection through both sets of apparatus in a tank of water indicated that at low rates, air tended to be released consistently through a few large diameter pores. Because these larger pores were somewhat randomly distributed, it did not seem to pose a major experimental difficulty and a decision was made to utilize these distribution systems. Subsequent tests indicated that a bubbling pressure of approximately 43 cm for the bubble bars and 32 cm for the soaker hose was required to initiate any gas release. Literally no pressure was required to force water through either apparatus; additional measurements indicated that water or air would move much more readily through both the bubble bars and the soaker hose than would be passed by the matric permeability of the sediment. Most of the tests described in the following paragraphs were performed with a bubble bar as the distribution system but it is not believed that any different behavior would have been observed if a soaker hose had been used.

When the bubble bar was used as the source for vertical pore water flux, the problem of water release at the container walls was solved and flow was almost always observed directly above the bubble bar. It was originally intended to perform the water injection experiments by applying a constant pressure head to the bottom of the sample much as might be experienced by a groundwater driven flow. However, this proved to be infeasible since the majority of the water flux was through the aforementioned channels. The issue is that the water flux rate was not directly linked to pressure head in those circumstances. Consequently, a decision was made to perform constant flux experiments in both the flume and the flux chamber experiments. Because of the different objectives in the two experiments, the methods for controlling the water flux varied between the two setups; the method for water injection in the flume experiments consisted of using a flow meter to regulate the flow rate at a pre-selected value.

Originally, a decision was made to follow this same approach for the gas injection, but difficulties were experienced that did not allow this approach to be implemented in the experiments. The problem was that if a gas injection rate was set with the flow meter, initially the gas would flow into the sediment. This would result in a local increase in

sediment pressure and a decrease in gas flow through the meter, possibly even falling to zero. Increasing the control valve setting to increase the flow would only cause the situation to be repeated until eventually, the gas erupted from the sediment, again through a well defined channel. At this point, the resistance to gas flow would suddenly decrease and the gas flow rate would dramatically increase. Consequently, another setup for managing the input of gas to the base of the sediment was adopted; this procedure is described in Section 3.3 and a similar setup was implemented for both sets of experiments.

Observations of the gas ebullition process is described by the occurrence during the course of a flux chamber experiment, but the observations in the flume experiments support the idea that the same process occurred in those experiments. Differences between the two types of experiments will be noted in the following discussion. As gas was applied at the bottom of the sediments, gas pressure built up within the bubble bar distribution system and the surrounding sediment. At some point, one would see a bulge develop on the sediment surface (Figure 3.2a) and a large bubble would erupt from the bulge, normally followed by several smaller diameter bubbles. The initial bubble could be as large as 5 cm diameter or more and often had the form of a spherical cap bubble. It can be observed that a large amount of sediment is entrained into the bubble wake and is lifted up into the water column (Figure 3.2b and 3.2c). This sediment was partially composed of small chunks of aggregated sediment that tended to settle out fairly quickly but some of the sediment appeared to be individual particles and could be carried all the way to the water surface. The subsequent bubbles that were released following the initial one tended to be smaller and entrain less sediment; thus there appears to be a correlation with bubble size and sediment entrainment. Typically if the air pressure applied was not excessive, bubble release would stop after a short period of time and the process would repeat itself, gas pressure build-up, bubble release, pressure drop, and cessation of bubble production. However, it was noted that bubble release tended to be from relatively few locations, more variable at the beginning of an experiment and more consistently from the same locations as the duration of the experiment proceeded. It was also noted that as time went on, the bubble diameters tended to become smaller and more constant in size,

in the range of about 0.5-1.0 cm diameter and the amount of sediment entrained with the same bubble size declined with time. It is hypothesized that this is due to some sort of armoring process on the walls of the channel through which the bubbles rose. In the flux chamber experiments, these channels became increasingly well-defined and about 1 cm in diameter and an actual hole a few cm deep in the sediment surface was observed to develop. In the flume experiments, the channels were not so well defined, probably because the flume experiments were of a much shorter duration. It is also noted that periodically, a new channel could form in either set of experiments, usually close to a previous one and the gas flow would be diverted to the new channel. Also, as the experiment proceeded, the injection of air resulted in almost immediate bubble production that was continuous until the air pressure was nearly completely relieved as opposed to the more intermittent type of bubbling events near the beginning of the experiment.

Additional preliminary experiments were performed to bubble air through sediment covered with a sand cap. The behavior was somewhat similar in this situation but with some important differences. A higher pressure buildup was required to initiate the first bubbling event, as expected, presumably due to the increase in internal pressure within the sediment due to the submerged weight of the sand. The bubbles tended to be more constant diameter (roughly 0.5-1.0 cm) throughout the duration of the experiment and were more constant in other behavior over the duration of an experiment. Figure 3.3 shows a bubble release event from the sand surface. Initially, small amounts of sediment were entrained in the bubble wake, but the sediment color was not consistent with the Anacostia sediments, so it is presumed that the entrained material is fine material present in the sand itself. If the experiment was conducted for a sufficiently long time, eventually dark sediment with a color consistent with that of the Anacostia sediment would be seen being entrained into the water column although in considerably smaller amounts than in the uncapped sediment experiments. In a few cases, air bubbles were observed to occur along the tank walls, a situation depicted in Figure 3.4. Again the air is observed to flow through a distinct channel. The channels were never straight and vertical but it is not known if this can be generalized to the more common channels forming away from the

tank walls. The channels appear to be smaller in diameter than the bubble diameters being released at the sand interface. In one test, the locations of the air release were carefully noted and the sand carefully excavated below these positions. What was observed was that a fair amount of the Anacostia sediment was transported up into the sand but it was filtered out and did not penetrate through the entire sand layer. The cross-sectional area occupied by the Anacostia sediment was considerably larger than the channel diameter observed on the tank wall, possibly suggesting a slight migration of the channel as the pore spaces in the sand became clogged with the finer-grained Anacostia sediment.

Samples of AquaBlok® aggregate were obtained from the manufacturer and subjected to a number of preliminary tests prior to placement in any of the actual experiments. It is noted that any placement of the AquaBlok® on a sediment bed was performed very carefully, literally initially placing it piece by piece by dropping less than a cm with a small water layer depth over the sediment bed. Once a layer or two of the AquaBlok® was placed, then subsequent amounts of material could be placed more rapidly. All placement was performed under water to allow only the submerged weight of the AquaBlok® to bear on the underlying sediment. This procedure created a fairly distinct interface between the sediment and the AquaBlok® and is most likely not representative of what happens during field placement conditions. Preliminary tests were required to determine how to create an AquaBlok® layer of the desired thickness. Since the material hydrates upon exposure to water, the final layer thickness increases during the hydration process. For example, in order to create a 10 cm thick AquaBlok® layer, approximately 6.5 cm of material would need to be initially placed. In general, the thinner the desired layer thickness, the greater was the relative increase in the thickness during the hydration process. Once the AquaBlok® was placed, it took approximately 24 hours to reach a final thickness although most of the increase occurred during the first few hours.

Even if the AquaBlok® surface was initially smooth and level following placement, it did not tend to remain that way as the hydration process proceeded. Generally a somewhat irregular surface would develop, especially pronounced for smaller total

AquaBlok® layer thickness, and there would be small mounds develop on the surface, generally in the range of 5-10 cm in horizontal diameter. If one stuck a finger into the mound, it was obvious that the mound was essentially hollow inside. These mounds tended to subside with time but were observed to persist for days to a few weeks. It is difficult to state with precision what the long term behavior was since the only experiments that persisted for more than a week or so involved other phenomena such as gas ebullition.

Interesting behavior was observed when water or gas pressure was applied beneath the AquaBlok®. A preliminary experiment was performed in a 15 cm wide tank in which air was applied to a bubble bar embedded in sand with an AquaBlok® layer placed on the sand. As the gas pressure slowly built up, a small horizontal crack was observed to open at the interface between the sand and the AquaBlok®. The crack continued to grow as observed in Figure. 3.5 and the AquaBlok® layer was heaved up considerably in the center. It was deformed like a flexible beam but eventually cracks began to form on the upper surface and as the cracks penetrated through the entire layer thickness, gas was eventually released through the AquaBlok®. It was felt that the particular behavior observed may have been due in large part to the small tank width and the ability of the AquaBlok® to slip along the glass walls of the tank. A series of tests were performed for different thicknesses of AquaBlok® layers in a set of flux chambers that were sub-divided to produce horizontal sections of 45 cm by 45 cm. Either air or water was applied through bubble bars embedded in sand beneath the AquaBlok®. Sand was used as a medium to ensure uniform pressure distribution beneath. Observations of the rupture of the AquaBlok® in the various experiments indicated that most commonly, rupture would begin along one wall in much the same process as described above. In a less common, but still fairly frequent failure mode, the AquaBlok® would begin to mound near the center of the tank and the mound would grow in the sense of a volcano until eventually the layer ruptured. In one or two cases, the rupture would develop at the corner of the tank with an uplift of a block of the material. These last two failure modes are shown in Figure 3.6.

In these experiments, the AquaBlok® layer was placed and allowed to hydrate for at least a day. Then the pressure beneath the AquaBlok® was slowly increased over a period of days by injecting either air or water through the bubble bar until the AquaBlok® was observed to rupture. Table 3.1 presents the results of these observations. Although there is some variation in the individual experiments, it is interesting to note that the pressure head required to rupture the AquaBlok® is apparently independent of whether air or water pressure was used, of AquaBlok® layer thickness, and of failure mode. Additional tests may need to be performed to investigate this behavior in more detail. AquaBlok® is also reported to be self-healing if the cap is damaged in some way. These experiments were not continued to observe whether the cracks would re-seal if the pressure beneath the cap was removed since it is presumed that some pressure would generally be present under AquaBlok® caps placed in field environments where pore water flux or gas ebullition are present.

One of the sets of three flux chamber experiments performed involved the application of a vertical pore water flux through uncapped sediment, through sediment with a sand cap, and through sediment with an AquaBlok® cap. A number of observations were made during the conduct of this set of experiments that are potentially revealing as to flow behavior. After the completion of the experiments, dye was added to the injected water to observe how it was passing through the sediment/cap layer. There were distinct differences in observations for the three setups. For the uncapped sediment, the dye was observed to be coming through a fairly large number of small channels. These were typically on the order of 2-5 mm in dimension and seemed to be more like elongated cracks as opposed to circular openings. There were often clusters of several of these openings in close proximity to each other in different general locations around the sediment surface. After dissection of the sediment following completion of the experiment, residual dye within the sediment appeared to be moving through larger cracks that appeared to be connected with more than one of the surface openings. With the sand cap, the water above the sand was observed to slowly increase in dye intensity but no distinct locations where dye could be seen exiting the sand were observed. It is presumed that since the pore water flux was much less than the permeability of the sand,

the sand acted as no significant barrier to water movement and it just passed uniformly through the sand. Similar water pressure heads were required to drive the same pore water flux through the sand capped and the uncapped sediments; thus it appears that similar processes in the sediment layer controlled the water migration.

An initial pressure head on the order of 20 cm was applied to the AquaBlok® capped experiment. Almost immediately, the AquaBlok® cap started to lift along one of the long walls of the flux chamber so the pressure was immediately reduced to about 5 cm. With this small pressure head, the lifting along the side wall subsided but a mound on the AquaBlok® surface started to grow near the center of the tank. After 4 weeks, the water pressure was again increased to about 20 cm and the AquaBlok® cap lifted quickly and ruptured within a few hours after the application of pressure with only about 10 cm of pressure head required to cause the final rupture. Cracks appeared both in the central mound as well as along the tank walls in several locations. Water could be observed to be flowing through one crack through the AquaBlok® along one of the short sides of the tank. For the duration of the ten week experiment, the head required to move a given flux of water through the sediment/cap system was much less than in the other two experiments, suggesting some large scale channel or crack through the sediment itself. When the dye was added to the injection water, dye started appearing through several openings in the AquaBlok®. There were two fractures along the walls of the tanks but several more along the mound formed in the center of the tank. These openings were generally less than 1 cm in diameter and one could not perceive the actual opening in most places, even with the dye flowing out. However, there were appearances of large surface cracks in the vicinities of the dye escape locations. Figure 3.7 shows some of these locations with the dye escape through them.

3.3. Experimental Apparatus

The flume experiments were conducted in a 7.5 m long, 0.6 m wide flume (Figure 3.8). The test section was located about 3.5 m downstream from the flume inlet which consisted of an inlet tank with a converging section connected to the upstream end of the flume. Screens and other flow straightening devices were present in the inlet tank to

provide a uniform approach flow. The test section was approximately 2.00 m long, with a 0.3 m wide depressed cavity installed in a false floor in the bottom of the flume to be filled with the sediment and/or capping material. The choice of conducting experiments in a relatively large sediment bed came particularly as a result of some concerns related to ebullition and seepage experiments. Gas and water migration rates suggested from field measurements are simply too large to be consistent with Darcy-based flow through the fine-grained sediments typical of the Anacostia site. The implication is that either pore water or gas migration through cohesive sediment beds likely occurs through isolated channels. In fact, formation of the channels was confirmed with the preliminary experiments described in the previous section. Therefore, it was planned to ensure that the evolution of the flow channels would be independent of cavity side-wall effects that might dominate the experiment if an inadequate bed size was to be studied and that the test bed surface area was sufficiently large to accommodate the formation of several channels. Furthermore, by having a test section with only half of the total width of the flume, wall effects on the flow were minimized.

The depth of the sediment cavity in the flume was changed according to the specific experiment. In general, the bed thickness was fixed to 10 cm both for sand and the Anacostia River sediment beds. For the cases where the Anacostia River sediment together with the cap material was used, each layer was 10 cm in order to be consistent among the experiments.

Non-cohesive sediment incipient motion experiments (d_{50}=160 μm, d_{50}=500 μm and d_{50}=1200 μm) were conducted in a setup where an additional false floor in the cavity under the sediment bed was used to provide pore water transport through the bed. Within the cavity, a platform covered with geotextile was placed to support the sediment while allowing free migration of pore water into or out of the sediment depending on the applied pressure beneath (Figure 3.9). The hydraulic head at the bottom in the cavity beneath the sand bed was measured with a piezometer and the head difference between the cavity and the water flowing above the sand bed was determined. The injection (positive hydraulic gradient) or suction (negative hydraulic gradient) discharge was also

metered. Prior to the experiments, to check if the distribution of the vertical pore water transport was uniform, fluorescent dye was added into the injection system and it was visually observed that the existing experimental setup provided a uniform distribution across the bed (Figure 3.10a). Two-dimensionality in the flow was also observed in the formation of the ripple patterns formed after the beginning of sediment transport as indicated in Figure 3.10b. In this figure, the dyed segments are located upstream of the ripple crests where injected dye is entering the flow stream while the lighter colored sediments are in the lee of the crests where dye has been washed out of the sand transported over the crest and subsequently deposited in the wake.

It was initially intended to utilize the aforementioned apparatus for the experiments involving cohesive Anacostia River sediment with pore water flux. However, initial observations showed that vertical water or gas flow would tend to occur through well-defined channels in the cohesive sediment beds preferentially along container walls, potentially impacting the experiments. As explained in the previous section, it was discovered that a simple way to resolve this issue was to supply the fluid away from the container walls and then to allow the vertical channel flow to develop within the interior of the sediment bed. For the flume experiments, the injection system consisted of a set of parallel soaker hoses which are generally used for yard irrigation purposes, composed of hydrocarbon-based materials with a large number of small openings in the hose walls. Six individual soaker hoses with center to center spacing of approximately 4 cm were connected to a common source and ran the length of the test bed. The inflow was metered in at the desired rate.

Ebullition was simulated by air injection in a similar fashion to the water injection using another set of five soaker hoses with the same center to center spacing placed under the water injection soaker hoses (Figures 3.11 and 3.12). The placement of soaker hoses provided uniform water or air injection away from the cavity side-walls. Attempts to supply air at a constant rate met with some difficulties as explained in the previous section. This situation was eventually resolved by adopting a novel methodology to ensure that a long term average gas flux was maintained through the sediment. The

concept developed allowed the maintenance of the desired gas flux through a number of discrete additions of gas at intervals that were short compared to the total duration of the experiment. This procedure was implemented with the idea in mind that gas release was presumed to be through a series of discrete release events and the chosen procedure would be capable of reproducing such a set of events. The apparatus in Figure 3.13 schematically indicated how this was accomplished and Figure 3.14 shows the implementation in the laboratory. Water was supplied to Bottle A at the desired rate of the gas flux although in a series of discrete additions at ten minutes intervals for the flume experiments. The water source was supplied through a trap so that air could not escape back through the water supply hose. This water addition compressed the air in Bottle A, increasing the pressure which was then transmitted directly to Bottle B. When the air pressure in Bottle B increased to a level required to initiate bubbling through the sediment, the bubbling event would relieve pressure in the bottles and eventually the bubbling would cease until the addition of more water increased the pressure again to a level required to initiate a new event.

The two-bottle system was preferred to a one-bottle system. In case Bottle A became full during the experiment; it was isolated from Bottle B and could be emptied without losing any pressure in the system before continuing the experiments. Even if Bottle A became full during the experiment, the change in the total air volume compressed did not change too much compared to a one bottle system. Therefore, a constant long term average air injection rate was achieved. It was observed that the initial bubbling event in each experiment required more pressure to cause gas release compared to subsequent experiments. Capped sediment configurations generally required a higher initial pressure to cause a gas release, so a larger Bottle A was used in those experiments without creating a need to empty the bottle during an extended experiment. Often an initial volume of water was added prior to an experiment to create an initial pressure within the sediment that would initiate air release events soon after the commencement of an experiment rather than waiting a long time for the pressure to build up within the system. Adjustments to the size of Bottle A were made when a higher or lower air injection rate was applied to the bed in order to best meet the needs of that experiment; these

adjustments could be anticipated prior to the experiment (based on the application of pressure volume relations with the ideal gas law) so there was no need for a trial-and-error adjustment of the bottle volume.

Advective flow rates in the flume were varied to create conditions spanning the critical shear stress required to initiate sediment transport and these discharge rates were measured with two different methods depending on the experiment. For the non-cohesive sediment stability experiments, the flume received the water from a constant head supply and the flume was operated in a once-through mode. A venturi meter was used to determine the discharge that was regulated with a control valve. The water level over the test bed was controlled by means of downstream weirs and flow depths were measured by a point gauge. In almost all the incipient motion experiments, the depth was approximately 25 cm. Resuspension experiments with the cohesive sediment with or without caps were performed by converting the flume to a recirculation mode. A recirculation pump was used to return the flow to the upstream head tank. An orifice meter installed in the return pipeline was used to measure the discharge rate. The depth in the flume was fixed to 0.25 m for all the resuspension experiments for consistency. This depth was again measured with a point gauge.

Different techniques were considered for the determination or measurement of the bed shear stress. As discussed previously in Chapter 2, there is no direct way to measure the local bed shear stress and indirect methods for computing the shear stress are required. Most previous approaches compute the bed shear stress as the residual of an integral momentum balance of which the shear stress becomes a small difference between a number of larger magnitude terms that cannot be determined with precision (e.g. see, Oldenziel and Brink, 1974; Rao and Sitaram, 1999). Constraints on the experimental apparatus can compound this problem. When a straight flume is not long enough to provide a fully developed turbulent boundary layer over the test section, the flow is not uniform and this fact would eliminate many of the simpler estimation methods. It was considered to be unacceptable to achieve a developed boundary layer by performing experiments at depths of a few cm since the resulting bulk flow Reynolds Numbers

would only nominally be above the transition from laminar to turbulent flow and therefore not representative of typical field conditions. It was felt that the best approach to estimating bed shear stress was to obtain local turbulence measurements close to the bed surface and to develop a procedure for converting these results to bed shear stress. Several sets of Acoustic Doppler Velocimeter (ADV) data were collected. An ADV (Sontek MicroADV, down-looking probe) probe is capable of measuring the instantaneous velocity components of the flow in all three dimensions. Vertical velocity profiles were measured at the middle of the flume width over the sediment bed as well as on a rigid boundary. Similar measurements were made at the downstream end of the bed. Then, a framework was developed comparing the boundary layer thicknesses determined from the velocity profiles to those determined from semi- empirical relationships available in the literature for turbulent boundary layers. The results confirmed that the turbulent boundary layer was not fully developed over the test section. The ADV measurements also provided data for a statistical analysis of the velocity fluctuations, and consequently the Reynolds Stress term which is proportional to the local turbulent shear stress. Therefore, in addition to the vertical velocity profiles, these measurements provided the data required to develop means to investigate local turbulence characteristics and from these, to estimate the bed shear stress. This approach will be explained in further detail in Chapter 4. It is important to note that ADV probe can only measure down to about 0.5 cm above the bed which needs to be taken into consideration for the development of a conceptual framework to compute the shear stresses at the bed level.

For the experiments involving the Anacostia River sediment, sediment concentrations in the recirculating water were inferred by monitoring the flow with a turbidimeter (Orbeco-Hellige 965-10AR), a device that measures light attenuation through a sample due to the presence of suspended solids in this application. In this experimental setup, the turbidimeter was connected to the return pipeline in the recirculating flume system downstream from the recirculation pump. It was presumed that the flow through the recirculation pump homogenized the flow providing for a relatively uniform sediment concentration that was subsequently sampled by the turbidimeter. A flow-through cell

was used to take continuous turbidity measurements which were then used to compute resuspension rates. The turbidimeter was connected to a data acquisition system through which the turbidity readings were recorded in terms of voltages which in turn gave the total suspended sediment concentrations by means of a calibration performed for this sediment relating turbidity to concentration (see Appendix A.1).

3.4. Non-Cohesive Sediment Bed Experiments

3.4.1. Sediment Properties

The non-cohesive sediment bed experiments were performed to determine the conditions under which incipient motion is observed in the presence of pore water seepage through the sediment bed. There are various definitions for initiation of motion criterion in the literature (Buffington, 1999). This issue will be further addressed in Chapter 4. In this study, initiation of motion was observed visually. During the early stages of the experimental studies, it was recognized that some of the properties of the sand such as uniformity of the sand blend and shape of the individual particles influenced the incipient motion observations. For some blends, it was difficult to observe a condition that would clearly define initiation of motion. After several trials, it became clear that a uniform blend with roughly rounded particles would provide the conditions where ripple formation at the incipient motion state could be used as the stability criteria for this investigation. This approach provided a more repeatable methodology for defining initiation of motion than other approaches investigated. Therefore, for the non-cohesive sand bed experiments all the sand blends were commercially produced and commonly referred to as *beach/lake sand.* The sand used in the experiments was thus relatively rounded and uniform in shape and size. Three sizes of sands, d_{50}=160 μm, d_{50}=500 μm and d_{50}=1200 μm were used for the main part of the non-cohesive sediment stability (incipient motion) experiments. There were difficulties locating the larger diameter sand and a compromise was required in that a less uniform sand was used for the d_{50}=1200 μm experiments. The median grain sizes of these sand blends were measured using standard sieve tests (Figure 3.15). Other than the experiments with these sand sizes, tests on the effectiveness of caps utilized sand with similar specifications to that placed at the

Anacostia demonstration site. The median size of this sand material was determined to be 340 μm. This sand is commonly referred to as concrete sand and follows general specifications for grain size distribution and that used in the experiments was obtained locally. This sand did not have the rounded characteristics of the sands used in the other experiments. In addition to the tests investigating the effectiveness of the cap in terms of reducing the resuspension of contaminated sediments, initiation of motion tests were performed on this sand for completeness.

3.4.2. Parameters Tested

Non-cohesive sediment stability experiments involved varying flow induced shear stresses and positive/negative pore water transport rates through the sediment bed. For each sand size, a baseline experiment without pore water flux was conducted to define a critical bed shear stress value at which incipient motion was observed. The flow rate in the flume was increased until incipient motion was observed. In these experiments, the initiation of motion was defined by running the experiment for about 15-20 minutes and watching for the formation of ripples on the sand bed surface. It was difficult to observe motion of individual sand particles until a ripple started to form after which the disturbance of the smooth surface triggered more significant sediment transport. Once the ripple formation was observed, the bed was defined as unstable and that flow condition was defined as the incipient motion condition. Repetitions of the same experiment yielded quite repeatable results using this methodology. It is not clear exactly how this definition of incipient motion compares to definitions used in previous studies but the results presented in Chapter 4 are consistent with the commonly accepted Shields curve.

After a base critical bed shear stress induced by the advective flow was determined for each sand size, positive (injection) or negative (suction) hydraulic gradients were applied to the bed to investigate the effect of pore water transport on the bed stability. In theory, the range for the applied hydraulic gradients would have an upper limit of 1 which implies a quick sand condition. The applied hydraulic gradients were selected to be sufficiently large that an effect on sediment stability could be observed and they would cover as wide a range of values as possible. Chapter 4 will provide the details related to

the rates applied. Overall, three injection and two suction cases with different pressure gradients were considered. The flow rate through the bed was metered in both injection and suction experiments. An injection or suction experiment was conducted by first setting the hydraulic gradient to a predetermined value then increasing the advective flow rate in the flume until incipient motion was observed. This procedure was followed for all three sand beds but not for the Anacostia demonstration site sand bed. Only seepage fluxes reported in the literature were applied to the Anacostia demonstration site sand bed to investigate the cohesive sediment resuspension rates in the presence of this sand cap; these rates were insufficient to produce large hydraulic gradients through this sand and the effect of pore water seepage on sand cap stability was judged to be negligible based on the other test results.

3.4.3. Bed Preparation Procedure

Prior to each non-cohesive sediment experiment, sand was placed in the cavity and the bed surface was smoothed so that it was flush without any imperfections as much as possible. The flow in the flume was started gradually so that the bed surface was not disturbed during the flume filling process. Before each experiment, bed surface was re-leveled. There was a possibility to get different results if an experiment was repeated due to the small differences on how the bed surface was prepared. In order to confirm the results, each experiment was repeated at least two times.

3.5. Capped and Uncapped Cohesive Sediment Bed Experiments

3.5.1. Sediment and Cap Properties

The Anacostia River sediment used in the experiments was obtained from four drums of sediment that were taken from a site near the test caps. Before using a large amount of the sediment in the flume experiments, several small samples were taken out from the drums for the grain size analyses and sample cores were collected for permeability tests. Sediment grain size analyses were performed with hydrometer tests (see Appendix A.2). Standard procedures were followed in the performance of these tests. Sediment samples were obtained from two of the drums to check for consistency. Results are presented in

Figure 3.16. The median sedimentation diameter d_{50} is approximately 10 μm, placing the material well into the clay-size particle range. In addition to the grain size test, Atterberg limit tests were performed on representative samples of the cohesive sediment (see Appendix A.3). The plastic limit for the samples tested averaged to 43.4 percent while the liquid limit was 77.7 percent.

Several attempts were made to measure the permeability of the sediment. Preliminary measurements were made from sediment cores collected by pushing an 8-cm diameter acrylic tube into the sediment in one of the drums. A core length on the order of 20 cm was obtained by this procedure. The core was then subjected to a falling head permeability test. The initial test was performed by applying the water head to the top of the core. Results of the testing as presented in Figure 3.17 indicated a permeability that decreased with time as the measurement proceeded. It is presumed that this decline in permeability could have been associated with consolidation within the sediment core due to the pressure gradient applied across it or else small leaks along the sidewalls of the cylinder being closed; the testing converged to a hydraulic conductivity of 7.8×10^{-6} cm/s. A second experiment was performed by applying the water pressure to the bottom of the sediment core. In this state, the water pressure gradient would oppose the tendency of the sediment to consolidate and substantially larger hydraulic conductivities were measured on the order of 2.6×10^{-4} cm/s. It is also possible that leakage at the side walls of the cylinder contributed to this larger value. Finally, an attempt was made to measure the hydraulic conductivity of the disturbed sediment at the placement density. Given the results of the initial measurements discussed above, the measurement was performed by applying the water pressure from below to avoid the consolidation of the sediment due to the applied pressure. However, only very small water pressure heads could be applied without flow being initiated through a well-defined channel in the sediment. Once that condition developed, much larger water fluxes could be forced through the sediment without a significant increase in pressure head. Consequently, only very small pressure heads could be applied to the sediment in order to perform the conductivity measurement and it was difficult to perform accurate measurements. The estimated sediment hydraulic conductivity from this measurement was 4.4×10^{-6} cm/s or much closer to the initial

experiment performed in a downflow mode and it can be concluded that the first estimate is the more reasonable value.

Since the sediment in the drums was already disturbed from the time of their collection, a procedure was developed to provide a consistent method for bed preparation in order to conduct the resuspension experiments. Prior to placement into the cavity in the flume, the Anacostia River sediment was homogenized with water addition if necessary to achieve a desired bulk density. The selection of the target bulk density was rather arbitrary but was based on a decision to achieve a desired level of sediment consistency in order to be able to place the sediment conveniently in the test setup as also addressed in Section 3.2. The selected value of the bulk density was 1.4 g/cm^3 and the volumetric moisture content of sediment samples corresponding to this bulk density was determined to be 77 percent.

The sand cap material with median size of 340 μm which has similar specifications to that placed at the Anacostia demonstration site was tested for effectiveness in lowering the resuspension rates. Before conducting any resuspension experiments, the sand was thoroughly cleaned of dust by washing it with water to ensure that the turbidity measurements were not associated with fine material scoured from the sand cap. Another cap material, AquaBlok®, was also tested for effectiveness within the scope of this study. AquaBlok® is a patented technology used to minimize the resuspension of contaminated sediments into the water flow once placed on the sediment bed. This material consists of small sized aggregates covered with bentonite (Figure 3.18). When a mass of discrete and relatively hard AquaBlok® particles hydrate and bind, the mass transforms into a continuous and relatively soft body of material creating a relatively low permeability layer. The hydraulic conductivity of AquaBlok® has been recently reported as ranging from 10^{-7}-10^{-8} cm/s in a report released by U.S. EPA (2007).

3.5.2. Parameters Tested

In order to get a baseline set of resuspension data, advective flow experiments were conducted with the Anacostia River sediment. In this context, advective flow implies that

only the recirculating flow creating a bed shear stress without pore water or ebullition flux was examined. These experiments were conducted to determine the shear stress levels leading to resuspension in the flow. Based on the observations, a range of different discharge rates were chosen for the experiments creating shear stresses below and above critical shear stress. Initially for the resuspension experiments with only advective flow, a five-step discharge increase was taken as the experimental protocol, starting from a low shear stress level and incrementally increasing the shear stress. In all of the experiments (discounting the occurrence of ebullition generated resuspension), no apparent erosion was observed during the first two discharge rates. However to make sure that the effect of ebullition and/or seepage on the critical shear stress level (possible reduction in critical shear stress) was captured in the results, all the experiments were conducted with this 5-step discharge scheme. At each discharge step, the flow was run for one hour. Although it may be possible that this time interval has some effect on the results, this parameter was not investigated in the experiments. One hour long discharge steps made it possible to complete the experiments in a reasonable time frame adding up to 5 hours as the total duration of one experiment. Another important aspect influencing the decision on the duration of the experiments was the temperature increase observed throughout the experiment due to the energy added through the recirculation pump. The temperature increase was controlled by limiting the duration of the experiments. Average discharge rates applied over the bed during a resuspension experiment are given in Table 3.2 together with the corresponding estimated bed shear stresses. Shear stresses were calculated using free stream velocities (u_s) measured with the ADV but are correlated to the maximum value of the Reynolds stress in the vertical profile as described in Chapter 4. The reported free stream velocity is the maximum longitudinal velocity measured in the vertical profile, but the velocity was relatively constant beyond outside of the boundary layer which was typically on the order of 4-6 cm thick.

Ebullition fluxes have been reported in the literature as ranging from 0.01-48 cm/d (see Section 2.3.4). 1.2, 12 and 48 cm/d were the initial selected rates for the resuspension experiments. Applying these rates to the sediment bed surface area, gas discharge rates were calculated as 5, 50 and 200 ml/min. Pore water seepage fluxes were

reported as 0.01-124 cm/d (see Section 2.3.3). The selected rates were 0.12, 1.2 and 12 cm/d for the experiments. A narrower range was considered for seepage fluxes as lower rates were reported in the literature for fine-grained low permeability sediments. These fluxes would be converted to seepage rates for the experimental setup as 0.5, 5 and 50 ml/min. Some the lowest rates reported in the literature were eliminated due to the desire to see observable effects within the duration of a typical experiment which was approximately five hours. In the final testing, some of the selected lower rates were also eliminated, as preliminary experiments showed no observable effects. The details of the experiments conducted are provided in Chapter 5.

Effects of the same parameters on resuspension rates as mentioned above were also studied in the presence of the sand cap and the AquaBlok® cap when initial observations showed a necessity for investigation. During the AquaBlok® experiments, the shear stress levels normally applied to the bed throughout the rest of the resuspension experiments did not create any significant effect. Therefore, higher shear stress values were applied to the AquaBlok® bed within the limitations of the setup (Table 3.3). It should be noted that not every shear stress level in the AquaBlok® test was applied for an entire hour to limit the total duration of the experiment and the temperature increase in the recirculating water.

3.5.3. Bed Preparation Procedure

The bed preparation procedure was particularly important for the experiments involving cohesive Anacostia River sediment as initially, some problems were encountered regarding the reproducibility of the results. These issues were largely eliminated by defining well-controlled procedures for sediment bed preparation. Once the procedures for different types of experiments were developed, each experiment was repeated at least two times to confirm the results.

Since the Anacostia River sediment in the drums was already disturbed, it was not possible to conduct experiments with undisturbed samples. A decision was required to establish a consistent procedure for sediment bed preparation. After some initial

investigation, it was concluded that the best procedure would be to extract sediment from the drums, clean it of debris such as plastic, clam shells, sticks, etc., and mix it thoroughly to a density to be maintained consistently throughout all experiments. It was observed that the homogeneity of the sample also had some impact on the results. Therefore, it was necessary to mix the sample thoroughly before placing into the test cavity in the flume. In order to obtain a consistent sample density, a small sample of sediment was collected and weighed prior to each experiment. Results showed that the bulk density of the samples was about 1.4 g/cm^3 and among the experiments, the bulk density varied less than one percent, minimizing the effect of density variation on the results.

While it is known from literature that consolidation degree has a significant impact on erosion rates (Mehta et al., 1989 and Lick et al., 1995), this phenomenon was not considered as a parameter within the scope of this study. For each experiment, the sediment was placed and allowed to settle for 12-24 hours. There were practical limits on this time interval in order to conduct the large number of projected experiments. In addition, if the processes of pore water flux and gas ebullition were to be studied, it is not consistent with a natural system to allow the sediment to settle for 30 or 60 days, for example, without these processes being present and then to suddenly impose the process on a partially consolidated sediment. It is noted that although the term “settling” is applied above to the resting period between the placement of the sediment and the initiation of an experiment, the sediment density was sufficiently high that a separated water layer did not form above the sediment during the settling period. It is acknowledged that the sediments were tested at a lower density than that would be expected from in-situ consolidated sediments.

Four separate experiments were conducted consecutively over a four day period following each placement of the sediment. It was determined that after about four days of experiments, the sediment was consolidating, creating a denser layer at the bottom of the cavity. This effect was observed even though prior to each individual experiment, the sample was remixed in the cavity. Complete mixing in the cavity was difficult due to the

presence of the soaker hoses at the bottom of the cavity. After each four experiment set, all the bed material was removed from the cavity and remixed in an external tank and replaced into the test cavity. It became possible to obtain consistent test results in the experiments following this procedure.

Another important aspect was to ensure that the prepared bed surface was flush and undisturbed as much as possible for each experiment. Every bed sample had to be prepared extremely carefully. To keep the sediment sample surface undisturbed while filling the flume with water, a frame with 15-cm side walls surrounding the cavity was placed. Once the flume was full up to a certain level this frame was removed carefully and then the flume was filled to the required level slowly. The optimal bed preparation procedure was developed after many trials and the test procedure was carefully followed for each subsequent experiment.

Similar experimental procedures were followed with the sand cap and AquaBlok® cap experiments but bed preparation had some differences. For the resuspension tests with the sand cap, the sand (d_{50}=340 μm) was applied carefully to the surface of the Anacostia River sediment layer in order to minimize mixing of the sand and the sediment (Figure 3.19). The bottom sediment layer was deep enough to cover the injection soaker hoses and the sand layer on it had a thickness of approximately 10 cm. For the AquaBlok® experiments, the thickness of the hydrated cap was again 10 cm but this time Anacostia River sediment was not placed underneath this layer as no ebullition or seepage resuspension experiments were conducted with this cap. This decision was based on the initial investigations leading to the development of protocols for seepage and ebullition experiments as described in Section 3.2. The results of the preliminary investigations revealed that due to excessive water or air pressure build-up, AquaBlok® ruptured and the location of the rupture and its characteristics were quite random. Once the cap was ruptured, the sediment was able to migrate into the water column freely through the cracks. It was felt that the experimental results would be completely dependent on the nature of the AquaBlok® rupture process involved in the specific experiment conducted and that meaningful results could only be determined by performing a sufficient number

of repetitions to provide a statistically significant data set. This was beyond the scope of the present investigation. Hence, stability of AquaBlok® cap was examined only for the effect of advective flow. For the experiments, AquaBlok® material was placed in the cavity and left to hydrate under water overnight (Figure 3.20). The next day, advective flow experiments were conducted by increasing the flow rate incrementally to reach a shear stress level destabilizing the bed.

3.6. Experimental Error and Uncertainty Assessment

Evaluations were conducted to define uncertainties in experimental measurements. The sources of these uncertainties are related to the instrumentation or uncontrollable experimental processes and specific decisions made to develop some of the experimental and data analysis procedures. For example, related to the cohesive sediment experiments, there is no accepted standard to follow in order to conduct these experiments. Although the procedures developed follow a general strategy often implemented by other researchers, there is no consensus on duration of the time increments for each discharge step or sample preparation, etc. Each of these factors may influence the results. These issues are all acknowledged and investigations were performed being internally consistent.

The turbidimeter provides perhaps the most important data required for this study which is the total suspended sediment concentrations determined from the turbidity measurements. Therefore, fluctuations in the data which were observed in all of the experiments were evaluated (Figure 3.21). Some of the relatively large peaks were directly related to an event when an air bubble was passing through the flow-through cell. As the turbidimeter takes the readings utilizing the reflection and transmission of light beams when they are passed through the fluid body with suspended sediment particles, an air bubble results in a large peak. Although this was observed visually watching the flow reaching to the sampling cell in the turbidimeter, several exploratory tests were conducted to investigate and confirm the relationship between large peaks and air bubbles. These tests explained below showed that the large peaks in the signal were not present when air bubbles were not present. However, the smaller amplitude fluctuations

seemed to exist consistently throughout the experiments which could be related to the experimental setup. Exploratory tests conducted were set up so that the possible influence of the specific flume setup used in the experiments was ruled out. In one control test, the flow-through cell system was arranged such that the turbidimeter took the readings from a small amount of water with constant suspended sediment volume recirculated by means of a small pump. Even though a declining trend during the experiment was observed because of the sediment deposition in the water container, the same fluctuations as in the flume experiments were observed (Figure 3.22). Here, there was no bubble transport through the system because of the way the experiment was set up. Similar results were obtained when a sample of the same water-sediment mixture was put into a discrete sample vial (the measurement did not involve the flow through cell) and the concentration was measured. In this experiment, sediment deposited with time in the sample cell over the duration of the experiment which resulted in an overall decline in the turbidity.

The above mentioned tests were repeated on a water sample with less suspended sediment concentration to check whether the turbidimeter was giving a constant fluctuation value or fluctuations depended on the concentration of the mixture. Computations showed that higher concentration sample measurements resulted in higher standard deviations and lower concentration sample measurements resulted in lower standard deviations. The standard deviations computed using 10-sec samples (to avoid significant effect of concentration decrease due to deposition) were on the order of 4-5% of the 10-sec averages. These results indicate that the observed fluctuations are solely as a result of the precision of the turbidimeter and are on the order of 5% of the sample concentration.

Another potential instrumentation error could be related to the flume discharge measurements. In order to examine this issue, discharge measurements from the venturi meter and orifice meter were compared to the discharge computations using ADV velocity profile measurements. All ADV data were collected so that the accuracy of the measurements was satisfactory with a frequency of 30 Hz and at very high correlations

such as 95% or higher most of the time. This high correlation value indicates that the noise level in the signals was significantly low. The differences in the discharges calculated from measurements vary between 5-10% on average depending on the discharge value. It should be noted here that ADV velocity profiles are formed using the measurements taken at a limited number of vertical samples along the middle section of the flume. Furthermore, computation of the discharge from the velocity profiles involves some mathematical approximations.

All the experimental procedures and setups were developed so that the experiments would be reproducible and in the end, to provide consistent results. However, there might be some observational errors involved especially in the incipient motion experiments. A significant amount of effort was put into performing these experiments so that consistent results would be derived from the experiments. Most of the time, each experiment was repeated at least twice or until a consistent result could be achieved. On the other hand, the experiments with the Anacostia River sediment had some other challenges involved considering the complicated nature of cohesive sediments. The protocols which did not exist in the literature were developed minimizing the uncertainty levels as much as possible. Yet, there may be some issues that are difficult to control with a high precision such as homogeneity of the sediment sample used. It is unknown how much the sediment matrix changes among the experiments or how much a minute difference in the bulk density would influence the results.

Figure 3.1: Air bubbles released along the side-wall of the permeability test core due to the lowered water pressure on the sediment.

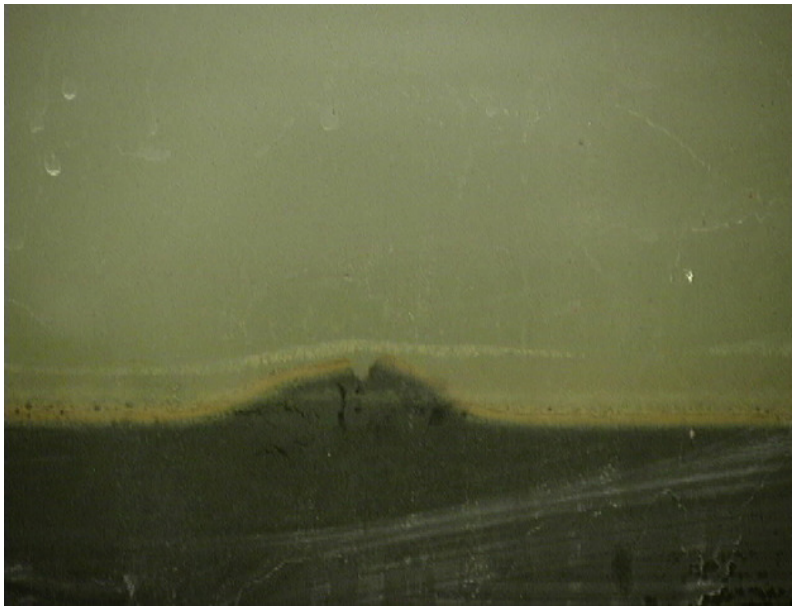

Figure 3.2a: Bulge development on the Anacostia River sediment surface just before the release of an air bubble.

Figure 3.2b: Air bubble is released and some sediment is entrained into the water column in its wake.

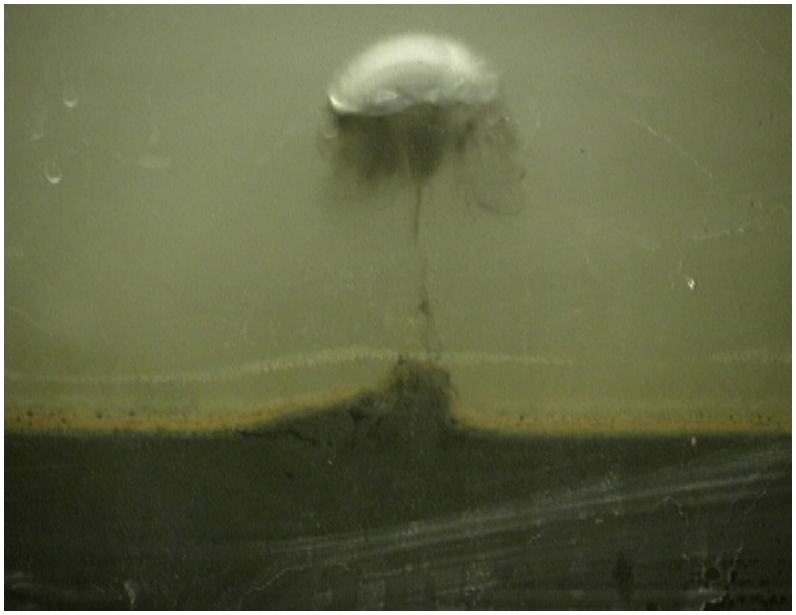

Figure 3.2c: Sediment is lifted up into the water column with the bubble.

Figure 3.3: Bubbles released through a sand cap.

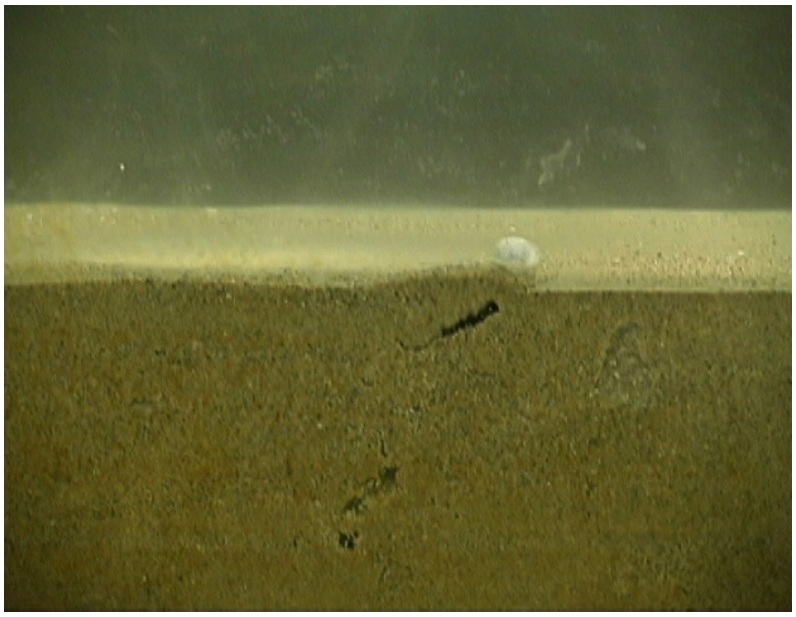

Figure 3.4: Channel formation and an air bubble along the side-wall of the tank (sand cap).

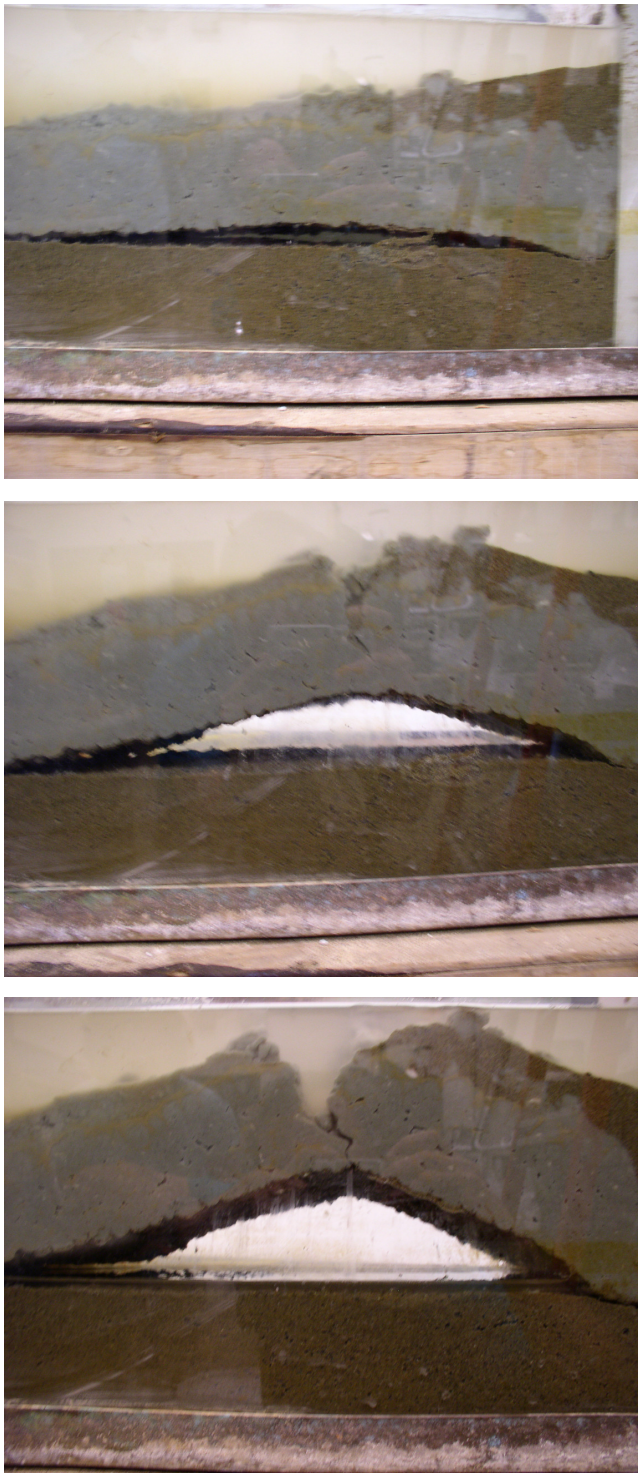

Figures 3.5: Evolution of the AquaBlok® - sand interface separation and subsequent cap failure due to air pressure build-up.

(a)

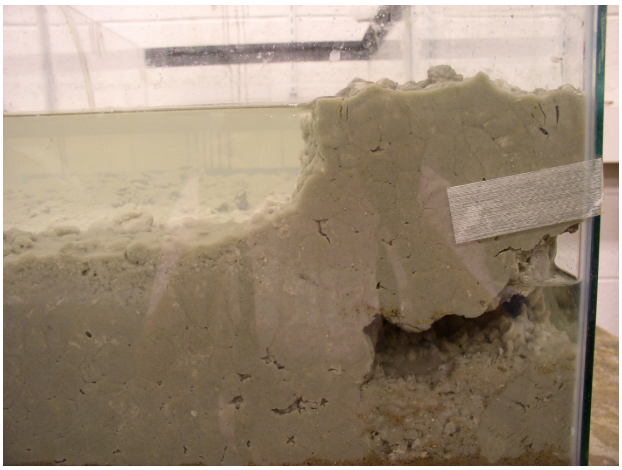

(b)

Figure 3.6: Two failure modes of AquaBlok® due to air pressure build-up: (a) mound formation near the center of the tank followed by its rupture (side and plan views), (b) uplift and rupture at the corner of the tank.

Fluid Applied	AquaBlok® Thickness (cm)	Pressure Head Differential at Failure (cm)	Mode of Failure
Air	5.0	27.5	Mound in center of tank
Air	5.5	27.5	Mound towards one wall
Air	6.0	20.0	Crack 4 cm away from wall
Air	7.0	25.0	Mound in center of tank
Air	10.5	22.0	Mound in center of tank
Air	13.5	25.0	Lift along one wall
Water	5.0	25.0	Mound in center of tank
Water	7.0	27.5	Lift along one wall
Water	9.0	25.0	Lift along one wall near corner
Water	10.0	20.0	Mound in center of tank plus cracks along wall (4-week test)
Water	13.0	22.5	Uplift of block in corner of tank

Table 3.1: Observed failure modes in flux chamber experiments when air or gas flow was applied beneath the AquaBlok®.

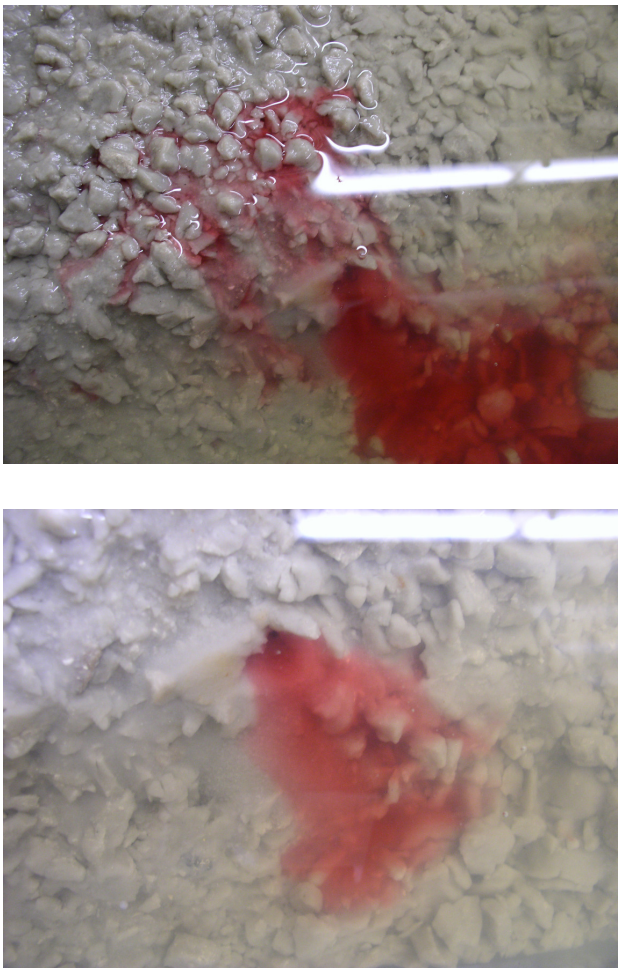

Figure 3.7: Dye escape through fractures in AquaBlok® at several locations formed due to water pressure build-up.

Figure 3.8: Test section and the general setup of the flume that can be run either in a once-through mode or in a recirculating mode.

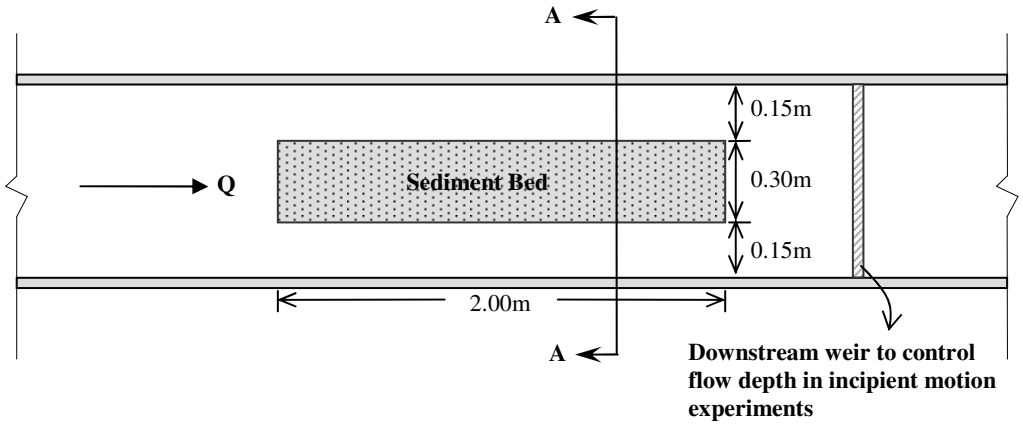

(a)

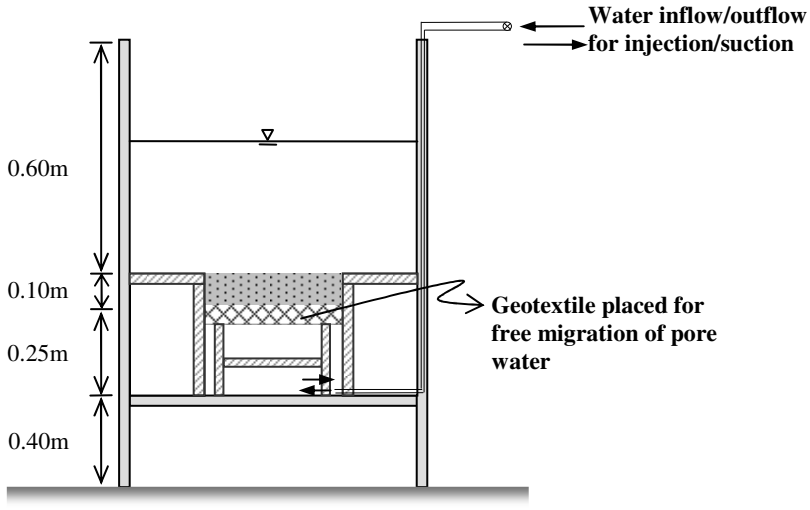

Section A-A

(b)

Figure 3.9: (a) Plan view of the test section, (b) Cross section of the flume and cavity showing pore water flux setup for non-cohesive sediment incipient motion experiments.

Figure 3.10: (a) Under a very low advective flow rate in the flume, the plan view of the test section after fluorescent dye was added to the injection system in order to test the uniformity of the seepage distribution over the whole bed, (b) Plan view of dyed ripple formations after application of a high flow rate over the bed (flow direction is from bottom to top of the photographs).

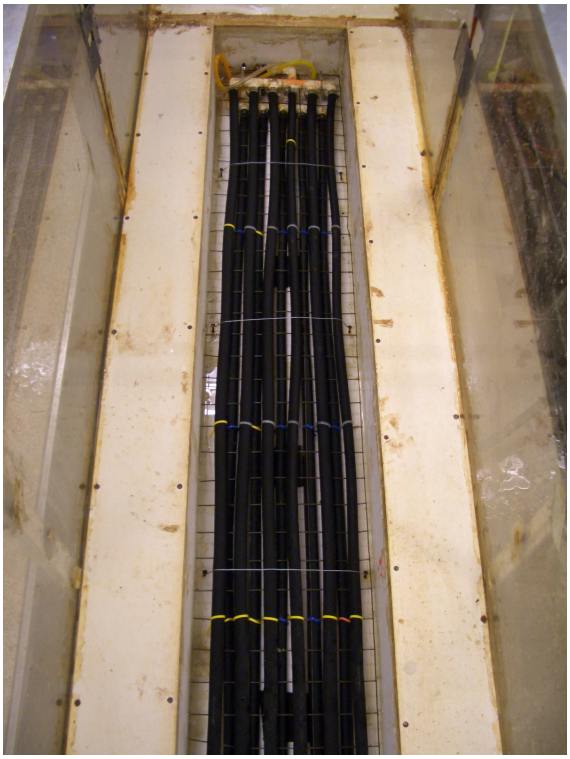

Figure 3.11: Soaker hoses capable of providing uniform seepage and ebullition away from the cavity side-walls for the resuspension experiments.

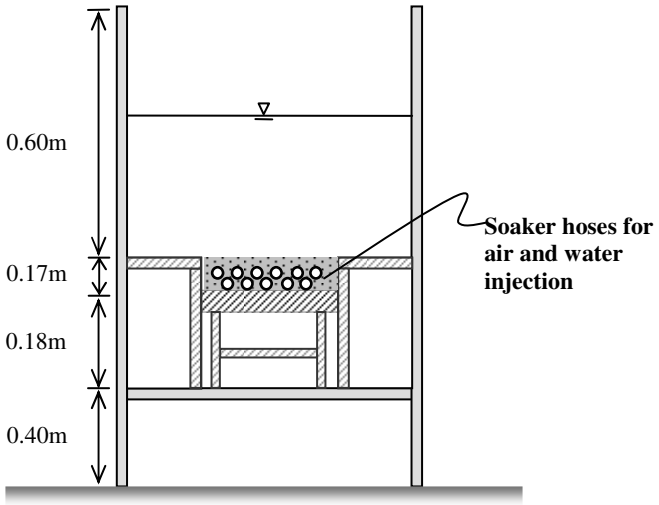

Figure 3.12: Cross sectional view of the flume showing the layout of the soaker hoses, water injection was through the upper row of hoses while air injection was through the lower row.

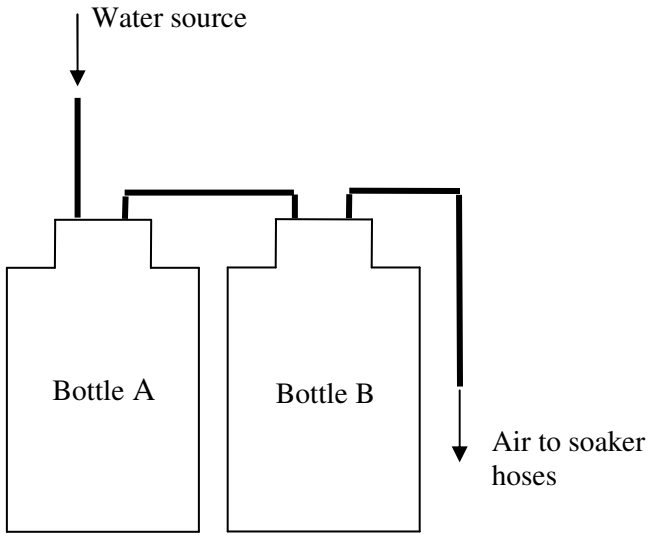

Figure 3.13: Schematic of the apparatus to develop gas ebullition through sediment beds.

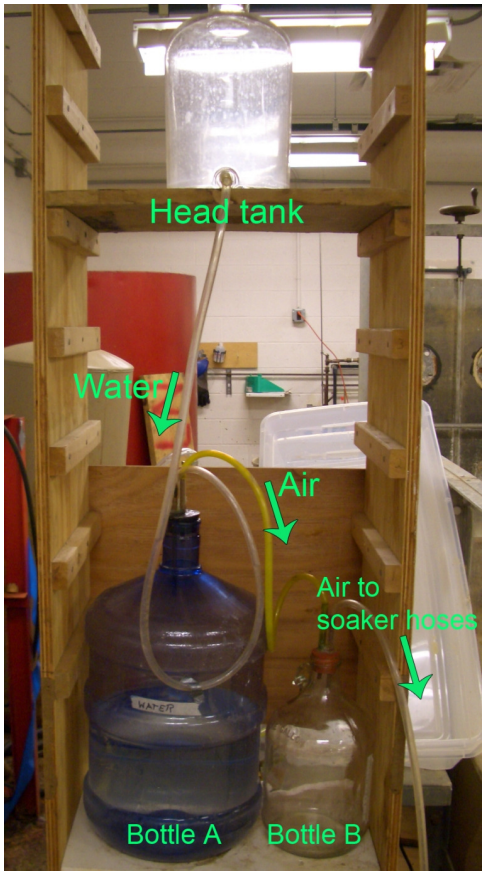

Figure 3.14: Implementation of the gas ebullition apparatus.

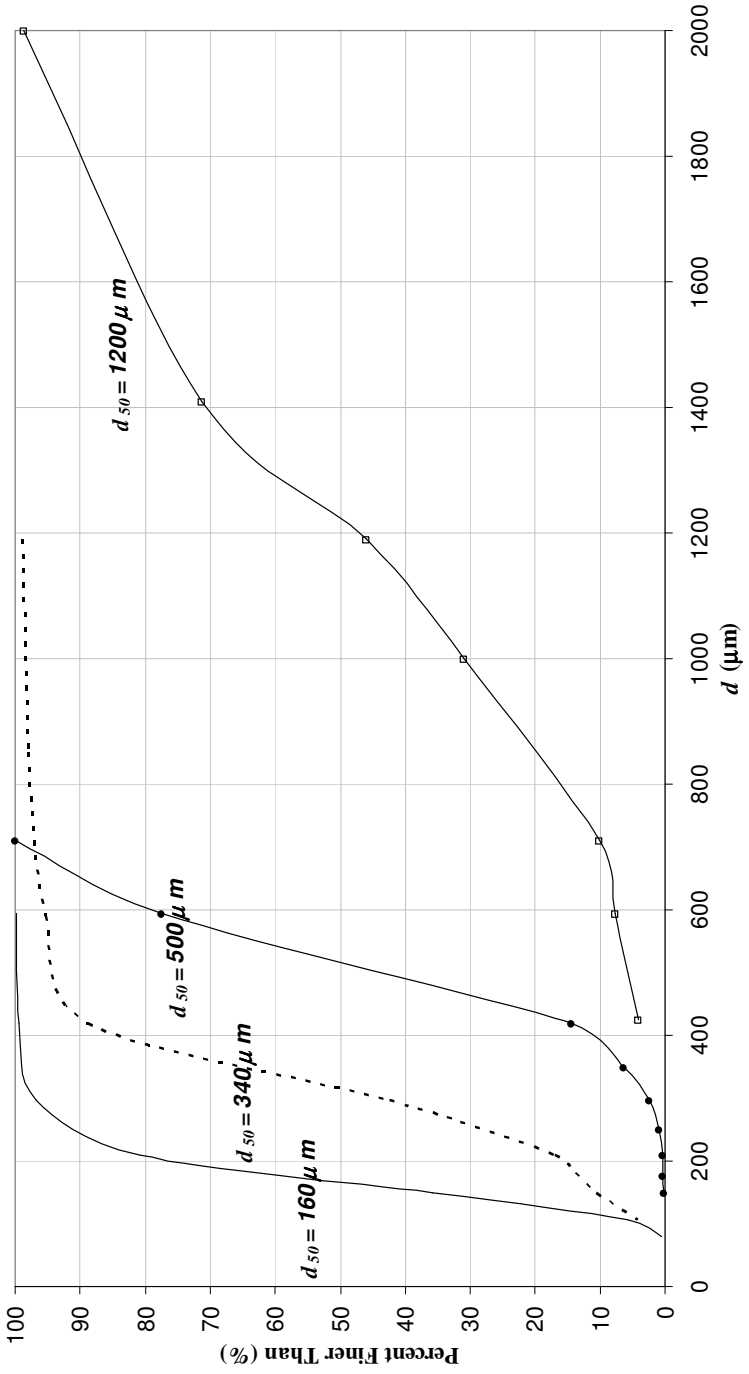

Figure 3.15: Sieve analyses for non-cohesive sediments.

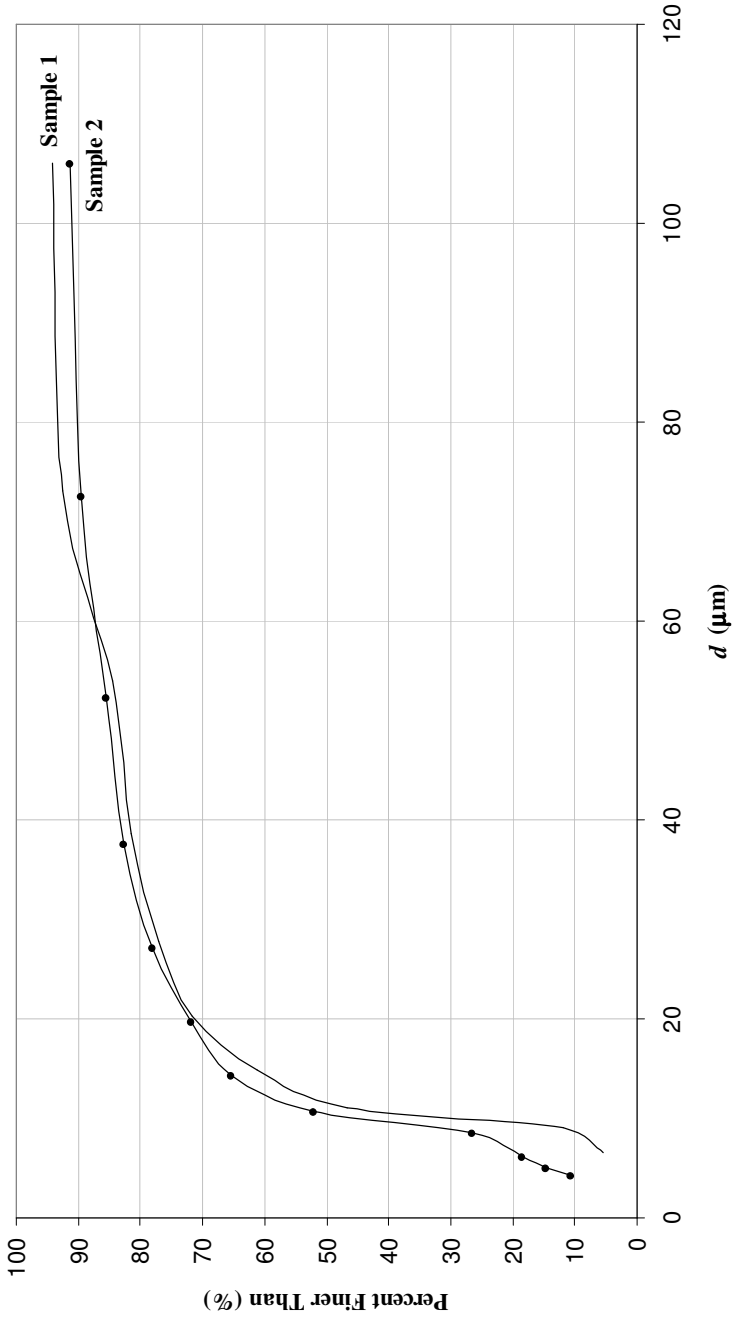

Figure 3.16: Hydrometer test results for the two Anacostia River sediment samples.

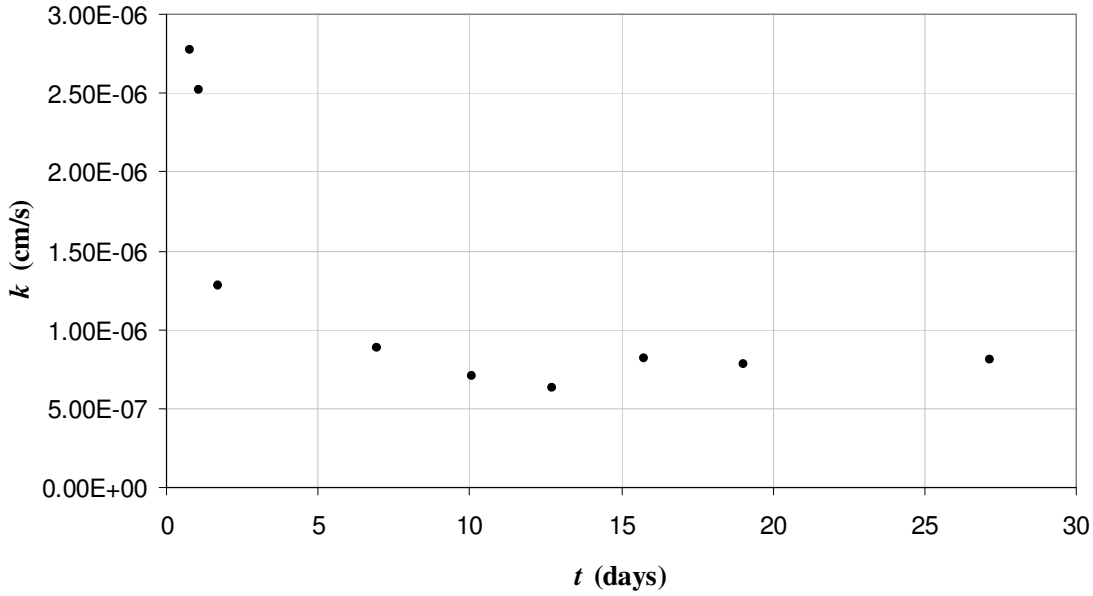

Figure 3.17: Hydraulic conductivity versus time measurements from downflow permeability tests.

(a)

(b)

Figure 3.18: (a) AquaBlok® cap material (bentonite covered small aggregates), (b) Various sizes of aggregates under the bentonite layer.

Q (m^3/s)	u_s (cm/s)	τ (N/m^2)
0.033	25.511	0.153
0.036	27.996	0.180
0.041	31.027	0.214
0.046	34.513	0.257
0.051	38.454	0.309

Table 3.2: Average discharge, free stream velocity and estimated bed shear stresses applied to the test section for resuspension experiments.

Q (m^3/s)	u_s (cm/s)	τ (N/m^2)
0.033	26.494	0.164
0.035	29.538	0.197
0.041	32.374	0.231
0.046	35.883	0.275
0.051	39.515	0.324
0.056	42.685	0.370
0.058	45.220	0.408
0.069	53.921	0.552
0.078	60.454	0.671
0.101	79.276	1.067
0.126	108.935	1.839
0.142	115.488	2.032
0.143	132.324	2.565

Table 3.3: Average discharge, free stream velocity and estimated bed shear stresses applied to the test section for AquaBlok® experiments.

Figure 3.19: (a) The Anacostia River sediment placed in the cavity covering the soaker hoses right before placing the sand cap over it, (b) Careful placement of the sand cap over the sediment.

Figure 3.20: (a) AquaBlok® bed before hydration, (b) AquaBlok® bed under water after 21 hours of hydration.

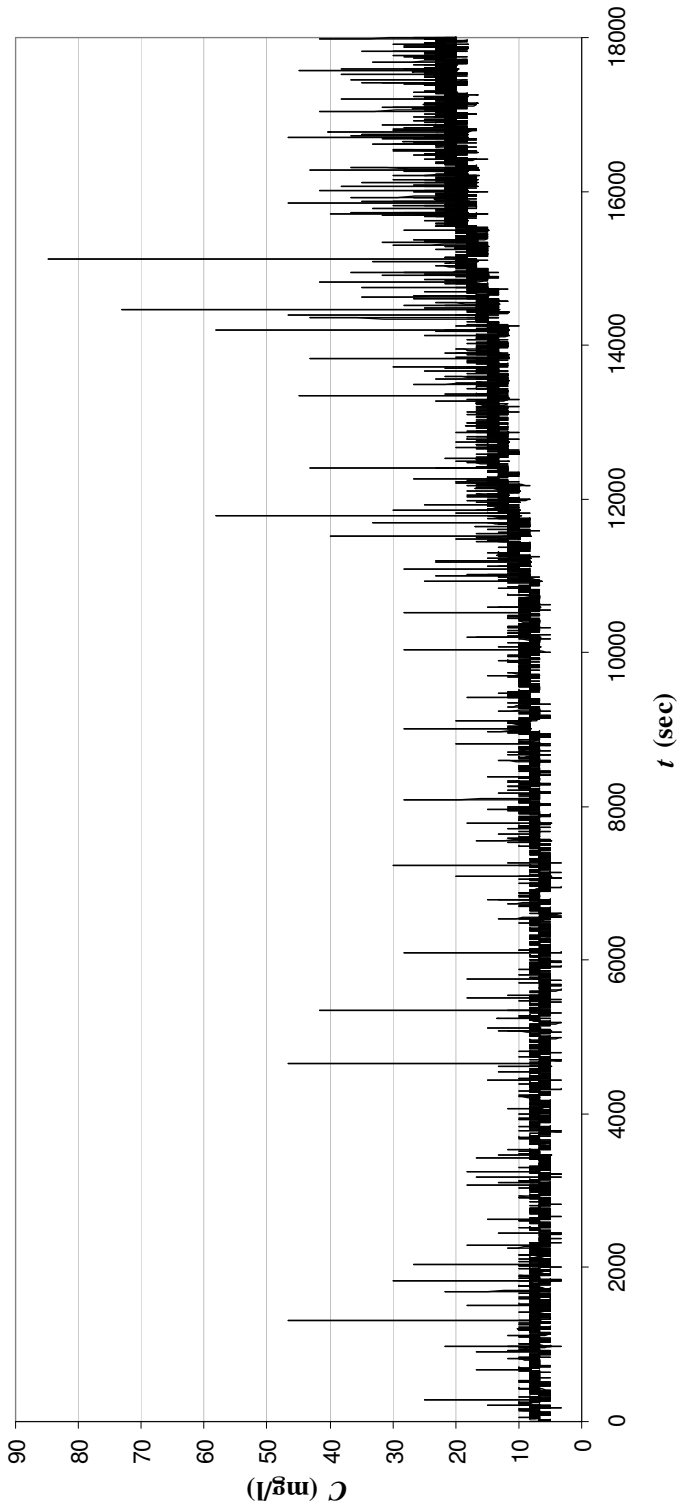

Figure 3.21: A typical concentration versus time graph from a resuspension experiment showing the signal fluctuations.

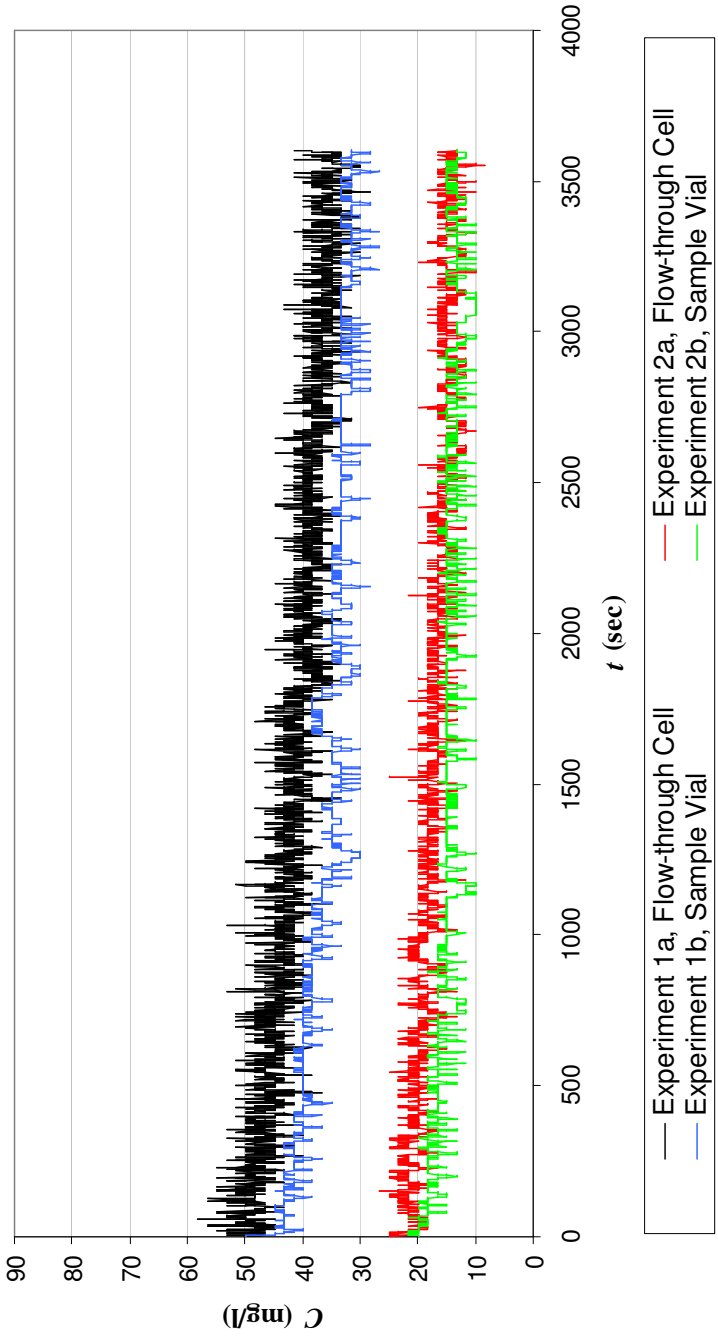

Figure 3.22: Results of the exploratory experiments measuring concentrations of two different sediment-water mixtures (experiments 1 and 2) using a flow-through cell and a discrete sample vial.

CHAPTER 4

STABILITY OF NON-COHESIVE SEDIMENT BEDS SUBJECT TO PORE WATER FLUX

Commonly used methodologies for predicting stability of non-cohesive sediment beds are typically based on correlations with bottom shear stresses associated with hydrodynamic events such as advective river flow or estuarine tidal episodes. In these predictions it is assumed that there is a critical shear stress above which sediment is eroded at increasing rates with higher shear stresses. In addition to the hydrodynamic processes, another process that could to sediment destabilization is vertical pore water pressure gradients due to groundwater flow through the stream bed which could be a result of ground water table changes or tidal fluctuations in estuaries. This destabilizing effect may be additive to hydrodynamics forces, resulting in erosion under hydrodynamic conditions that would otherwise be below critical shear stresses or higher erosion rates than expected based on hydrodynamic conditions alone.

In this chapter, the results of a series of experiments conducted with three different sizes of non-cohesive sand, d_{50}=160 μm, d_{50}=500 μm, and d_{50}=1200 μm are presented. Supplemental investigations testing the stability of a sand cap with similar specifications to that placed at the Anacostia demonstration site are also included. The results are presented within the framework of an interaction of fundamental forces acting on a bed particle. Results from previous investigations are also compared to the present results to the extent possible. Interpretation of the results will provide a clear insight to the effect of vertical pore water movement on the bed stability which would in turn provide a stability design criteria for the sand caps employed in contaminated sediment remediation strategies.

For the experiments, a constant head water supply is provided at the bottom of the sand bed to provide different rates of vertical water movement through the sediment bed for either injection (vertical pore water flux into the water column) or suction (vertical pore water flux into the bed) conditions. The influence on the critical shear stress for initiation of motion is compared to the zero pore water flux condition in order to determine the magnitude of vertical hydraulic gradient required to produce a significant change in the critical shear stress.

4.1. Incipient Motion Criteria and Calculation of Bed Shear Stress

Incipient motion is defined as the condition where the grains forming the bed are dislodged and set into motion. It is assumed that the movement is very small and can be detected visually or by extrapolating the bed-load transport curve to a shear stress level that bed-load movement ceases. The benchmark study conducted by Shields (Buffington, 1999) also reports these two different methods to define incipient motion criteria. As Shields' work is derived from different descriptions in textbooks and journal articles, it is not well understood which method he actually used during his studies. However, he noted that in case of a bed with mixed grain sizes, the beginning of movement can not be established by the extrapolation method because of the possible early mobilization of finer particles. Various other investigators followed different approaches to identify incipient motion which can explain some of the variation in results. Kramer (1935) defined the weak movement of sediment which seems to agree with Shields' critical condition. Yalin (1976) tried to minimize uncertainty related to visual observations and defined the incipient motion criterion using a non-dimensional number relating the number of detachments per area of observation and time of observation. At incipient motion, this number needs to be maintained as a constant finite number close to zero.

In this study, several preliminary experiments were conducted in order to determine an incipient motion criterion providing the most consistent results. These experiments were conducted with locally produced sand that had been sieved to separate into different size fractions. Working with one size fraction initially, it was found to be difficult to obtain consistent results for initiation of motion using a criterion based on visual

observations. Additional experiments were conducted with a commercial grade of uniform quartz sand. After further experimentation with these sand blends, it was discovered that the initiation of motion could be consistently defined by running an experiment at a given shear stress level for an extended period of time and noting when ripples began to form on the sediment bed surface. Once ripples started to form, local variations in shear stress due to the evolution of the bed forms caused a more rapid ripple development, creating a clear threshold condition. At each shear stress level, running the experiment for 15-20 minutes was observed to be long enough to identify ripple formation. It is noted that this approach uses yet another definition of initiation of motion than the ones mentioned previously, but one which was well defined in terms of experimental observations. As described further below, it also gives results consistent with Shields curve. All of the subsequent experiments were performed with commercial "uniform" sands which could be considered as beach sand or more rounded than the angular sands from local glacial deposits. Observations suggest that the angularity of the sand has some effect on the initiation of motion but that effect was not explored systematically in this research. Later experiments with the material comprising the "sand cap" were conducted with angular local sands and this difference may somewhat influence the observed results.

For the injection and suction experiments, in addition to the advective flow, different rates of injection or suction were applied to the bed to determine the effect on the critical shear stresses. Initiation of motion was identified once again by observing the ripple development on the bed surface. In previous studies, the influence of pore water flux on sediment beds was investigated using seepage velocity as the defining criterion. However, it is known that if a quick condition exists over a sand bed at a vertical upward hydraulic gradient of 1, then there should be no shear resistance to the sand. Thus, in data analysis, hydraulic gradient should be a more relevant parameter. Figure 4.1 presents the relationship between the injection flux (velocity) through the bed grains, I computed using the measured injection rates and the measured hydraulic gradient, i for three different sand sizes where d_{50} represents the median grain size. These approximate relationships were confirmed by independent sand permeability tests. It was difficult to

measure precisely the gradient for the suction experiments as it varied depending on the consolidation degree of the bed over the duration of the experiment. Therefore, average suction hydraulic gradients were determined using the relation computed for the injection cases relating them to the metered suction rates. Details regarding the experimental setup are given in Chapter 3.

In the literature, investigations considering the stability of non-cohesive sediment beds address the initiation of motion conventionally expressed by the Shields curve (e.g., Vanoni, 1975; Rao and Sitaram, 1999) that outline the initiation of motion criteria in terms of the two dimensionless parameters as

$$\tau_* = \frac{\tau}{(\gamma_s - \gamma)d} \quad \text{and} \quad \mathrm{Re}_* = \frac{u_* d}{\upsilon} \tag{4.1}$$

in which τ is the bed shear stress, γ_s and γ are the unit weight of sediment and water, respectively, d is the effective sediment diameter, u_* is the shear velocity defined by $\tau = \rho u_*^2$ and υ is the kinematic viscosity of the fluid. A moment balance analysis considering three principal forces acting on an idealized (spherical) non-cohesive sand particle: the drag force F_D, the submerged weight of the particle F_W and a lift force F_L leads to the derivation of τ_*. Flow normal to the bed may be included as a seepage force F_J in this balance (Figure 4.2). Here drag force, lift force and upward directed seepage force produce destabilizing moments. In case of suction, the seepage force is reversed which would stabilize the particle. The forces acting on the sand particle can be formulated as

$$F_W = \frac{4}{3}\pi\left(\frac{d}{2}\right)^3 (\gamma_s - \gamma) \tag{4.2}$$

$$F_D = C_D \pi\left(\frac{d}{2}\right)^2 \frac{\rho u^2}{2} \tag{4.3}$$

$$F_L = C_L \pi \left(\frac{d}{2}\right)^2 \frac{\rho u^2}{2} \tag{4.4}$$

$$F_J = \frac{4}{3}\pi \left(\frac{d}{2}\right)^3 \gamma i \tag{4.5}$$

where u is a local velocity in the vicinity of the sphere, C_D and C_L are drag and lift coefficients, respectively. In this formulation the seepage force is assumed to be produced by a linear pressure gradient deviation from hydrostatic conditions (i) and this linear pressure gradient produces a force similar to the buoyant force and in the same direction in the case of injection. Since the forces due to both linear pressure variations act through the center of volume of the sediment particle, regardless of actual shape, the effect of the seepage force can be directly incorporated into a modified definition of τ_* although possibly with a correction factor to account for the local variation of the head gradient at the sediment/water interface such as suggested by Martin and Aral (1971). This latter approach assumes that a simple constant correction of the piezometric head gradient within the sand bed can be used to estimate the local gradient at the sediment/water interface where the particle is dislodged.

Since the various forces listed above are not in the same direction, a moment balance is required to determine the condition for neutral stability. For the moment balance analysis, an assumption is required to specify the moment arm which would basically depend on the specific packing arrangement of the idealized spherical sand particles. However, the moment arm about the particle contact point can be considered to be proportional to the particle diameter without loss of generality. Another assumption needs to be made to specify the local velocity used in the drag and lift forces. Modifications are also required for non-ideal particle shapes. Nevertheless, the Shields' formulation can be derived under the assumption that the local velocity, u at a distance z from the bed is related to the shear velocity u_* by the logarithmic velocity profile for a hydrodynamically rough boundary as

$$\frac{u}{u_*} = \frac{1}{\kappa} \ln \frac{z}{k_s} + 8.5 \tag{4.6}$$

where $\kappa =$ von Karman constant which has a value of approximately 0.4; $k_s =$ equivalent roughness height, $z =$ vertical distance from the boundary (Olson and Wright, 1990). For hydrodynamically smooth boundaries, this formulation requires consideration that sediment transport is initiated by the process of turbulent bursts and streaks in order to presume the same velocity scaling for the local velocity. Under the assumption that the local velocity scales with the shear velocity, a moment balance derived considering the forces acting on a non-spherical sediment particle would yield the following relationship:

$$\rho u_*^2 \propto (\gamma_s - (1 + Si)\gamma) d \tag{4.7}$$

where S represents an adjustment to the internal hydraulic gradient within the sediment bed representing the effect of the altered flow pattern at the sediment/water interface as proposed by Martin (1970), and Martin and Aral (1971). They suggested that the seepage force experienced by the particles comprising the uppermost sediment layer would be different from that for the particles more than several layers deep because of the difference in flow pattern associated with the flow moving through the interface. Martin and Aral considered a different force balance applied to the whole bed rather than individual particles. They used the void ratio of the sediment bed to describe the surface area exposed to shear by the flow. Thus, their correction factors must be modified by the factor $1 - n$ with n being the bed porosity in order to be consistent with the present formulation. By converting their adjustment factors to a factor that could be used in the moment analysis explained above considering the individual particles and then excluding the physically unrealistic high values ($S > 1$), the average S value was estimated as 0.85 from an arithmetic average of the individual values from all their experiments. It is noted that minor changes on this coefficient did not have a significant effect on the current results as will be shown later in this chapter. Finally, this formulation suggests a modified Shields' parameter τ_{*m} as

$$\tau_{*m} = \frac{\tau}{(\gamma_s - \gamma(1 + Si))\, d} \tag{4.8}$$

such that in the absence of pore water flux where $i = 0$, it reduces to the conventional Shields parameter. From Equation 4.8, it can be seen that i must be fairly large, say greater than about 0.1, in order to have an effect on bed stability.

There are several methods available for the evaluation of bed shear stress. A conventional application would involve derivation of τ from bulk flow parameters including a resistance coefficient if they can be determined accurately. Another typical method is to compute bed shear stress by fitting the logarithmic law of the wall to the measured velocity profiles. If it is possible to measure the water surface slope S_W, then bed shear stress can be computed according to $\tau = \gamma h S_W$ where h is the water depth for a wide channel. Still another way is to use a Preston tube which would involve measuring the local dynamic pressure and relating it to the bed shear velocity by the assumption of near wall logarithmic velocity profile. When the Reynolds shear stress profile is available, the bed shear stress can also be estimated by extrapolating it to the boundary. However, it is essentially impossible to make direct accurate measurements of bed shear stress, especially in the presence of vertical pore water movement. Therefore the bed shear stress needs to be inferred by indirect measurements and the results may be significantly dependent on the specific assumptions employed in the analyses. All of the methods listed above rely on the assumption of uniform flow. In all of these methods, the derived bed shear stress would need to be adjusted for the effect of injection or suction. Furthermore, as described in Chapter 3, the experiments were performed for conditions of a developing boundary layer even in the absence of suction or injection and the flow is therefore not spatially uniform.

A significant issue to be considered in the bed shear stress computations is that in a straight flume, there is a region of boundary layer growth starting from the channel inlet and, depending on the flume length and the water depth, the turbulent boundary layer will not be fully developed at the test section. Consequently, the flow will not be uniform. In

order to resolve this issue, a water depth as low as a few centimeters could be chosen to perform the studies (e.g., Rao and Sitaram, 1999). Although this issue was recognized in the design of the experiments conducted for this study, it did not seem realistic to conduct experiments with shallow depths as it may alter the turbulence characteristics relative to typical prototype conditions. Therefore, a decision was made to perform experiments in which there was a developing boundary layer. According to standard boundary layer theory, the bed shear stress decreases with downstream distance (Schlichting, 1979). However, if the test section is sufficiently far downstream from the channel inlet, the variation of the bed shear stress even over the 2 m long test bed over which the experiments were performed should be sufficiently small so as not to impact the experimental results significantly. This was consistent with the experimental observations; if the longitudinal variation of shear stress were important, the observation of initiation of sediment transport should be confined to the upstream end of the test bed. However, the visual observations of initiation of motion indicated that the locations where sediment transport began to occur could be anywhere along the test bed and perhaps more related to minute imperfections of the bed surface.

In this study, it was decided to determine bed shear stresses based on measurements of Reynolds stresses with an Acoustic Doppler Velocimeter (ADV). Although there are several issues with this approach as discussed further below, this methodology does at least rely on local measurements made near the bed surface and should be subject to the least uncertainty. ADV measurements provide instantaneous velocity components in three dimensions and therefore the velocity profile above the center of the sediment bed can be obtained. It is also possible to measure Reynolds stress which is proportional to the turbulent shear stress using a statistical analysis of velocity fluctuations. However, it is not possible to take measurements close to the bed with an ADV probe. The ADV probe used has a sample volume of a cylinder roughly 1 mm in horizontal diameter and 9 mm in height. Once the center of the sample volume is within approximately 0.5 cm above the bed surface, a portion of the sample volume is located within the bed and therefore the measurement is not valid. Thus, the probe can only measure down to about 0.5 cm above the bed and the bed shear stress needs to be computed from the available

Reynolds stress profiles. However, as the bed surface is approached, the turbulent stress is only a fraction of the total shear stress and some methodology to estimate the bed shear stress would need to be employed even if the probe could measure down to the surface.

For a two-dimensional uniform flow, an elementary force balance indicates that the shear stress distribution must be linear from zero at the free surface to the maximum value at the bed (dashed line in Figure 4.3b). The Reynolds stress profile for a turbulent flow is indicated by the solid line in the same figure. Computation of the bed shear stress from the Reynolds stress profile usually involves extrapolation of the profile to the channel bottom. In the case of a developing turbulent boundary layer as employed in this experimental investigation, the Reynolds stress profile cannot be linearly extrapolated to the wall because of characteristics of the profile having a stress free region outside the boundary layer (basically zero Reynolds stress) and a sharp gradient towards the wall (Figure 4.3a). The most relevant parameter that could be utilized in the bed shear stress estimation here is the maximum Reynolds stress in the profile which will be assumed to be proportional to the boundary value as in uniform flow. It is known that for a uniform flow the maximum Reynolds stress is approximately 75-85% of the extrapolated bed shear stress suggested by the data reported in previous studies regardless of the boundary roughness or presence of injection or suction (Prinos, 1993; Nikora and Goring, 2000; Dey and Cheng, 2005). Because of the nature of the profile indicated in Figure 4.3a, it is expected that the maximum Reynolds stress would be a smaller fraction of the bed stress and it is assumed that for the particular measurements at a fixed location along the channel and a relatively small range in velocity, the fractional value can be approximated as a constant to be determined in the analysis that follows.

A procedure consisting of a series of calculations was developed to estimate bed shear stress. The ultimate purpose of this procedure was to be able to calculate bed shear stress from ADV measurements in a practical and reasonably accurate way. If the ADV measurements were taken in close proximity to a sediment bed, the local turbulence created by the wake of the probe might disturb the bed surface and alter the measurement results. It may also be possible that having a porous sediment bed as a boundary has some

effect on reflection of the acoustic waves, thus on measurements. Therefore, several sets of ADV stream-wise velocity profiles were taken at the middle of the test section on a rigid boundary at different discharge values. The locations of ADV sampling volumes along the vertical cross section of the flow were chosen so that representative profiles can be formed from the collected data. In addition to the average three dimensional velocity measurements, the covariance of the velocity fluctuations can be calculated with a statistical analysis by the use of the ADV data (Table 4.1) as

$$Cov(XZ) = \overline{u'v'} \tag{4.9}$$

where u' and v' are the velocity fluctuations in the longitudinal and vertical directions. Then, a local shear stress, $\tau_{\exp}$ close to the bed can be computed using the maximum covariance of the profile as

$$\tau_{\exp} = -\rho Max.Cov(XZ) \tag{4.10}$$

The covariance is a direct output of the data analysis program used to compute velocity and turbulence statistics from a sample measurement. The maximum measured covariance was selected avoiding the issue of where specifically to take a measurement along the vertical cross section of the flow, especially in the case of injection or suction which alters the velocity profile, potentially displacing the maximum value from the location observed in an experiment with no pore water seepage. It is presumed that covariance profile data collected captured the maximum covariance or a value very close to the maximum. The shear stress calculated using Equation (4.10) needs to be modified in order to estimate the shear stress at the bed level. The Blasius equation can be utilized for this purpose which is an empirical formulation to calculate the bed shear stress, τ_0 for developing turbulent boundary layers on smooth flat plates. With this formulation, the bed shear stress (Olson and Wright, 1990) is defined relating free stream velocity, u_s and distance along the flume, x as

$$\tau_0 = 0.03 \rho u_s^2 \left(\frac{\upsilon}{u_s x} \right)^{1/5} \tag{4.11}$$

and in terms of local boundary layer thickness δ, the bed shear stress is expressed as

$$\tau_0 = 0.0233 \rho u_s^2 \left(\frac{\upsilon}{u_s \delta} \right)^{1/4} \tag{4.12}$$

where δ, for a turbulent boundary layer is given as

$$\delta = \frac{0.382x}{(u_s x / \upsilon)^{1/5}} \tag{4.13}$$

At the upstream end of a flat plate, the boundary layer is laminar and therefore the turbulent boundary layer relation may not be applied over the entire upstream end of the flume. Therefore, it was necessary to estimate the location of the transition from laminar to turbulent boundary layer. In the literature supported by observations, the transition from laminar to a turbulent boundary layer is reported to occur when the longitudinal Reynolds number is approximately 3.5×10^5 to 5×10^5 (Schlichting, 1979). The transition Reynolds number, Re_t can be defined as

$$\mathrm{Re}_t = \frac{u_s x_t}{\upsilon} \tag{4.14}$$

where x_t is the distance from the inlet of the flume to the transition location for the purposes of this study. For this experimental setup, it was estimated that the transition was located where the Reynolds number was approximately 4.5×10^5. This was determined by a trial and error procedure. First, a transition Reynolds number is assumed which determines the transition distance, x_t from Equation (4.14) and then a laminar boundary layer thickness at the transition point can be computed as

$$\delta_t = \frac{4.91 x_t}{\mathrm{Re}_t^{1/2}} \tag{4.15}$$

The effective origin of the turbulent boundary layer is located a little further upstream of the transition location. If the computed laminar boundary layer thickness at the transition point is plugged into Equation 4.13 (matching laminar and turbulent boundary layers at the transition), then it is possible to determine the distance between the effective origin of the turbulent boundary layer and the transition point. Using the distance from the effective origin of the turbulent boundary layer to the measurement location, the turbulent boundary layer thickness can be calculated by Equation (4.13). Once this value is compared to the boundary layer thickness estimated from the ADV velocity profile measurements, the assumed Reynolds number is modified until the computed and estimated boundary layer thicknesses match. After the transition Reynolds number and thus the location of the transition are defined, the bed shear stress can be computed using Equation (4.12).

As explained previously, the Reynolds stress obtained by the ADV measurements would be assumed to be proportional to the bed shear stress. The ratio between the shear stress derived from the measurements and the bed shear stress calculated from the empirical turbulent boundary relationship has been calculated as 0.60 on average (Table 4.2) for the measurements over the solid boundary. The individual values in the table deviate only a little from the average value with a few exceptions that appear to be associated with measurement error and therefore it appears reasonable to estimate the bed shear stress in the flume with no suction or injection as

$$\tau = \frac{\tau_{\exp}}{0.60} \tag{4.16}$$

In the case of vertical pore water transport, especially if the rate is high, the final bed shear stress above needs to be modified due to momentum transfer associated with the inflow (Cheng and Chiew, 1998a; Maclean, 1991). Considering the momentum exchange

between the flow and the sand bed in the presence of suction or injection, the bed shear stress can be computed by

$$\tau_i = \tau - \rho u I \tag{4.17}$$

where I is the injection or suction flux (velocity) and u is the local stream velocity at the bed level. I can be calculated as

$$I = \frac{q_i}{A} \tag{4.18}$$

where q_i is the metered injection or suction rate and A is the bed surface area. The sign convention is positive for injection velocity and negative for suction velocity. $\tau_{\exp}$ that is used in the computation of τ in Equation (4.17) is taken from the Reynolds stress profiles measured over the sand bed in the presence of injection or suction depending on the specific experiment. However one final issue still remains since the local stream-wise velocity at the bed where the vertical velocity is taken to be I is not measured. One additional approximation is required to complete the analysis.

The local stream velocity at the bed level utilized in Equation (4.17) can not be measured directly because of the ADV probe's limitations. Thus, it is required to be estimated from the velocity measured at a small distance from the boundary (generally on the order of 0.5 cm). Extrapolating the logarithmic velocity profile to the bed level would be the best approximation in this case although the flow is not uniform. In the development of relations for standard flat boundary layer such as Equations (4.11)-(4.13), an assumption is made implying that the velocity profile behaves as if it is locally uniform within the boundary layer. Consequently, the velocity profile in a two-dimensional flow is usually considered to follow the logarithmic velocity distribution given by Equation (4.6) which applies to hydrodynamically rough walls. In this study, however, the boundaries span hydrodynamically smooth to rough, depending on the grain size studied. As the injection or suction velocities for smaller grain size beds are much

lower than those for d_{50}=1200 μm, assuming that the same velocity profile is valid for every case would not result in a bad approximation of the bed shear stresses estimated by Equation (4.17). In order to take into account the effect of injection or suction on the stream-wise velocity, a modification to the logarithmic law for the velocity profile was proposed by Cheng and Chiew (1998b) which has a similar form to the one proposed by Schlichting (1979) and it is given by the following:

$$\frac{u}{u_*} = \left(\frac{1}{\kappa}\ln\frac{z}{k_s} + 8.5\right) - \frac{I}{4u_*}\left(\frac{1}{\kappa}\ln\frac{z}{k_s} + 8.5\right)^2 \tag{4.19}$$

Then, using Equations (4.6) and (4.19), the average stream-wise velocity measured by the ADV close to the bed can be extrapolated to the bed level where $z = 2k_s$ which was selected somewhat arbitrarily but consistent with the literature and $k_s = d_{50}$. Equivalent roughness height, k_s could also be defined in different ways such as using $3d_{90}$ suggested by van Rijn in 1984 which will be investigated in the next section or d_{65} suggested by Einstein (Vanoni, 1975) which is not much a different value compared to d_{50}.

4.2. Results and Discussion

Several previous experimental studies were conducted to investigate the role of injection and suction through a porous stream bed on the resistance to bed erosion. Contradictory findings have been reported as the results of these studies. For example; while Oldenziel and Brink (1974) and Cheng and Chiew (1999) noted a tendency for decreasing bed stability for increasing injection rates and the opposite tendency with increasing suction rates, experimental results reported by Rao and Sitaram (1999) indicated that suction reduces the stability of the bed particles whereas injection does the opposite. In this study, it was intended to understand the reasons for these conflicting conclusions and some probable causes have been identified by investigating the experimental procedures and the procedures used in the data analysis. One issue which is

related to the experimental investigations is the water depth chosen to be worked with. In order to conduct the experiment in a straight flume with a fully developed turbulent boundary layer, some researchers performed studies with a water depth as low as 2-3 cm (e.g. Rao and Sitaram, 1999). An implication of this is the altered turbulence characteristics associated with the low bulk Reynolds numbers of their flows, making it difficult to generalize the results. More importantly, it appears that the major issue is the selection of the method used in computation or indirect measurement of bed shear stress. The specific assumptions employed in previous analyses appear to significantly affect the results and it also appears that some of the previous studies did not estimate the bed shear stresses accurately, potentially leading to incorrect conclusions.

Before making any attempt to draw some conclusions from the results of this investigation, in order to clarify some of the issues in advance, it is useful to explore the effect of suction and injection on velocity and Reynolds stress profiles of the flow. For this purpose, a series of velocity profiles were measured for flows with and without vertical flux through the sand bed. The results of some typical experiments are provided in Figures 4.4 to 4.7. An anomaly is observed in the velocity profiles presented here and also in some other profiles recorded either for measurements around 30-40 cm/s or at a depth 3-4 cm above the bed. This is not a real effect and it is believed that this is due to an unknown artifact of the ADV probe and has been observed in other studies measured with the same model of ADV probe. The measured velocity profiles demonstrate the intuitive result that when the pore water flow is upwards into the free stream flow, the lower velocities near the bed are pushed further out into the flow. Similarly, when there is suction into the bed, higher velocities persist closer to the bed surface as the lower momentum flow near the boundary is removed from the main flow. The two sets of measurements contain velocity profiles where the free stream velocity is similar in a case without suction or injection and in experiments with high injection or suction rates. This result implies that if one used the surface velocity or the discharge to characterize the flow (e.g., to estimate the bed shear stress from the Manning equation), injection into the flow will actually serve to reduce the bed shear stress at a common surface velocity or discharge compared to a zero injection condition. It is believed that this situation has led

to confusion in the past in discussions on the influence of bed injection or suction on sediment stability. Since most accepted bed stability criteria are shear stress based, it is irrelevant how the velocity or discharge required to initiate sediment transport varies with injection or suction; the only thing that is important is how the shear stress varies. Thus it was observed during this experimental investigation that sometimes a greater discharge was required to initiate sediment motion but at the same time, a lower estimated bed shear stress was experienced and therefore by shear stress-based criteria, the bed is less stable. It is certain that a vertically upwards pore water flux results in an upwards piezometric pressure gradient since this is a key aspect of elementary theory of flow in porous media. Therefore one would intuitively expect that injection decreases bed stability while suction increases it.

Figures 4.8 to 4.11 provide partial support for this argument. In these figures, plots of the profiles of the covariance of the vertical-longitudinal velocity fluctuation correlations are presented for the same experimental conditions as shown in Figures 4.4 to 4.7, respectively. The covariance is proportional to the Reynolds stress which is the turbulent shear stress and the results clearly show that at the same free stream velocity injection increases the local turbulent shear stress while suction decreases it. The effects are more pronounced the larger the hydraulic gradient. This observation describing the effect of suction on Reynolds stress was also implied by Schlichting (1979) who suggested that suction reduces the boundary layer thickness and a thinner boundary layer is less prone to become turbulent. Prinos (1995) also studied numerically the effects of bed suction on the structure of turbulent flow by solving the Reynolds-averaged Navier-Stokes equations supported by the experimental data by Maclean (1991) and reported the same behavior of decreased turbulent shear stress in case of bed suction.

These results are counter to some of the qualitative behavior discussed in the literature (e.g, Cheng and Chiew, 1998a) on the role of suction or injection on bed shear stress and this may have led to some of the contradictions in the literature on bed stability in experiments with pore water seepage. One could argue that in the case of injection the smaller local velocity gradient due to the displacement of a given velocity further out into

the flow would indicate a smaller bed shear stress; nevertheless this would only be valid for a laminar flow where the bed shear stress is dominated by the laminar flow effects that are directly proportional to the velocity gradient. In this study, even for experiments when the turbulent shear stress was lowered due to suction, the flow was still turbulent over the test section as the free stream velocity was not affected by the suction rates. This implied that bed shear stress was dominated by the turbulent characteristics of the flow.

The bed shear stresses corresponding to the conditions when the incipient motion was observed were computed employing the procedure explained above in cases of suction, injection and in the absence of any injection or suction. The results are given for d_{50}=160 μm, d_{50}=500 μm, and d_{50}=1200 μm in Table 4.3. In order to clearly identify the effect of seepage on bed stability, relatively high injection and suction hydraulic gradients that may not commonly exist in natural systems were applied to the beds. Since the range of gradients examined were similar for all three sand sizes, the actual seepage velocities will vary considerably (see Figure 4.1). A possible question of whether bed hydraulic gradient or seepage velocity is the key parameter controlling bed stability can be readily evaluated from the results of these experiments. The results corresponding to the suction experiments for 500 μm are not included here since no ADV measurements were taken to be used in the computation of bed shear stresses. Those results will be considered further below, however. The sand blend that has specifications similar to the sand cap used in the Anacostia River with median grain size of 340 μm was also tested for stability under the effect of advective flow-induced shear stress. Injection rates matching the field conditions were applied on this sand only for the purposes of resuspension experiments reported in Chapter 5. The maximum injection gradient applied according to the reported field conditions was only in order of 5-6% of the minimum hydraulic gradient applied to the rest of the non-cohesive sediments and according to Equation 4.8, should have a negligible effect on bed stability. Computed bed shear stresses versus applied hydraulic gradients for all beds with different median grain sizes are given in Figure 4.12. It can be seen from the data that for all the sand sizes suction tends to stabilize the bed and injection does the reverse as implied by the elementary force balance presented earlier. This result is also consistent with the results of direct Reynolds stress measurements

noted previously. When the bed consisted of large grain sized sediments such as 1200 μm, in order to observe an effect of the suction or injection, pore water fluxes were increased to relatively high levels but with velocities still well below 1% of the free stream velocities.

An investigation was made regarding the assumption for the equivalent roughness height, k_s in the computation of bed shear stresses for the cases of injection or suction. According to the assumption implemented in this analysis, k_s was approximately equal to d_{50} and the level of the bed was defined at a distance of $2k_s$ from the boundary. Additional computations have been performed on the data for the 1200 μm sand bed to demonstrate the most extreme of a potential influence on the results due to this assumption. This sand bed involved relatively high injection and suction velocities which were incorporated into the bed shear stress calculations through Equation (4.17) and any assumption made in the process of the bed shear calculations for this sand bed would potentially affect the results the most. In order to make an assessment, $k_s = 3d_{90}$ has been considered which was suggested by van Rijn in 1984. Then the bed level was assumed to be at the distance where the ADV data were collected closest to the bed since $3d_{90}$ was a quite large value for equivalent roughness height. By this way, it was basically not necessary to extend the logarithmic velocity profile to the bed to determine the velocity at the bed level as measurements were made close to this distance from the bed. The results given in Figure 4.13 show somewhat significant influence on the injection cases but not altering the general nature of the conclusions. Apparently, although the conclusions are not affected by this assumption, the magnitude of the bed shear stresses might be affected sufficiently to change the specific values computed.

For comparison purposes, the well-known Shields curve defined by his experimental data and modified by additional data over the years can be drawn by segments (Figure 4.14) which are approximate piece-wise relationships defined by Bonnefille (Raudkivi, 1998) or by van Rijn (1984) and the details of these relationships are given in Appendix A.4. Many other researchers conducted experiments investigating non-cohesive sediment

bed stability in an attempt to clarify some of the questionable aspects of Shields' work and Yalin and Karahan (1979) compared Shields curve to various researchers' data including theirs. When the data provided by them are plotted on a graph, an extended Shields curve can be formed. Figure 4.14 shows Shields curve defined by Bonnefille's and van Rijn's relationships and its extension by using the experimental data provided by Yalin and Karahan. When the data collected in this study are incorporated into this graph (but without the modified shear stress incorporating the bed hydraulic gradient defined in Equation (4.8)) after the necessary computations, it is seen that the results show some scatter that appears to be somewhat greater than traditionally observed in some experiments without suction or injection. However the trends for individual grains sizes, especially the 160 and 1200 μm sizes don't follow the general trends of the Shields curve. The dimensionless shear stress is then modified to account for the effects of suction and injection (Equation (4.8)). Table 4.4 and Figure 4.15 demonstrate the results of the modification using a value of 0.85 for the S coefficient suggested by Martin (1970), and Martin and Aral (1971). Computation of the modified Shields parameters eliminate much of the scatter in the data but even more importantly, the data for individual grain sizes tend to follow the general trends of the Shields curve much better than the un-modified data in Figure 4.14. The data for d_{50}=1200 μm lie below the Shields curve but basically parallel to it. This may be due to the fact that the grain size distribution is fairly broad for that particular sand and smaller grain sizes in the distribution are responsible for the observed initiation of motion. Figure 4.16 is presented to show that some variation in the S value (e.g., 1 or 0.65) does not change the presented results significantly.

There are a number of assumptions that were employed in the determination of the bed shear stress used in the computation of the modified dimensionless shear stress and the grain Reynolds number used in the modified Shields curve. It is likely that a more rigorous determination of a procedure to determine the bed shear stress would result in better agreement with the traditional Shields curve, but there is a fair disagreement in the literature regarding even what the Shields curve is supposed to be. The presented results are considered satisfactory in verifying the methodology for incorporating the effects of

suction or injection on bed stability with a straightforward and simple modification of the traditional dimensionless shear stress used in the Shields curve.

The framework for determination of the initiation of motion for non-cohesive sediment beds presented in the preceding sections is supported by the experimental observations, subject to the uncertainties associated with the determination of the bed shear stresses from the measured turbulence. However, these results do not provide a framework to typical applications since the types of measurements collected in this study will not generally be available. There is a requirement for the development of a methodology to start with data or predictions that would be commonly available (i.e. for sediment beds without seepage) and extend that information to apply for application with higher rates of suction or injection. Typical applications would have measurements available of the variation of discharge and water depth or else predictions of discharge and water surface elevation (given the channel geometry). This data can be used to compute a bed shear stress τ that is appropriate in the absence of injection or suction through the use of the Manning equation or other resistance relations. In order to estimate the bed shear stress with suction or injection τ_i, it is necessary to develop a relationship between τ_i and τ as a function of relevant flow variables.

A common approach is to assume that this ratio is a function of the momentum contained in the injection flow relative to the free stream momentum (Turcotte, 1960; Cheng and Chiew, 1998a). The ratio of these two momentum fluxes should be a primary variable influencing the flow at the bed although there may be other factors that influence the flow behavior. The ratio of the fluxes per unit area is simply I/U where I is the injection or suction velocity through the bed and U is some characteristic velocity describing the free stream flow. The data from the current study for the 1200 μm sand are used to explore the functional dependence since it involves the data that cover the widest range of the velocity ratio. The bed shear stress τ is computed from the relation in Figure 5.1 developed for flow over a solid surface as explained in Section 5.1.1. Although the data are somewhat limited, Figure 4.17 indicates a fairly consistent relation among these

data. In this analysis U is taken as the measured free stream velocity. Cheng and Chiew (1998a) also performed a somewhat similar evaluation but only for flows with bed injection. Their Figure 15 shows quite a bit of scatter in the individual data but a smooth curve is estimated through these data. Their smooth curve is reproduced on Figure 4.17 and is seen to be quite consistent with the data from the current study where they overlap. A second order polynomial is fitted through the data for 1200 μm sand, yielding the relation

$$\tau_i / \tau = 1.23 - 152(I/U) + 10181(I/U)^2 \tag{4.20}$$

In principle, the leading constant should be 1.0 when $I = 0$. This is likely to be slightly greater due to the greater shear stress over the rougher sand bed surface compared to the original solid boundary from which Figure 5.1 was developed. Some improvement in prediction could be achieved by making an adjustment to account for this effect but neglecting the effect will have only a small influence on the subsequent results. The computational procedure in the following comparisons will be to compute the bed shear stress τ in the absence of injection or suction by a means appropriate to the particular data and to use Equation 4.20 to transform it to an estimate of bed shear stress including the effects of bed seepage. The hydraulic gradient through the bed i as well as the seepage velocity I will be either provided or estimated from the available data in order to make this computation.

A survey of the literature indicates limitations in all of the available data in order to perform the intended comparison with the exception of the data collected in the present study. It is noted that there are two additional experiments involving bed suction with the grain size of 500 μm for which ADV Reynolds stress measurements were not performed but which are included in the following comparison. Experiments by Rao et al. (1994) include measurements for both bed injection and suction but do not specifically include observations of the incipient motion condition. Rather, they classify individual experiments as to whether there was observable bed transport or not. It would be possible to take the two experiments closest to the incipient motion condition and compare where

they fall on the modified Shields curve, but for some grain sizes there are considerable differences between the flow conditions for the two experiments, rendering a definitive conclusion relatively meaningless. Cheng and Chiew (1999) made observations for experiments with bed injection only. Unfortunately, they only report the depth to which the maximum measured velocity was observed instead of the total water depth. Preliminary computations using this depth as representative of the total flow depth gave results that were consistent with a too small water depth and the results of this study were not analyzed further. Rao and Sitaram (1999) provide data for observations of incipient motion for experiments with either bed suction or injection and thus appear to be the most meaningful results available for comparison. Their data do not include measurements of the hydraulic gradient through the sediment bed so it needed to be estimated. There are other less useful aspects to their data. They performed experiments with fairly small flow depths, down to as small as 2-3 cm in some instances and this may have influenced their results. Also, in their study, they considered seepage velocity to be the critical variable in determination of bed stability so maintained this value roughly constant over the range of sand sizes (0.58-3.0 mm) considered in their study. This resulted in somewhat significant hydraulic gradients for the smallest sand size but increasingly smaller values as the grain size increased, and the effect of hydraulic gradient through the bed becomes negligible with the large grain sizes. However, since this is the most comprehensive data set to compare the proposed methodology (with the exception of the current data) these data will be utilized in the comparison.

An initial comparison is made with the current data set, including the suction data for the d_{50}=500 μm. The analysis is quite straightforward in this case since all of the parameters required for the analysis are available. The measured free stream velocity was used as the characteristic velocity U in the analyses. The results of the analysis are presented in Figure 4.18. This presentation of data is comparable to the results presented in Figure 4.15 with the data appearing somewhat more consistent due to the smoothing effect of the data fit in Equation 4.20. Since Equation 4.20 was obtained with the use of the 1200 μm data, one would expect it to appear similar, but the two smaller grain sizes provide a level of confirmation for the proposed approach. One would observe better

agreement for the two smaller grain sizes if the constant 1.23 in Equation 4.20 is replaced by 1.0 in order to reproduce the correct behavior for zero bed seepage as indicated in Figure 4.19.

The data of Rao and Sitaram (1999) require some transformations in order to perform a comparison of the proposed methodology. First of all, the data in that study include values for mean velocity and depth. Because of the very small depths, the bed shear stress was predicted using the Darcy-Weisbach equation (Equation 9-5b in Olson and Wright, 1990) for fluid resistance together with the Haaland equation (Equation 9.18 in Olson and Wright, 1990) to predict the friction factor which is applicable for a wide range of Reynolds numbers and relative roughness. The equations were used with the hydraulic diameter equal to $4A_0 / P$ with A_0 the cross sectional area and P the wetted perimeter. The mean flow velocity was used as the characteristic velocity in Equation 4.20 to estimate the actual bed shear stress. Finally, the hydraulic gradient was estimated from the given grain size and bulk flow velocity through Darcy's law and the approximation that the hydraulic conductivity (m/s) could be related to the grain size (mm) by $k = 0.005d^2$. This latter approximation is consistent with estimating equations provided in the literature (e.g., Bear, 1979). It is also consistent with the measurements collected in this study and with the data reported by Cheng and Chiew (1999). When these data are transformed in this fashion, they agree fairly well with the results of the current study as indicated in Figure 4.20. Given the limitations in the Rao and Sitaram data, this level of correspondence with the modified Shields curve is considered to be quite acceptable.

The data collected during this study and the presented analyses clarify many issues related to data interpretation and conclusions reported in previous studies including several contradictory ones. It has been understood that it is crucial to examine bed stability by evaluating the critical bed shear stress in a way that all the different effects of seepage either on the flow or on the sediment bed particles are considered together. Bed shear stress needs to be determined by accounting for the effect of seepage properly. Commonly used bed shear stress computation methods are not valid when there is seepage mostly because the flow is not uniform. Either in a lab study with measurements

of Reynolds stresses or in a more typical application where for example; discharge and water depth is known, it is possible to compute bed shear stress in the presence of seepage using the methodology suggested in a relatively simple way. Application of the proposed methodology on the data provided by Rao and Sitaram (1999) showed that their measurements and observations are in fact consistent with the results of this study.

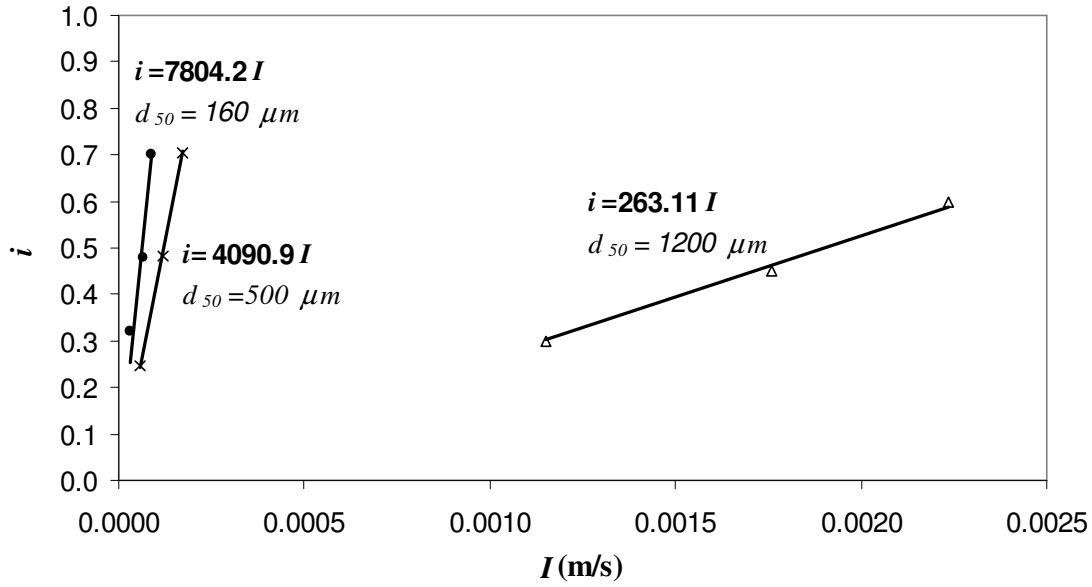

Figure 4.1: Seepage flux versus hydraulic gradient plot for different sand sizes.

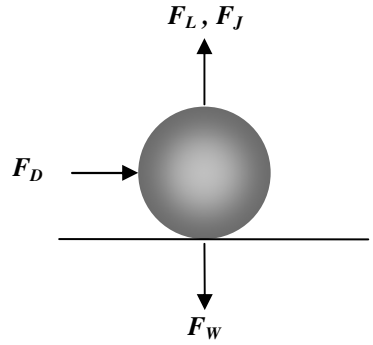

Figure 4.2: Forces acting on a sand particle.

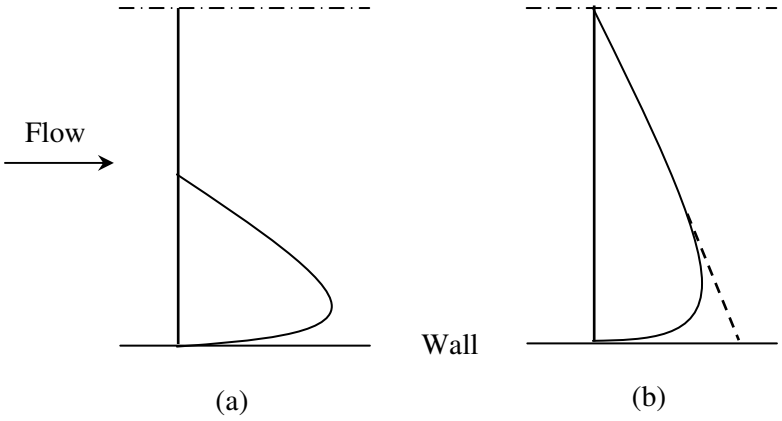

Figure 4.3: Graphical representation of Reynolds stress profiles for (a) a non-uniform flow with a developing turbulent boundary layer and (b) a uniform flow with a fully developed turbulent boundary layer.

Q (m^3/s)	z (cm)	u (cm/s)	$Cov(XZ)$ (cm^2/s^2)
0.023	0.498	9.747	-0.271
	1.001	11.312	-0.334
	1.503	12.070	-0.328
	1.999	12.831	-0.347
	2.502	12.952	-0.277
	2.990	13.817	-0.225
	3.994	13.949	-0.192
	6.006	14.760	-0.047
	9.990	14.439	0.006
	16.008	13.995	-0.044
	17.779	14.292	-0.039
Q (m^3/s)	z (cm)	u (cm/s)	$Cov(XZ)$ (cm^2/s^2)
0.029	0.496	12.790	-0.346
	0.992	14.693	-0.547
	1.508	15.519	-0.459
	2.005	16.112	-0.463
	3.022	16.141	-0.446
	4.031	18.101	-0.255
	6.011	18.732	-0.068
	10.014	18.755	0.077
	16.007	18.448	-0.048
	18.733	18.558	-0.100
Q (m^3/s)	z (cm)	u (cm/s)	$Cov(XZ)$ (cm^2/s^2)
0.036	0.489	16.871	-0.585
	1.003	19.156	-0.795
	1.501	20.640	-0.744
	2.019	21.858	-0.748
	2.489	22.518	-0.692
	3.004	20.935	-0.677
	3.990	24.000	-0.420
	6.007	25.482	-0.069
	10.038	25.352	0.074
	15.998	24.886	-0.067
	17.794	25.138	-0.174

Table 4.1: ADV data collected showing average stream-wise velocities (u) and Coveriances ($Cov(XZ)$) measured at the middle of the test section on a rigid surface for different discharge rates (Q) (Cont'd on the next pages).

Q (m^3/s)	z (cm)	u (cm/s)	$Cov(XZ)$ (cm^2/s^2)
0.041	0.494	22.039	-0.942
	1.002	24.789	-1.082
	1.497	26.275	-1.059
	2.008	27.581	-1.125
	2.485	28.954	-0.867
	3.008	29.133	-0.845
	3.969	30.833	-0.609
	6.031	31.980	-0.015
	9.996	31.749	0.159
	16.002	30.756	-0.010
	17.988	30.651	-0.079
Q (m^3/s)	z (cm)	u (cm/s)	$Cov(XZ)$ (cm^2/s^2)
0.051	0.504	27.557	-1.155
	1.017	30.992	-1.658
	1.502	32.221	-1.679
	2.003	34.284	-1.752
	2.502	34.926	-1.397
	3.008	35.840	-1.441
	3.987	37.351	-1.028
	6.003	39.003	-0.191
	10.014	39.039	0.247
	16.019	37.500	-0.074
	17.909	37.581	-0.233
Q (m^3/s)	z (cm)	u (cm/s)	$Cov(XZ)$ (cm^2/s^2)
0.060	0.507	36.352	-1.759
	0.990	40.681	-2.112
	1.494	42.580	-1.975
	2.008	44.157	-1.496
	2.499	45.394	-1.232
	2.995	46.089	-0.763
	4.000	47.287	-0.166
	6.007	46.898	0.178
	9.998	45.804	0.257
	16.002	44.685	-0.013
	17.469	45.000	-0.090

Table 4.1: ADV data collected showing average stream-wise velocities (u) and Coveriances ($Cov(XZ)$) measured at the middle of the test section on a rigid surface for different discharge rates (Q) (Cont'd).

Q (m^3/s)	z (cm)	u (cm/s)	$Cov(XZ)$ (cm^2/s^2)
0.068	0.510	35.430	-1.991
	1.008	38.684	-2.821
	1.495	40.462	-3.006
	2.003	41.867	-3.119
	2.503	43.265	-2.817
	2.965	44.241	-2.886
	4.002	46.222	-2.526
	5.982	48.608	-1.559
	9.988	49.909	-0.075
	16.006	49.812	-0.712
	18.042	50.996	-1.425
Q (m^3/s)	z (cm)	u (cm/s)	$Cov(XZ)$ (cm^2/s^2)
0.081	0.509	45.512	-2.932
	1.007	52.309	-3.028
	1.496	48.981	-3.065
	1.999	51.109	-2.956
	2.498	51.505	-2.872
	3.031	53.249	-2.312
	4.036	55.172	-1.929
	6.016	56.625	-0.671
	10.006	58.257	-0.093
	15.992	61.180	-1.760
	17.769	62.205	-1.807
Q (m^3/s)	z (cm)	u (cm/s)	$Cov(XZ)$ (cm^2/s^2)
0.091	0.497	48.029	-3.525
	0.997	54.815	-4.200
	1.486	57.579	-4.501
	2.009	60.070	-4.083
	2.510	61.441	-4.207
	2.998	63.383	-3.147
	3.991	66.989	-2.437
	6.005	69.295	0.042
	10.016	69.457	1.553
	15.981	70.179	2.673
	17.157	71.134	3.050

Table 4.1: ADV data collected showing average stream-wise velocities (u) and Coveriances ($Cov(XZ)$) measured at the middle of the test section on a rigid surface for different discharge rates (Q) (Cont'd).

Q (m^3/s)	z (cm)	u (cm/s)	$Cov(XZ)$ (cm^2/s^2)
0.100	0.493	54.481	-3.771
	1.000	60.995	-5.020
	1.498	63.340	-5.343
	2.004	66.463	-5.040
	2.487	68.122	-5.187
	3.015	69.142	-4.368
	4.003	72.492	-2.836
	6.002	75.721	-1.373
	10.025	76.101	2.517
	16.019	78.988	-1.648
	17.661	80.388	-1.099

Table 4.1: ADV data collected showing average stream-wise velocities (u) and Coveriances ($Cov(XZ)$) measured at the middle of the test section on a rigid surface for different discharge rates (Q) (Cont'd).

Q (m^3/s)	u_s (cm/s)	$Max.Cov(XZ)$ (cm^2/s^2)	τ_{exp} (N/m^2)	τ_0 (N/m^2)	τ_{exp}/τ_0
0.023	14.439	-0.347	0.035	0.058	0.598
0.029	18.755	-0.547	0.055	0.085	0.644
0.036	25.482	-0.795	0.080	0.137	0.580
0.041	31.749	-1.125	0.112	0.198	0.568
0.051	39.039	-1.752	0.175	0.283	0.619
0.060	45.804	-2.112	0.211	0.375	0.563
0.068	49.909	-3.119	0.312	0.434	0.719
0.081	58.257	-3.065	0.307	0.569	0.539
0.091	69.457	-4.501	0.450	0.777	0.579
0.100	76.101	-5.343	0.534	0.911	0.586

Table 4.2: At different discharge rates, free stream velocities and shear stresses (τ_{exp}) calculated from the Maximum Covariances and shear stresses (τ_0) calculated from the turbulent boundary layer theory, and their ratio.

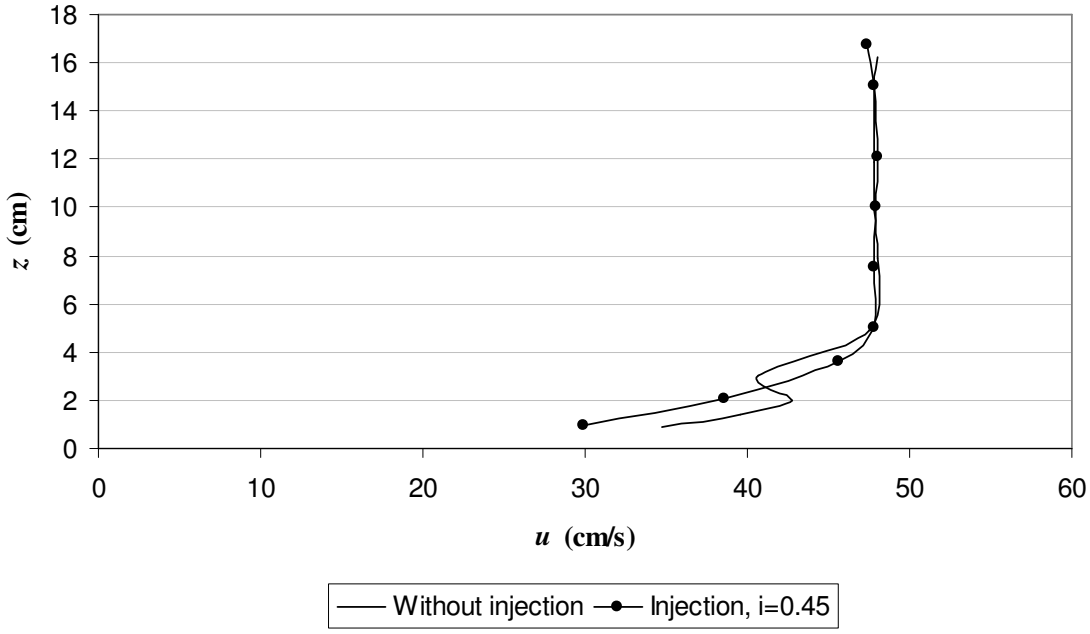

Figure 4.4: Longitudinal velocity profiles at same free stream velocity for experiments with strong injection (hydraulic gradient=0.45) and no injection conditions (d_{50}=1200 μm).

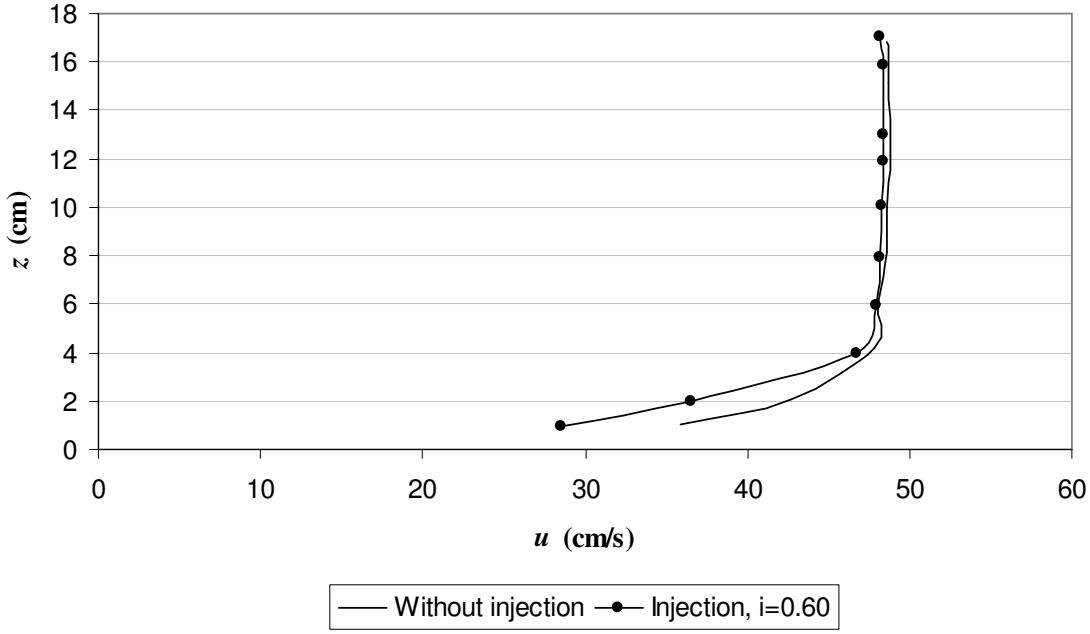

Figure 4.5: Longitudinal velocity profiles at same free stream velocity for experiments with strong injection (hydraulic gradient=0.60) and no injection conditions (d_{50}=1200 μm).

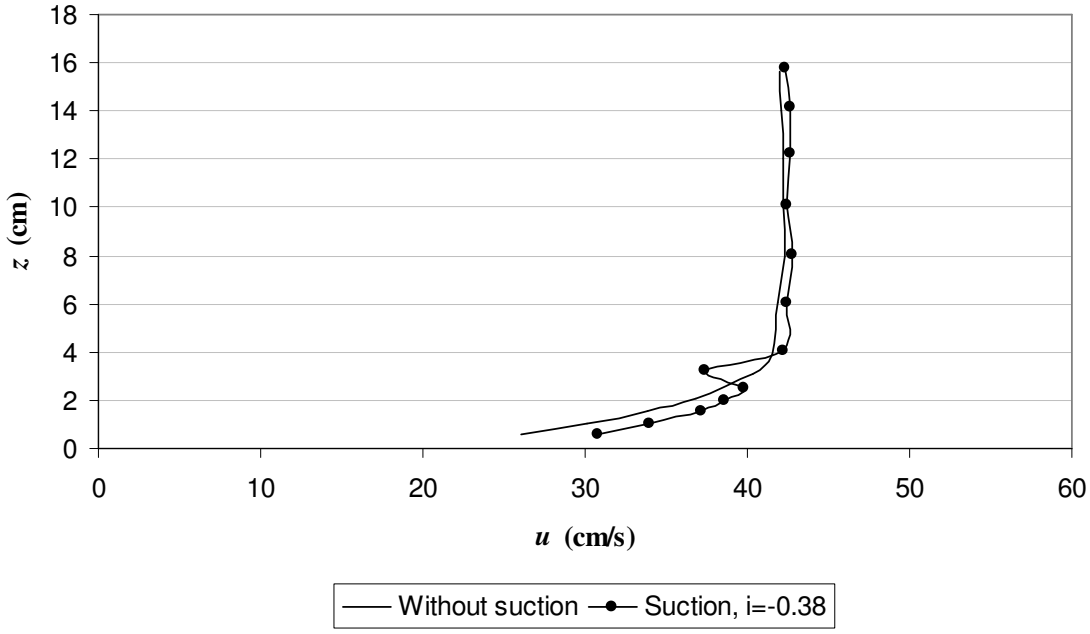

Figure 4.6: Longitudinal velocity profiles at same free stream velocity for experiments with strong suction (hydraulic gradient=-0.38) and no suction conditions (d_{50}=1200 μm).

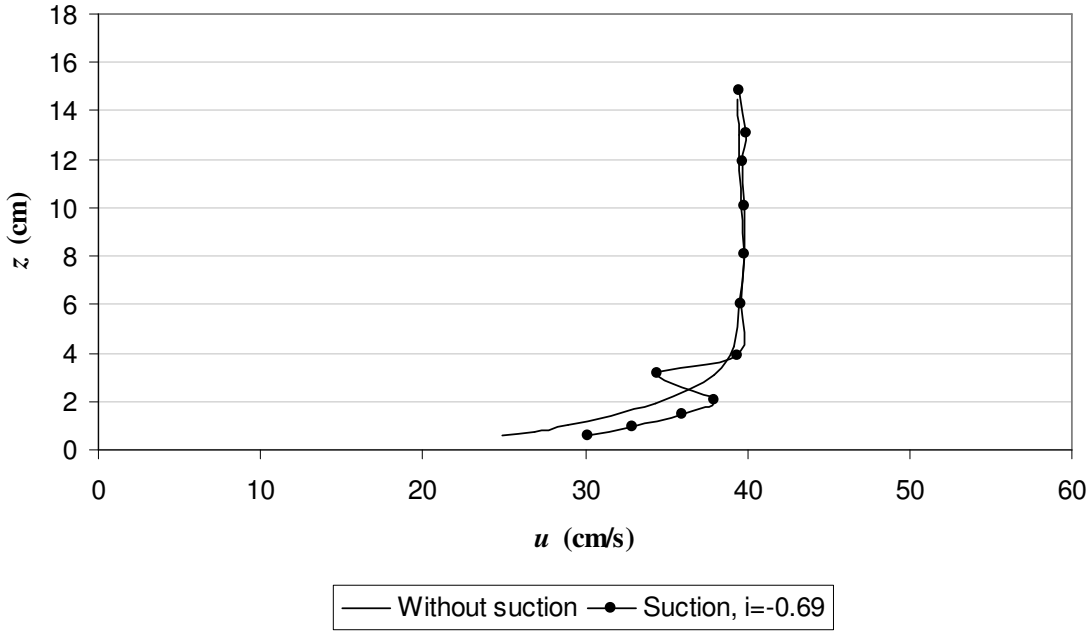

Figure 4.7: Longitudinal velocity profiles at same free stream velocity for experiments with strong suction (hydraulic gradient=-0.69) and no suction conditions (d_{50}=1200 μm).

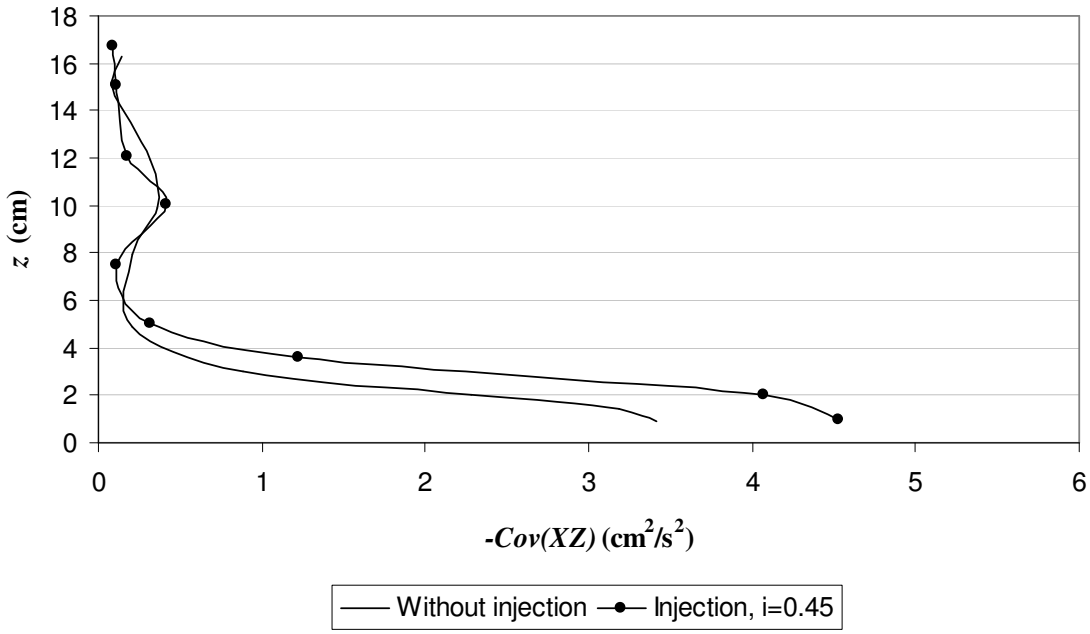

Figure 4.8: –Covariance(XZ) profiles at same free stream velocity for experiments with strong injection (hydraulic gradient=0.45) and no injection conditions (d_{50}=1200 μm).

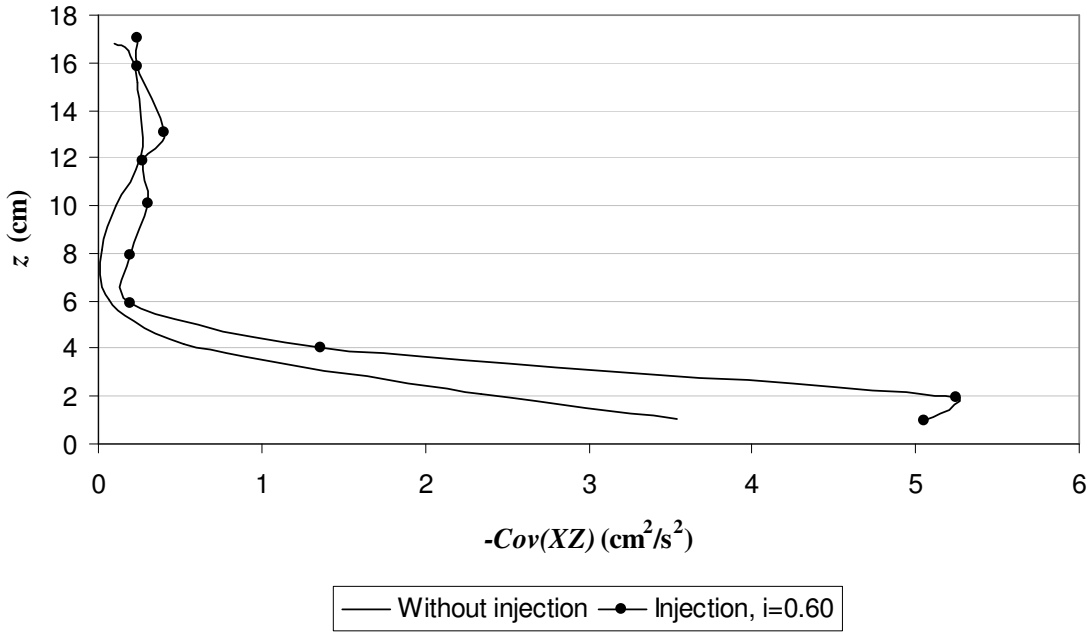

Figure 4.9: –Covariance(XZ) profiles at same free stream velocity for experiments with strong injection (hydraulic gradient=0.60) and no injection conditions (d_{50}=1200 μm).

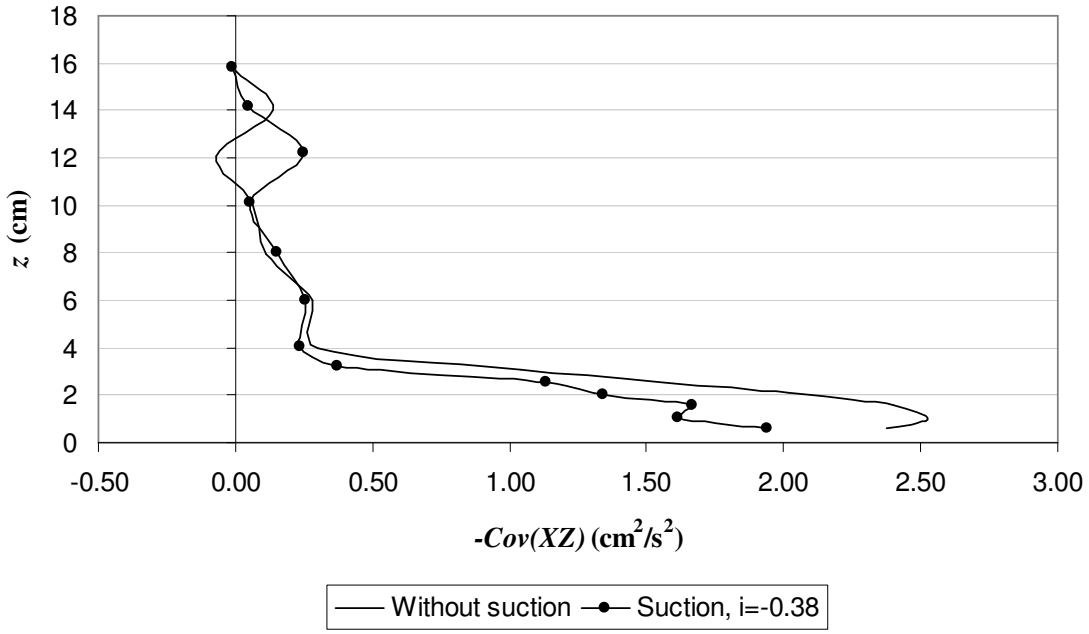

Figure 4.10: –Covariance(XZ) profiles at same free stream velocity for experiments with strong suction (hydraulic gradient=-0.38) and no suction conditions (d_{50}=1200 μm).

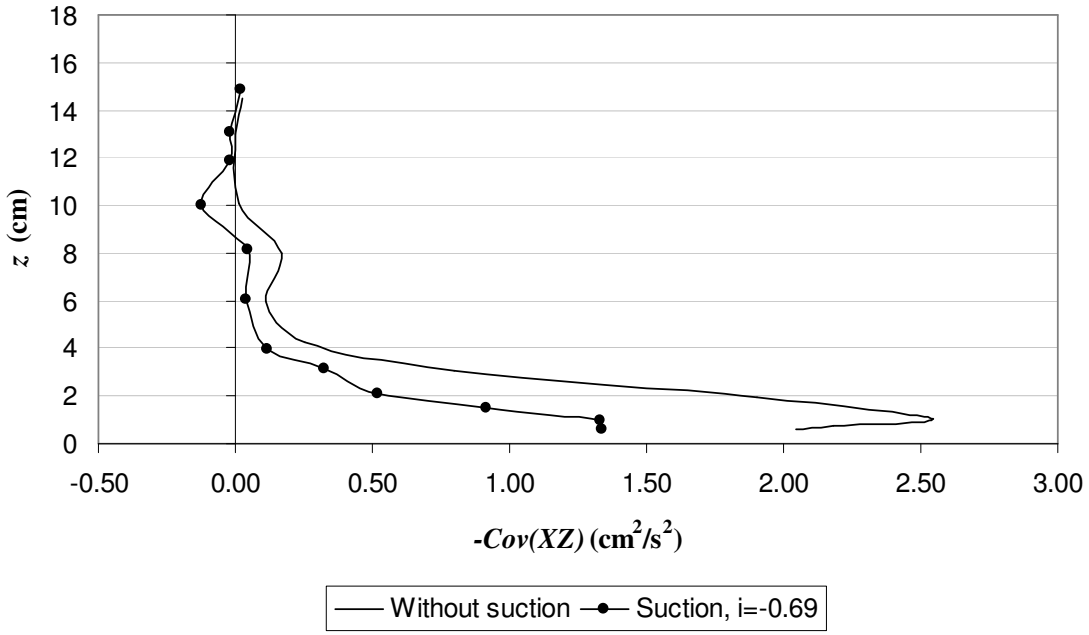

Figure 4.11: –Covariance(XZ) profiles at same free stream velocity for experiments with strong suction (hydraulic gradient=-0.69) and no suction conditions (d_{50}=1200 μm).

d_{50}=160μm			
i	V_i (m/s)	u_s (m/s)	τ_i (N/m^2)
0.000	0.000000	0.2978	0.1741
0.320	0.000033	0.2890	0.1696
0.480	0.000065	0.2796	0.1548
0.700	0.000090	0.2763	0.1602
-0.441	-0.000057	0.3279	0.2847
-0.844	-0.000108	0.3363	0.2487
d_{50}=500μm			
i	V_i (m/s)	u_s (m/s)	τ_i (N/m^2)
0.000	0.000000	0.3229	0.2344
0.248	0.000059	0.3229	0.1994
0.481	0.000117	0.3117	0.1951
0.706	0.000173	0.3047	0.1915
d_{50}=1200μm			
i	V_i (m/s)	u_s (m/s)	τ_i (N/m^2)
0.000	0.000000	0.4515	0.4918
0.300	0.001150	0.4684	0.3461
0.450	0.001760	0.4737	0.3341
0.600	0.002236	0.4815	0.3526
-0.383	-0.001455	0.4233	0.6739
-0.689	-0.002619	0.3952	0.8297
d_{50}=340μm			
i	V_i (m/s)	u_s (m/s)	τ_i (N/m^2)
0.000	0.000000	0.2574	0.2595

Table 4.3: Hydraulic gradient, seepage velocity, free stream velocity and estimated bed shear stresses for different cases ($\tau_i = \tau$ when $i = 0$).

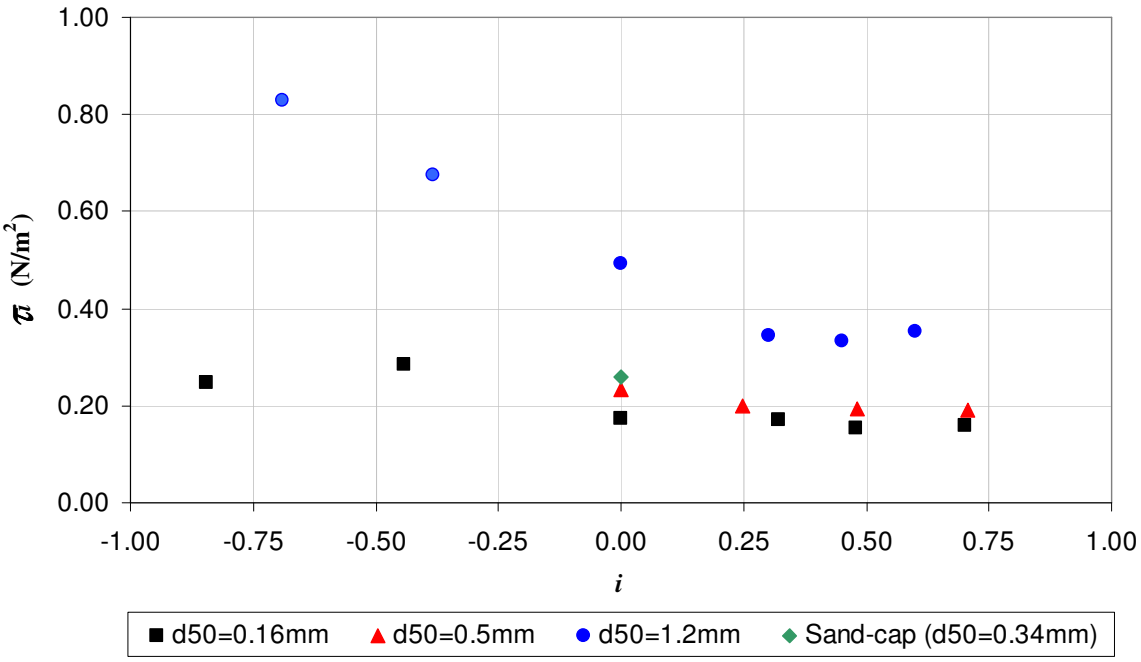

Figure 4.12: Hydraulic gradient versus bed shear stress graph for different sand beds ($\tau_i = \tau$ when $i = 0$).

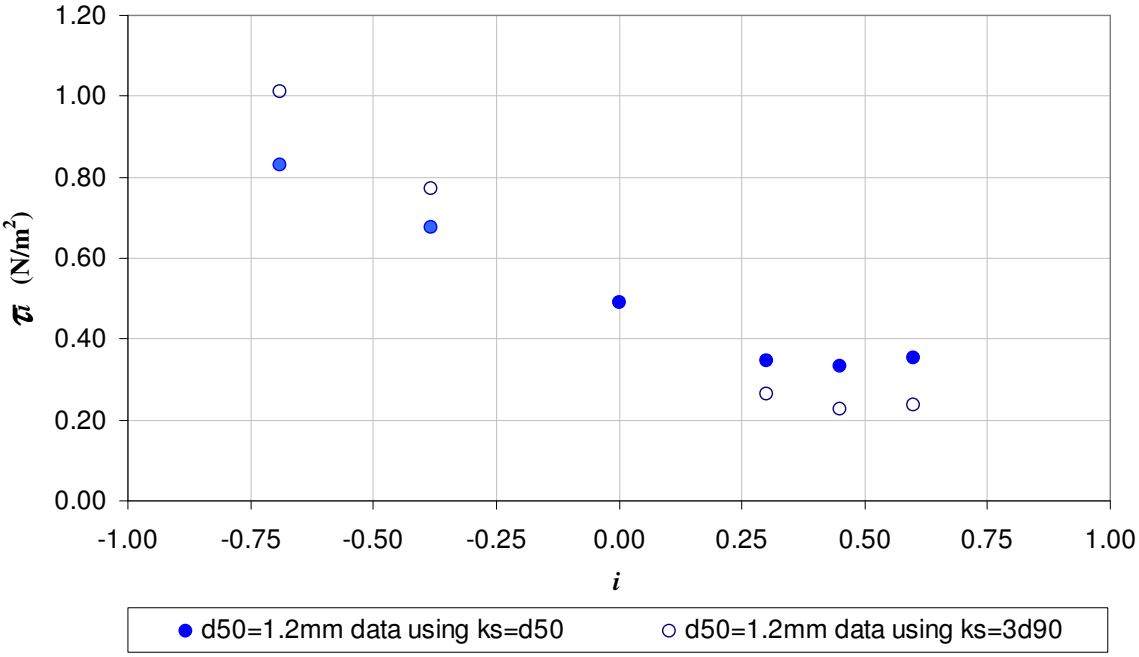

Figure 4.13: A comparison of bed shear stresses computed using $k_s=3d_{90}$ and $k_s=d_{50}$ (d_{50}=1200 μm and $\tau_i = \tau$ when $i = 0$).

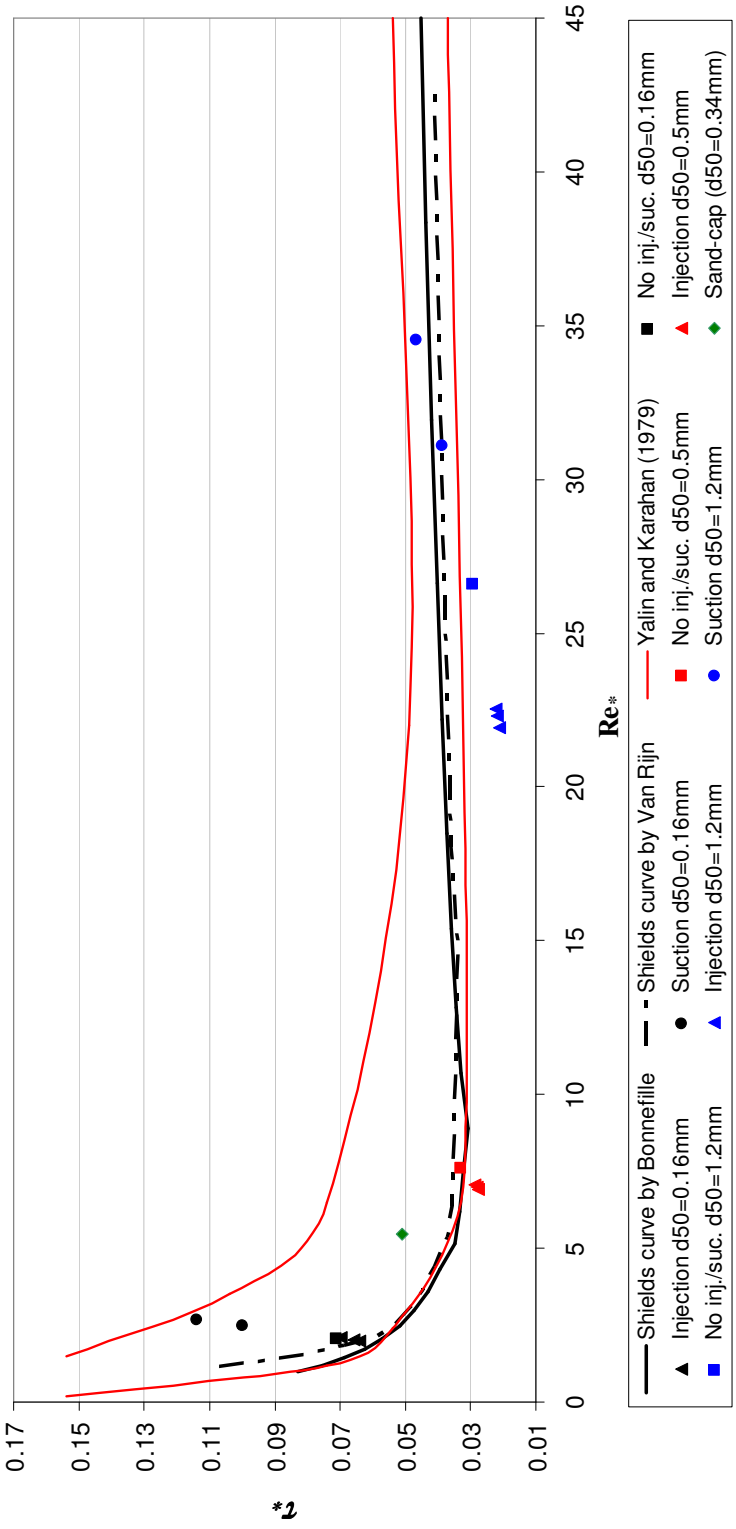

Figure 4.14: Experimental data on Shields curve.

d_{50}=160μm		
i	τ_{*m}	Re_*
0.000	0.0672	2.1110
0.320	0.0784	2.0837
0.480	0.0795	1.9910
0.700	0.0968	2.0249
-0.441	0.0896	2.6997
-0.844	0.0669	2.5230
d_{50}=500μm		
i	τ_{*m}	Re_*
0.000	0.0290	7.6550
0.248	0.0283	7.0604
0.481	0.0321	6.9835
0.706	0.0372	6.9188
d_{50}=1200μm		
i	τ_{*m}	Re_*
0.000	0.0253	26.6106
0.300	0.0211	22.3243
0.450	0.0224	21.9350
0.600	0.0263	22.5321
-0.383	0.0290	31.1513
-0.689	0.0315	34.5652
d_{50}=340μm		
i	τ_{*m}	Re_*
0.000	0.0472	5.4772

Table 4.4: Hydraulic gradients applied on sand beds together with computed modified Shields' parameters and grain Reynolds numbers.

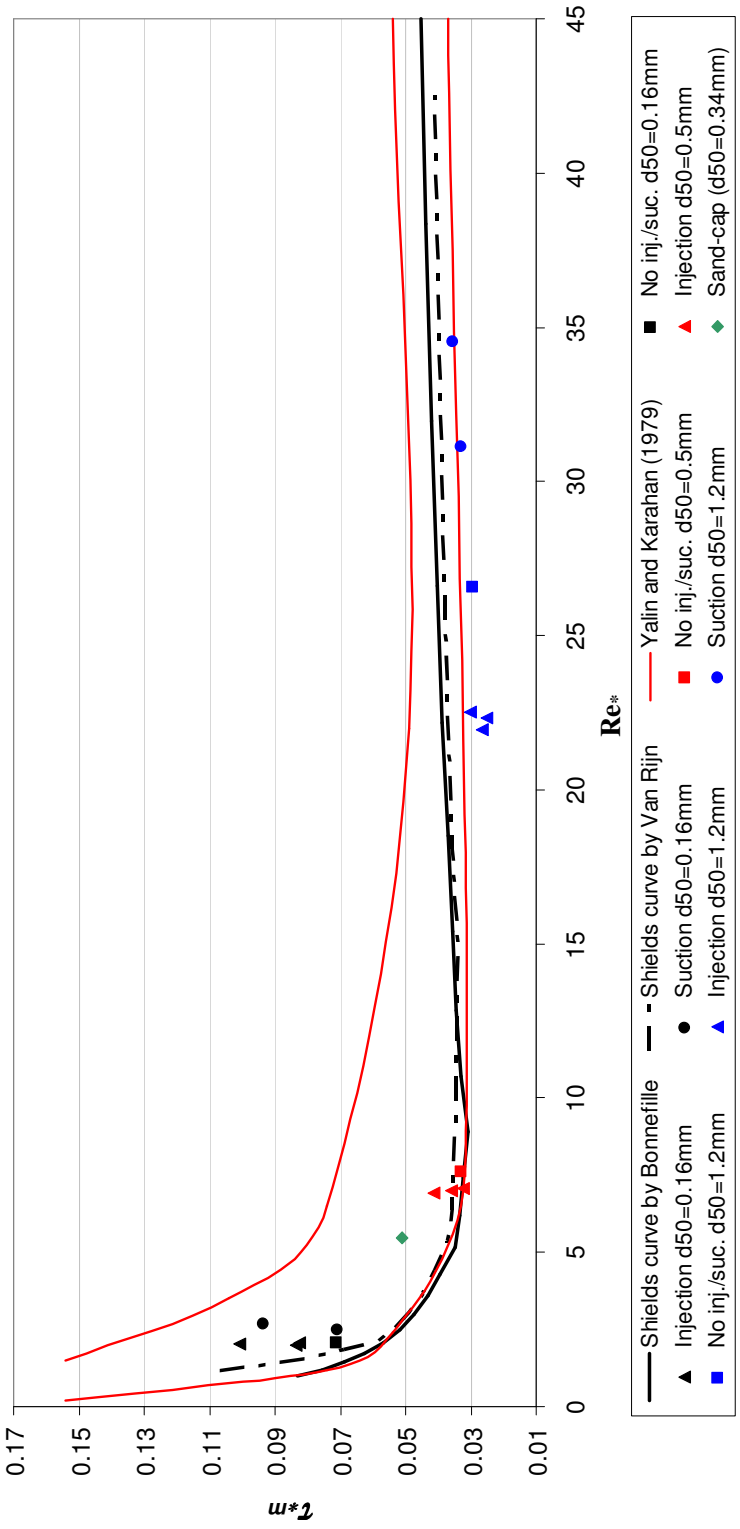

Figure 4.15: Experimental data on modified Shields curve.

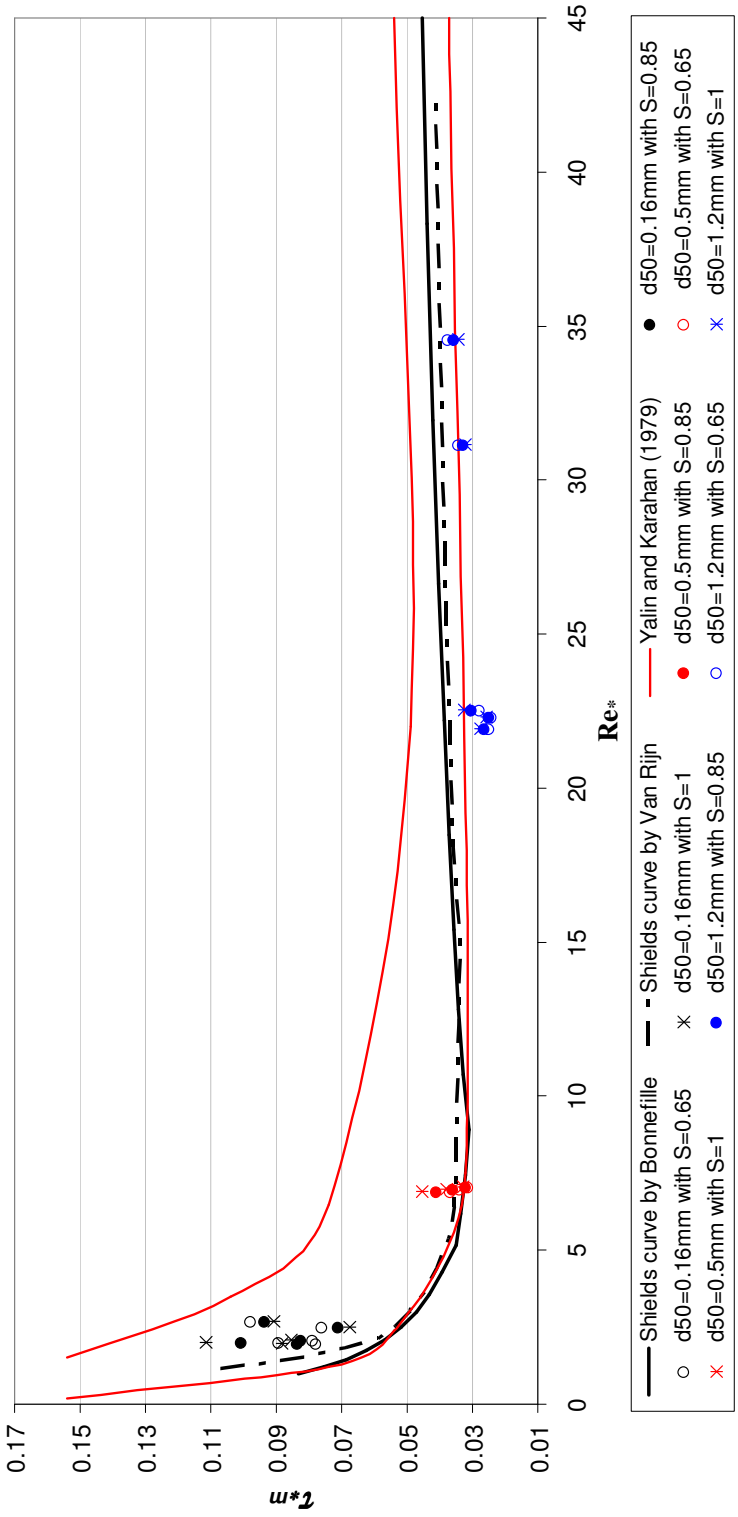

Figure 4.16: Experimental data on modified Shields curve considering S = 1, 0.85 and 0.65.

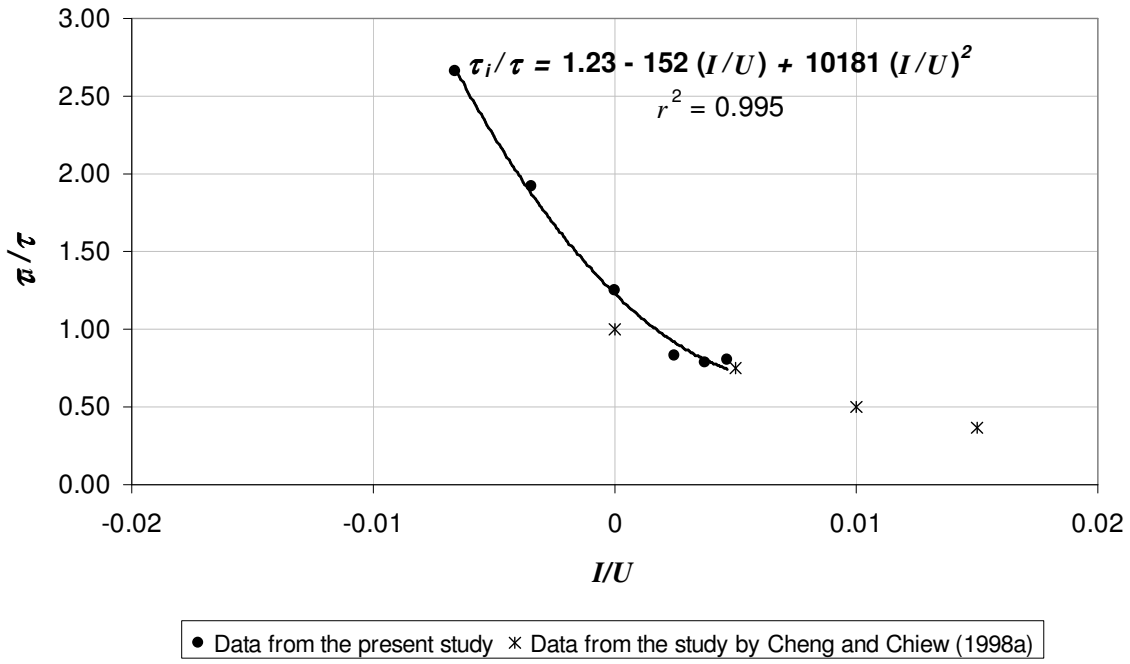

Figure 4.17: The functional dependence of τ_i/τ with I/U derived using d_{50}=1200 μm data together with the data trends from the study by Cheng and Chiew (1998a).

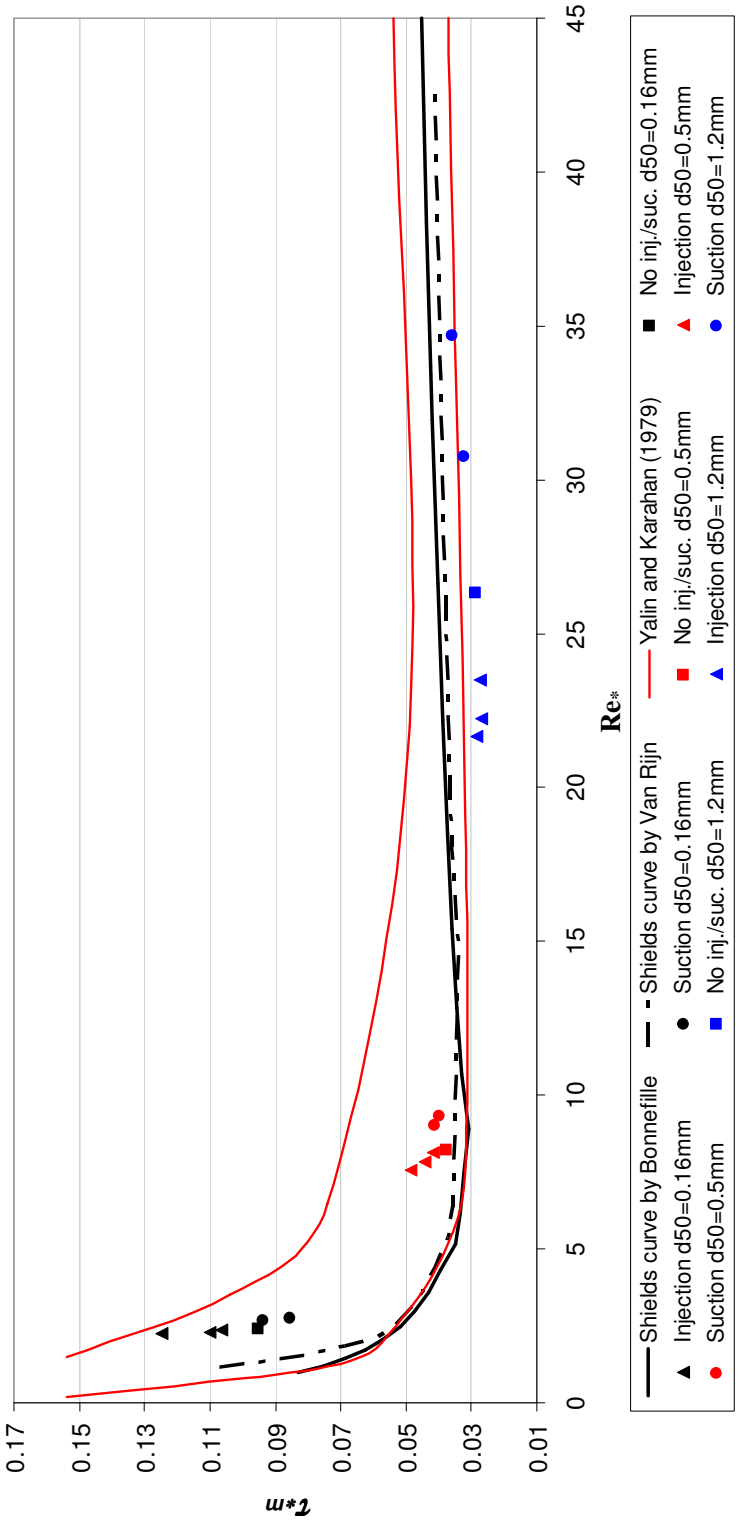

Figure 4.18: Results derived from the bed shear calculations using the second order polynomial relating τ_i / τ to I / U as given by Equation 4.20.

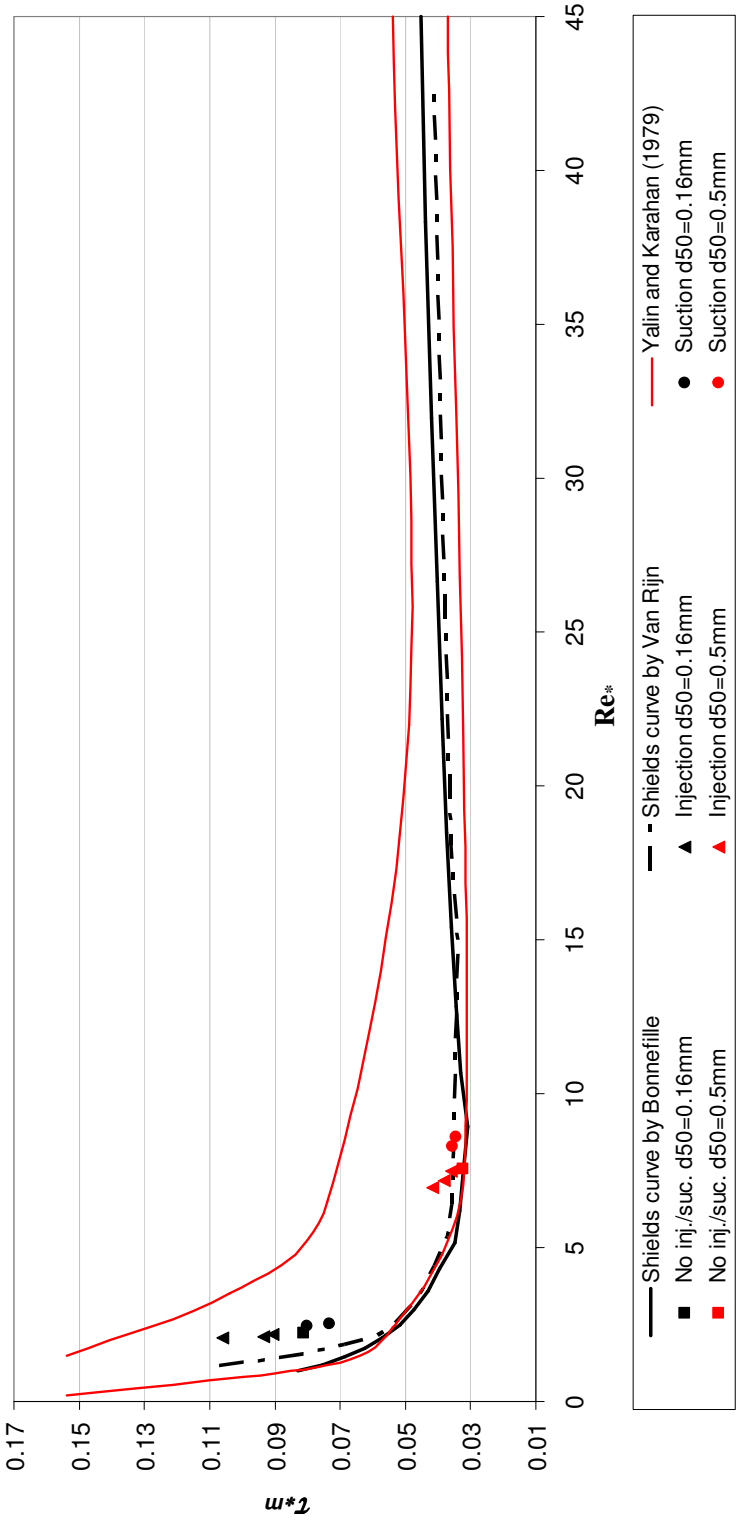

Figure 4.19: Results derived from the bed shear calculations using the second order polynomial relating τ_i / τ to I / U with the difference of coefficient of "1" to reproduce the correct behavior for zero bed seepage (applied for smaller sizes 160 µm and 500 µm).

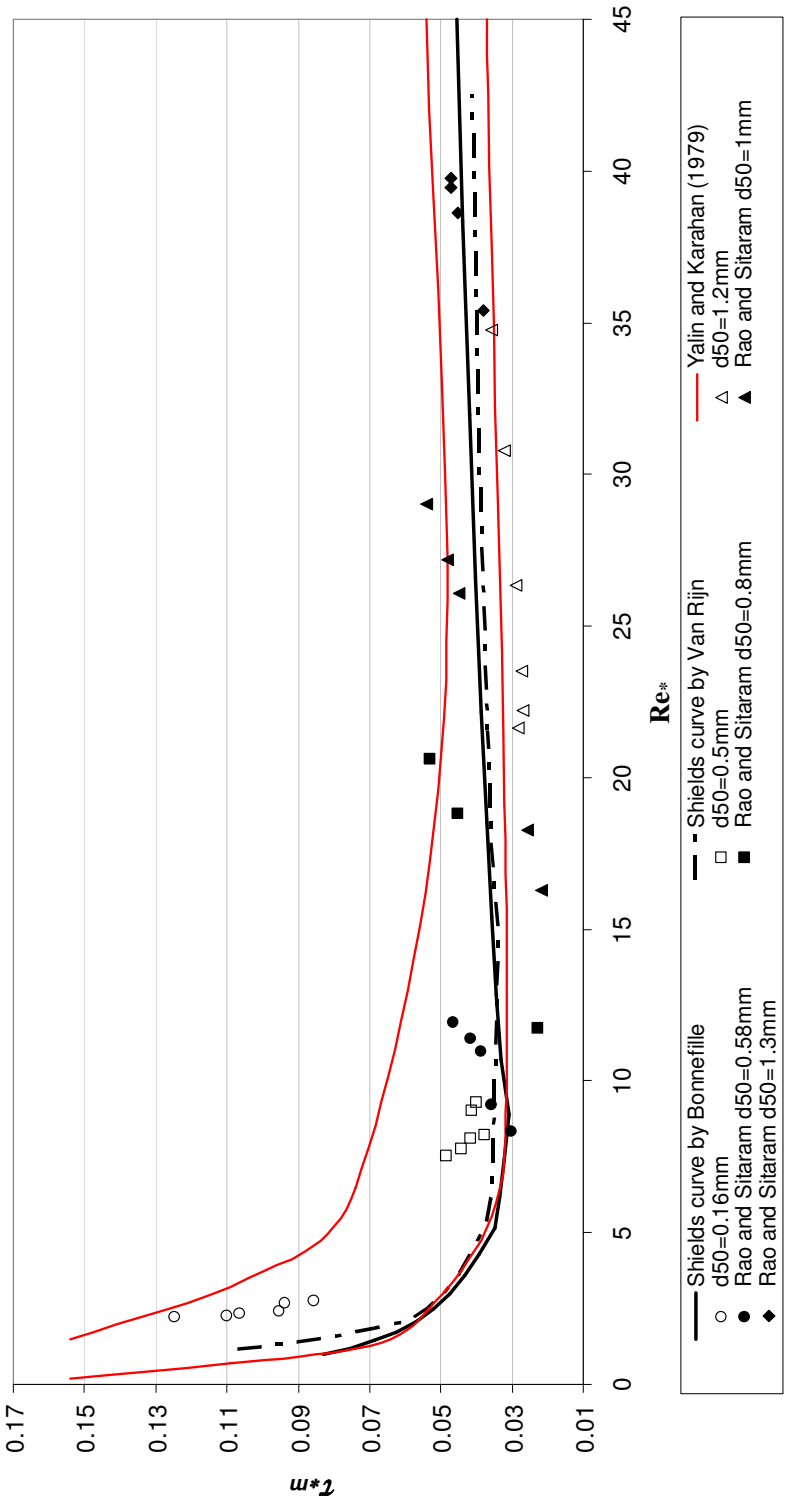

Figure 4.20: Results of the present study in comparison to the results of Rao and Sitaram (1999) after some transformations were performed in order to make a comparison.

CHAPTER 5

STABILITY OF COHESIVE SEDIMENT BEDS AND EFFECTIVENESS OF SAND AND AQUABLOK® CAPS IN REDUCING THE RESUSPENSION RATES

Cohesive sediments contain significant amounts of clay minerals. The cohesiveness of the sediments arises from electro-chemical forces in the clay-water medium and through these forces cohesive beds resist erosion. Research has shown that many factors influence the erosion resistance of cohesive sediment beds, including hydrodynamics, sediment characteristics, and chemical and biological properties of the surrounding medium. Unlike sand, which can be characterized by its grain size distribution, cohesive sediments are much more difficult to characterize; consequently, investigating erosion stability of cohesive sediment beds while controlling all the factors involved is practically infeasible. A comprehensive list of parameters to characterize cohesive sediments was provided by Berlamont et al. in 1993 (also presented in Chapter 2). The list consisting of 28 parameters included some of the commonly mentioned parameters such as grain size, bulk density, Atterberg limits, permeability, consolidation, gas content, mineralogical composition, organic content, etc. In addition, the literature studying the effect of hydrodynamics on erosion of cohesive sediments reflects by its variety the limited knowledge in this field. There is no established theory for calculating the rate of erosion of cohesive sediment beds. It has been more recently recognized that other processes that could affect cohesive sediment resuspension or bed destabilization are vertical pore water pressure gradients due to groundwater flow through the bed and gas ebullition due to microbial activity in contaminated sediment beds (e.g., Jepsen et al., 2000; Simon and Collision, 2001). Caps designed to isolate contaminated cohesive beds from the water column and therefore reduce the resuspension and transport of contaminants to other

sites, are also subject to the effects of hydraulic forces, pore water movement, and ebullition. There is only limited knowledge in the literature related to these processes.

In this chapter, the results of a series of experimental investigations performed using the natural cohesive bed material from the Anacostia River are presented. The objective of these investigations was to provide a better understanding and quantification of the impacts of advective flow, pore water flux (water injection) and gas ebullition (air injection) on the physical stability of cohesive sediments and resuspension rates with or without caps. Experimental studies involved measurement of suspended sediment concentrations in the water column to compute resuspension rates under the effect of the aforementioned factors. Contaminated sediment carried in suspension is presumed to facilitate contaminant mass transfer to the water column. A number of sets of uncapped cohesive sediment bed experiments provided the baseline resuspension data for comparison purposes in the investigation of the effectiveness of sand and AquaBlok® caps in minimizing resuspension.

Research concentrating on laboratory tests in this field has some benefits such as being able to control the test conditions in a flume or the specific properties of the test samples. On the other hand, the sediment itself will have changed due to the effects of transport and storage which may result in losing some site specific information. Even flawlessly designed experimental strategies may not be representative of field conditions. The steps taken to develop the procedures to be followed while conducting the experiments were explained in Chapter 3. It should be noted that due to lack of standard procedures in the literature almost all the procedures followed were developed specifically for this investigation. Some compromises (e.g., using sediment in a slurry form without letting it consolidate) were made along the way in order to be internally consistent and conduct all the planned experiments in a reasonable time frame.

5.1. Results and Discussion for the Effect of Advective Flow

5.1.1. The Anacostia River Sediment Bed

Advective flow experiments were conducted with the Anacostia River sediment beds prepared as described in Chapter 3. These experiments involved only flow induced shear stress applied to the bed without pore water or ebullition flux and were conducted to determine the bed shear stress levels leading to resuspension in the flow as well as rates with increasing shear stress. These sets of experiments provided the data for a reference state without a cap and without the effects of ebullition and pore water fluxes. Contribution of ebullition and pore water fluxes to resuspension rates and the impact of presence of a cap on resuspension rates were identified in comparison to the results of these advective flow experiments.

A five-step discharge increase was taken as the experimental protocol, starting from a low shear stress level with no resuspension and incrementally increasing the shear stress. At each discharge increase, the flow became steady within a few minutes and initial short term velocity fluctuations observed would not affect the bed stability over the vast majority of the time increment (one hour) that the shear stress increment was applied. It was also observed that when the experiments were first started, the startup of the recirculation pump created significant vibrations in the flume and the sediment in the cavity was shaken as a whole without creating any resuspension or erosion on the surface. This was attributed to the cohesiveness of the sediment and the high viscosity of the mixture.

Although bed shear stress levels were adjusted to be approximately the same among the experiments, in order to account for small differences, they were calculated using a correlation relating free stream velocity to the bed shear stress. For each discharge step, one ADV free stream velocity measurement was taken immediately downstream of the test section. The relationship given in Figure 5.1 relates bed shear stresses determined from the maximum value of the Reynolds stress across the flow depth as described in Chapter 4 and free stream velocity. Average discharge rates applied over the bed during a

resuspension experiment are given in Table 5.1 together with the corresponding shear stresses and free stream velocities. At each discharge step, the flow was run for one hour. One hour long discharge steps limited the total duration of an experiment as temperature increase was observed due to the recirculating nature of the setup. Conceptually, bed shear stress is influenced by viscosity which depends on fluid temperature. An increase in water temperature by 10 ^{o}C for typical ambient water temperatures which was also the range of temperature change observed during the experiments, results in approximately a 20% reduction in kinematic viscosity. The influence of this change on shear stress is a 4% decrease as shear stress is approximately proportional to the 1/5th power of viscosity (Equation 4.11). It appears that even though the change in viscosity is significant, the change in shear stress is much less and would tend to decrease erosion rates. On the other hand, there might be some other influences of temperature increase such as on the local turbulence characteristics of the flow or the inter-particle bonds of the cohesive sediment itself. Taylor and Vanoni in 1972 reported that an increase in temperature may increase the intensity of the high-intensity turbulence fluctuations at the bed responsible for dislodgement and transport of bed particles. Kelly and Gularte (1981) suggested that increasing water temperature increases rates of sediment resuspension. It is recognized that further investigations would be required to examine the effect of temperature on the erosion or resuspension rates for the Anacostia sediment.

It was observed that as the shear stress applied to the sediment bed surface was increased, chunks of sediment particles were torn from the surface layer, creating stripe-like formations on the sample surface. Figure 5.2 shows the eroded sediment bed surface in which the lighter colored layer is the uppermost oxidized sediment layer and the underlying darker layer is seen at the eroded locations of the bed. Large scale scour holes did not form in the sediment bed over the duration of the experiment at the levels of shear stress applied. Only the portion of the sediment that was removed from the bed and carried in suspension in the flow was measured with the turbidimeter. This was considered to be the most relevant quantity in the consideration of contaminant mass transfer to the water column since mass transfer from sediment carried in suspension would more readily facilitate mass transfer compared to chunks of sediment sliding along

the bed and potentially subsequently deposited in lower energy zones downstream from the point they were scoured. In practice, resuspension rates calculated using suspended sediment concentrations within the flume are usually assumed to be equal to the total erosion rates. From here on, the terms “resuspension rate” and “erosion rate” will be used interchangeably referring to the rates calculated from the turbidimeter concentration measurements. In theory, however, the erosion rate consists of two components, resuspension rate and bed load transport rate. The potential importance of bed load transport as a component of cohesive sediment erosion was indicated by Debnath et al. (2007). In this study, as the sediments in suspension are assumed to be responsible of the transport of the contaminants in the flow, only resuspension rates were measured and considered in the computations.

Sediment concentrations monitored by the turbidimeter due to increased shear stress levels induced by advective flow are given in Figure 5.3. This figure also shows the results of 3 repetitions of the same experiment for the purpose of demonstrating the variation in the data caused by the uncertainty involved in different aspects of the experimental investigation. The concentration versus time graph shows that there is no significant erosion on the bed during the first two hours of the experiment. For the rest of the duration of the experiment, resuspension is evident with increasing rates as the shear stress level is increased. The initial concentration reading is due to the resuspended material left in the flume from a previous experiment even though the flume and pipe system was flushed with water after each experiment. The raw data exhibit short term fluctuations because of the precision of the turbidimeter; moving averages for the concentration values were computed to smooth these fluctuations. Data trends are revealed much more clearly in the concentrations computed from the moving averages. The trends are consistent with the results of previous studies on sediment resuspension that have been conducted in a similar experimental framework (e.g., see Parchure and Mehta, 1985; Lick et al., 1995; Piedra-Cueva and Mory, 2001; Amos et al., 2003; Ravens, 2007). Since the flume water is being recirculated in the experiment, a constant slope to the concentration versus time plot would imply a constant resuspension rate. The trend observed in nearly all experiments is that the slope of the line is initially greater

after the elevated shear stress is applied and then the slope gradually decreases with time. It is assumed that this behavior is due to the removal of the least stable areas on the sediment bed at any applied shear stress and therefore, there is a time dependence to the resuspension process. Although this finding is widely reported in the literature, there is no generally accepted procedure for analyzing the data and computing the erosion rates. Deposition indicated by negative resuspension rates was sometimes observed when the bed was subjected to a low shear stress level. Also in some of the experiments, the rates for relatively short time intervals showed indication of possible temporary depositional behavior at higher shear stress levels although it is also possible that the observations are simply due to spatial variations in suspended sediment that are gradually smoothed out in the recirculating flow.

Research suggests that as the sediment consolidates over time, the bulk density of the sediment generally increases with depth and time as the pore water is expelled from the sediment and transported to the surface and consequently erosion resistance increases with depth (e.g., Mehta et al., 1989; Jepsen et al., 1997). Since the sample beds in this investigation were not allowed to consolidate over extended periods of time, it was not expected to have different layers of sediment with significantly different shear strengths and erosion of only a few millimeters of the sediment surface made the possibility of depth dependency a relatively minor factor. It is also noted that sediment beds subject to pore water seepage and/or gas ebullition will not consolidate as fast or in the same way as sediment beds not subject to these effects.

In almost all the experimental investigations reported in the literature, at the beginning of a shear stress level increase, the erosion rate is usually initially higher and then decreases with time. This time dependency has resulted in different interpretations of resuspension data and erosion rate calculations. For example, Ravens and Gschwend (1999) defined the erosion rate in two ways; one including the effect of the initial peak and secondly by excluding it and examining only the “plateaus” after the initial response passed. Tolhurst et al. (2000) averaged the resuspension rates over the entire shear stress step whereas Houwing (1999) assumed that the erosion rate for an applied bed shear

stress level was the initial peak value. Therefore different methods of analysis provide different values of parameters in various erosion-shear stress relationships. In this investigation, it was recognized that resuspension rates may be calculated in several different ways and the procedure used in analyzing the resuspension data would have some influence on the results. Although different schemes were considered, the final approach explained below was implemented making it consistent and well-defined. All the resuspension rate computations were performed on the moving averaged concentration measurements. Moving averages were calculated to smooth the data fluctuations related to the turbidimeter precision as mentioned previously. One five-hour experiment involved 18000 data points as one measurement was taken at every second. After some trial computations it was decided that 600-point data groups were required for moving average calculations in order to smooth the fluctuations effectively. Since 600 separate data points were used for each moving averaged data point, the total available data after performing the moving averages was 17400 for the rate calculations. For each shear stress level interval, rates were calculated in 10 min time increments excluding the moving averaged concentration data that were affected by the times surrounding the change in shear stress levels. For each shear stress interval, five resuspension rates were computed and the average of these resuspension rates was defined as the overall resuspension rate for that shear stress level (Figure 5.4). Resuspension rates generally tend to decrease towards the end of an hour; however they do not follow a consistent relationship that could be defined by a formula (e.g., see Figure 5.5). Averaged resuspension rates over an hour for each shear stress level yielded relatively consistent results when the results of the repetitions of the same experiment were compared. It is seen on Figure 5.4 that resuspension rates approach zero at an applied bed shear stress of around 0.18-0.21 N/m^2 which is assumed to be the range for the erosion threshold. Computations from the first two sets of advective flow experiments follow a quadratic shear stress-resuspension rate relationship defined as

$$R = M(\tau - \tau_c)^2 \tag{5.1}$$

where M is the resuspension rate coefficient, τ is the applied bed shear stress and τ_c is the critical shear stress. The values for the critical shear stresses for these two sets of data were determined as 0.194 N/m^2 and 0.181 N/m^2. The two other sets of results did not show such a consistent trend on the resuspension rates although in general resuspension rates were increased with increasing shear stresses similar to the first two experiments. Figure 5.6 shows the curve fitting performed by using the results of the first experiment with $r^2 = 0.986$ and the resuspension rates calculated using the data corresponding to the other three sets are also plotted on the graph to show the variation. For this relationship, M equals to 96.7 mg s^{-1} m^{-2} Pa^{-2} where τ_c is 0.194 N/m^2. An approximate error estimate (± 0.25 mg s^{-1} m^{-2}) was calculated using deviations from the curve fit rates and as the most repetitions were performed for advective flow only experiments, the same error estimation was used for the results of the pore water flux experiments presumably providing proper upper and lower error boundaries.

Similar power law relationships were also used in the results of Jepsen et al. (1997) whose experimental investigation of Detroit River, Fox River and Santa Barbara slough indicated a number of 2.23, 1.89, and 2.10 respectively as the exponent. They did not include a threshold for sediment erosion since the data did not indicate a clear threshold and bulk density was considered as another parameter in their expression. Ravens (2007) modeled his experimental data with a quadratic stress expression once again without including a threshold value. Lick et al. (1995) used a formula similar to the quadratic relationship used here relating the excess bed shear stress to erosion rates with the difference of a time dependency and reported 2.3, 2.5, 2.7, and 3.1 as the exponent for Fox River, Green Bay, Saginaw River and Buffalo River sediments, respectively. Regarding the determination of the critical shear stresses, the numbers reported vary significantly depending on many parameters. Several researchers have reported critical shear stress values in a range between 0.1-0.2 N/m^2 for surficial cohesive sediments (e.g., see Piedra-Cueva and Mory, 2001; Ravens and Gschwend, 1999; Houwing, 1999; Hunt and Mehta, 1985). Although the critical shear stress will be dependent on a number of different parameters, it is seen that the results of these experiments are comparable to

results obtained in other experiments performed on cohesive sediments in somewhat similar depositional environments.

Directly comparing the data from different studies may not be reasonable. The data collected with different devices (e.g. recirculating flumes, straight through flumes or pipes) may be difficult to compare due to some fundamental differences of flow structure, test surface area, time durations for the application of bed shear stress, and other factors. Most previous studies used shorter time intervals for measurement at a given shear stress. The measurement intervals were generally on the order of 10-20 min (e.g., Ravens and Gschwend, 1999; Amos et al., 1996; Maa et al., 1998). But the main difficulty arises from the fact that the calculation of the bed shear stress, erosion rate and erosion rate parameters, and the other data analysis procedures vary significantly among different studies. The issues associated with bed shear stress calculations were addressed in Chapter 4. A variety of erosion rate-shear stress relationships have been reported in the literature as addressed in Chapter 2. Furthermore, the dependency of the erosion potential of cohesive sediments on physical, chemical and biological factors which vary in both space and time affect the conclusions extensively. Bed preparation by using a thick slurry of sediment or a compacted sediment sample will definitely influence the results. Beds formed by allowing suspended sediment to deposit under a low flow velocity have been considered as another possibility for bed preparation by several researchers and it was shown to influence the erosion-shear stress relationships (e.g., Lau and Droppo, 2000).

5.1.2. Sand Cap

Incipient motion experiments on the sand material with specifications similar to the sand cap used in the Anacostia River with a median grain size of 340 μm showed a critical shear stress value of 0.260 N/m^2. The critical shear stresses computed from the results of the other incipient motion experiments with sand sizes d_{50}=160 μm, d_{50}=500 μm, and d_{50}=1200 μm are 0.174 N/m^2, 0.234 N/m^2, and 0.492 N/m^2 respectively. The critical shear stress for the graded sand with median grain size of 340 μm is larger than that for the d_{50}=500 μm sand. It was recognized during the incipient motion experiments

that some of the properties of the sand such as uniformity of the sand size distribution and shape of the individual particles influenced the incipient motion observations. It is believed that this discrepancy in the results arise from performing experiments with roughly rounded particles for all the incipient motion experiments except for the 340 μm sand which is more angular in shape.

The sand with the smallest grain size, d_{50}=160 μm has a threshold for mobility slightly less than the critical shear stress for the cohesive Anacostia River sediment. The ratios of the threshold bed shear stresses for sand beds to that for the Anacostia River sediment is given in Table 5.2 for comparison. As also mentioned before, cohesive sediments resist erosion mainly by the electro-chemical bonds and this result shows that even with a very small average particle size (10 μm) this cohesive sediment bed is more stable than a bed consisting of 160 μm sand particles that resist erosion through gravitational forces. It may not be the best decision to use this sand material in the design of a sand cap to increase the stability of the contaminated sediment bed as only modest increases in bed surface stability are achieved. Since the cohesive sediments were tested in an unconsolidated state, it is even possible that the shear resistance of the sand cap material is less than that for partially consolidated sediments.

5.1.3. AquaBlok® Cap

The effectiveness of AquaBlok® caps to prevent the resuspension of contaminated sediments into the water flow was intended to be studied within the scope of this investigation. However, the flux chamber experiments discussed in Chapter 3 revealed that there are limitations to what can be investigated in the flume studies. In regards to the seepage experiments, applied water injection would either leak along the side walls or accumulate beneath the AquaBlok® until the cap ruptured because of very low conductivity of the AquaBlok® material when hydrated. Similarly, in the ebullition experiments, it was observed that pressure build up under the AquaBlok® cap was released only through a surface rupture which would make the flow dynamics over the cap very complicated and strongly dependent on the geometry of the ruptured surface. Since the formation of the rupture is apparently quite random in time and space,

obtaining reproducible results in a laboratory experiment even with the relatively significant test bed surface area seems to be impossible and side wall effects would dominate the behavior of the experiment. In light of the experimental observations from the flux chamber experiments, it was decided to investigate the stability of AquaBlok® cap considering only the effect of shear stress induced by advective flow. The cap thickness was set at 10 cm to be consistent with the flux chamber experiments, but this should not have any impact on the observed results. Other test conditions were similar to the other experiments, except that much higher shear stresses were necessary to erode the AquaBlok® surface.

Results show that AquaBlok® is extremely stable without failure under even very high shear stresses and it is much more stable than any sand bed considered in this investigation. The AquaBlok® experiment was initiated with the shear stress values applied during the Anacostia River sediment experiments. There was no indication of overall destabilization of the bed for any of these shear stress levels. Therefore, shear stress values were increased further to observe the limitation to the stability of the AquaBlok® bed up to a shear stress of 2.565 N/m^2 which is approximately 5 times larger than the critical shear stress of a sand bed with d_{50}=1200 μm and 13 times larger than the critical shear stress of the Anacostia River sediment. The discharge rates applied over the bed are given in Table 5.3 together with the corresponding shear stresses and free stream velocities. It should be noted that not every shear stress level was applied for an entire hour to limit the total duration of the experiment. Looking at the surface of the bed after the experiment, it was observed that some bentonite was eroded from the surface and some small aggregate particles were carried downstream by bed load transport. However, the majority of the aggregate adhered to the bentonite layer underneath creating an armoring layer (Figure 5.7).

Concentration measurements in the water also confirmed the stability of the AquaBlok® bed and are presented in Figure 5.8 (see Appendix A.1 for turbidity-concentration calibration). There was no change in the turbidity values until very high discharge rates were reached at around Q= 0.069 m^3/s. At this point the turbulence

downstream of the raised test section led to resuspension of some bentonite covering the aggregate material that had been previously eroded and transported downstream and deposited just upstream from the pump intake. This resuspension was due to a strong inlet vortex at the pump intake and cannot be related to the general flow conditions over the AquaBlok® surface. The rise in turbidity late in the experiment is due to this resuspension of previously eroded bentonite material as opposed to a catastrophic failure of the AquaBlok® bed. It is noted that it would be difficult to explicitly define what constitutes the critical shear stress for the AquaBlok® material from observations. In this study, at every shear stress increase some of the loose aggregates were transported downstream or bentonite was sheared off the upper gravel particles. However, a short time after increasing the bed shear stress, the surface stabilized and it was not possible to observe additional bed deformation. It is unclear whether these observations should be interpreted to define a critical shear stress since the bed dislocations were only temporary in time. The U.S. EPA released a report in September, 2007 on the results of an experimental investigation indicating that shear stresses required to erode the AquaBlok® material were between 3.2 and 10 N/m^2. These experiments were performed with Sedflume and a small but finite erosion rate was used to define critical shear stresses.

5.2. Results and Discussion for the Effect of Pore Water Flux

5.2.1. The Anacostia River Sediment Bed

The selected fluxes for the seepage experiments were 0.12-1.2-12 cm/d. In terms of injection rates through the test bed, these fluxes are equal to 0.5-5-50 ml/min. These rates were considered in the experiments together with the procedure for the step-wise increased advective flow induced shear stress. Examination of the results at the 1.2 cm/d pore water flux indicated that 0.12 cm/d would not exhibit a discernable effect on resuspension rates. Even 1.2 cm/d had a minimal effect on the suspended sediment concentrations with essentially the same results as the concentration measurements in advective flow only experiments (see Figure 5.9). On the other hand, the 12 cm/d pore water flux significantly changed the suspended sediment concentrations (Figure 5.10). Both types of experiments resulted in very consistent suspended sediment concentration

measurements. When a pore water flux of 12 cm/d was applied to the bed, there was no visible vertical flow in the form of small jets (see discussion in Section 3.2) into the water column but visual observations were hampered by the turbidity in the recirculating water. Although it was not possible to observe any vertical flow in the form of jets, it is believed that resuspension rates were increased as a result of seepage channels formed in the sediment bed through which pore water flow entrained sediment into the water column consistent with the observations made in flux chamber experiments. It was observed that at the high seepage rate (12 cm/d), the density of the sediment bed after re-mixing of the sediment in the cavity was less than at the beginning of the experiment. It is speculated that flow in the immediate vicinity of the soaker hoses behaved more like a porous media flow for some distance until the seepage channels concentrated the pore water flow. It would therefore be expected that the sediment density close to the soaker hoses was reduced during the course of the experiment but that the sediment further away is much less impacted by the seepage except possibly in the immediate vicinities of the seepage channels. Density variations within the sediment bed were not investigated systematically; the main purpose of the sampling was to make sure that the bulk density of the material in the cavity matched the standards defined by the procedures developed previously. Therefore, no data was recorded in an organized manner documenting the degree of density changes related to the pore water transport experiments. The observations showed that after application of 12 cm/d pore water flux, density changes were much more significant compared to 1.2 cm/d pore water flux cases. Consequently, as opposed to the four successive experiments prior to bed removal and re-mixing, the sediment material was required to be taken out to mix with a denser sediment sample in order to maintain the constant bulk density among the experiments after only two 12 cm/d pore water experiments.

Resuspension rates were calculated employing the procedure explained previously. Figure 5.11 shows a comparison among the resuspension rates obtained from the first sets of advective flow, 1.2 cm/d pore water, and 12 cm/d pore water experiments. It is seen clearly that a flux of 1.2 cm/d does not cause a significant change in the resuspension rates; however, 12 cm/d affects the results, significantly increasing the rates. The results

from the first 1.2 cm/d injection experiment agree well with a quadratic shear stress-resuspension rate expression similar to the one used for advective flow experiments (Equation 5.1). The critical shear stress, τ_c and the resuspension rate coefficient, M for this set of data was determined to be 0.199 N/m^2 and 151.9 mg s^{-1} m^{-2} Pa^{-2}, respectively. The second data set for the 1.2 cm/d experiments does not indicate a clear power relationship. The curve fit with $r^2 = 0.992$ according to the first set of 1.2 cm/d data and variation of the data from the second experiment with respect to the fit is shown in Figure 5.12. Regarding the 12 cm/d pore water experiments, both of the two sets of data clearly follow a formula defined by the same quadratic relationship ($r^2 = 0.998$) with approximately the same relationship constants (Figure 5.13). The critical shear stress for these experiments was determined to be 0.190 N/m^2 and M equals to 507.9 mg s^{-1} m^{-2} Pa^{-2}. Table 5.4 summarizes the values of the parameters used in the quadratic shear stress-resuspension rate relationship corresponding to different values of pore water fluxes. According to the findings, M values are correlated to the injection fluxes through a linear relationship shown in Figure 5.14 and it is defined as

$$M = 33.76I + 103.65 \tag{5.2}$$

which clearly indicates that resuspension rates are increased by increasing injection rates although no significant change was observed in the critical shear stresses. It is presumed that density changes created by the pore water fluxes were not affecting the density of the surface layer maybe except in the location of the exit channels which enabled the critical shear stresses to remain at approximately the same values. In Equation 5.2, $I = 0$ relates to an advective flow experiment without any pore water flux applied. The reported mean seepage rates in the Anacostia River vary from a weak measurement of -0.049 cm/d to a moderate measurement of 1.1 cm/d (Horne Engineering Services, Inc., 2003). The reported high-end seepage rates for the Anacostia River due to tidal fluctuations range from 2.7 cm/d to 5 cm/d and thus, it is reasonable to expect a significant influence of pore water flux on the resuspension rates for the demonstration site.

A limited number of investigations has been reported in the literature regarding the effects of seepage on the erosion rates and these are not directly comparable quantitively to this study as a consequence of their experimental objectives and implementation techniques (e.g., Simon and Collision, 2001; Amos et al., 2003). Some other investigations that are somewhat related but still not comparable were also reported; such as investigations on the effects of the water content. The general conclusion from these studies is that the erosion threshold is inversely proportional to the water content of the sediment bed (e.g., Fukuda and Lick, 1980) Bulk density was another parameter considered widely in the previous studies showing that erosion rates are a very strong decreasing function of density (e.g., Roberts et al., 1998; Amos et al., 2003).

5.2.2. Sand Cap

The sand with d_{50}=340 μm was examined for its effectiveness in minimizing the resuspension rates under the influence of vertical pore water fluxes. The two injection fluxes applied, 1.2 cm/d and 12 cm/d did not cause any detectable suspended sediment concentration in the flume over the duration of the experiments. Apparently, the sand cap filtered all the contaminated sediment transported from the sediment layer underneath it. This is consistent with the qualitative observations made in the flux chamber experiments reported in Chapter 3. However, it is unknown if resuspension would occur after extended periods of time as suggested to be possible through the observations reported in Chapter 3. It is also noted that 1.2 cm/d and 12 cm/d pore water fluxes which are associated with relatively low hydraulic gradients (0.0015 and 0.015, respectively) did not cause any destabilization of the bed surface as expected from the results presented in Chapter 4. A low flow rate was used to re-circulate the flow in the flume without creating any destabilization on the surface of the bed due to the shear stress applied.

5.3. Results and Discussion for the Effect of Ebullition

5.3.1. The Anacostia River Sediment Bed

Considering the ebullition experiments, the observations from the flux chamber experiments and from the flume experiments were somewhat similar regarding the

physical processes associated with transport of sediment into the water column. Air migration tend to occur as a series of discrete "bubbling events" associated with a cyclical buildup of gas pressure within the sediment and a release of that pressure upon bubble release. This is consistent with discussions in the previous literature as well as observations of gas release from natural sediments transported to the hydraulics lab. This process is likely to be exacerbated in the tidally influenced Anacostia River as the tidal fluctuations in water level will create a cyclical variation in overlying pressure that should have a strong influence on the release of gas from the sediments. It is noted that this particular effect (tidally induced pressure variations) was not studied in the laboratory experiments. As the air bubbles emerge from the sediment bed, they carry a significant amount of sediment in their wakes. Observations showed that the amount of sediment resuspended depends on several factors such as bubble size, bubbling frequency and duration of bubbling. Once a channel is well-established in the sediment bed, there appears to be a reduction in the resuspension rate. This observation is based on both visual observations as well as turbidity measurements. Figure 5.15 shows one of the several channels that were formed in the sediment bed in the flume during an ebullition experiment. The size of the bubbles coming from the same channel tends to reduce over time if the bubbling is continuous. If a bubbling event from a channel stops at some point in time and restarts at a later time then the channel may heal itself to some extent. Consequently, the resuspension rates due to ebullition appear to be correlated to two time dependent processes, how long a bubbling event lasts and the time interval between successive events. It appears to be random where the channels form and at how many discrete points bubbling occurs at a given air flux rate. Therefore, considerable variation was observed among repeated experiments involving gas ebullition. The observations indicated multiple different bubbling locations formed over the surface of the entire sediment bed during the experiments suggesting that the results may be considered to be an aggregate of the effects averaged over the sediment bed surface area.

The initially selected ebullition fluxes were 1.2-12-48 cm/d. Applying these fluxes to the sediment bed surface area, air discharge rates can be calculated as 5-50-200 ml/min. These rates were considered in the experiments together with the step-wise increased

advective flow induced shear stress. Several experiments were conducted to investigate the effect of each ebullition rate. The investigations showed that 12 cm/d was a very high rate creating continuous air bubbling and this is felt to not be representative of occurrences in natural systems. 48 cm/d ebullition experiments were eliminated from further consideration because of this reasoning. On the other hand, 1.2 cm/d ebullition fluxes may end up with a situation where no air bubbling events occurred during some one hour measurements periods. One or two bubbling events lasting 20 minutes during the whole 5 hours of a single experiment was not definitive for the purpose of determining the added effect of ebullition on resuspension rate. Figure 5.16 shows the concentration measurements of a 1.2 cm/d ebullition experiment together with the result of an additional experiment that was conducted in order to observe the sole impact of ebullition on the resuspension rates. This latter experiment was conducted for each of the ebullition rates and consists of the application of a low shear stress not anticipated to cause any erosion of the sediment surface. During the regular (with shear stress increments) 1.2 cm/d ebullition experiment, only one ebullition event was observed during the first hour of the experiment creating higher suspended sediment concentrations compared to an advective flow experiment. On the other hand, one ebullition event was observed at a later time during a 1.2 cm/d ebullition with a very low shear stress flow experiment and then no further ebullition was observed. A short time following the end of the ebullition effect, there was also no further contribution to suspended sediment concentrations. It is generally observed in ebullition experiments that during the last hour of the experiment (highest shear stress level) resuspension rates closely correspond to those observed in an advective flow experiment with no ebullition. There are two possible explanations for that observation; one is that no ebullition occurs during that period of time and a second possibility is that the channels are formed in a well-defined configuration and the contribution of ebullition to the resuspension rates is minimal. In this particular case for both types of 1.2 cm/d ebullition experiments (with and without application of increasing shear stress increments) as the ebullition occurred only for a limited amount of time, there was no contribution of ebullition to the suspended sediment concentrations after bubbling stopped.

An additional ebullition flux of 2.4 cm/d (10 ml/min in terms of injection rate) was investigated in an effort to observe more ebullition events throughout the duration of an experiment. This rate also generally created fairly sustained bubbling in many of the experiments comparable to the 12 cm/d ebullition experiments, effectively limiting the ebullition rates that could be investigated with this experimental setup. Consequently, the 2.4 cm/d was the flux focused on for the remainder of the experimental investigation. Figure 5.17 shows the results for three 2.4 cm/d ebullition experiments together with the result of an advective flow only (no ebullition) experiment. In two of the three experiments, distinct ebullition events lasting between 20-60 min. were observed increasing the suspended sediment concentrations continuously through the duration of the experiments. Although the same experimental procedures were applied, one experiment resulted in a different outcome and corresponding concentration history. In this experiment, the ebullition event was continuous through the duration of the experiment and the effect of the ebullition on the concentration measurements was less compared to the other experiments. This is believed to be the result of formation of well-defined bubbling channels. It is noted that final slopes in all experiments are nearly the same suggesting that in the last hour of the experiment, the resuspension is dominated by the effect of the applied shear stress and independent of the ebullition rate which is the result of the formation of the well-defined channels. Figure 5.18 shows the result of the experiment with 2.4 cm/d ebullition under a very low but constant shear stress in comparison to the 2.4 cm/d ebullition experiment with the increasing shear stress increments. In the first experiment, the suspended concentration approaches a constant value (actually with a slight decrease) in the latter phases of the experiment, suggesting that ebullition is no longer effective in sediment resuspension. Since bubbling was observed during the latter phases of the experiment, the only explanation is that some process occurs where the channel wall through which the air escapes somehow becomes armored to further sediment removal. The data also suggest that since the low shear stress applied to the bed was ineffective in creating any resuspension, a decrease in suspended sediment concentration is observed, presumably due to deposition in quiescent areas within the flume.

The experiments with 12 cm/d ebullition flux resulted in continuous bubbling throughout the duration of the experiments. Figure 5.19 shows the results of two experiments in comparison to that of an advective flow experiment. The major difference observed between these two experiments was in the initial pressurization level required to start the bubbling; this effect was also observed for several other sets of experiments. Although the sediment bed was prepared applying the same procedure, sometimes it took more pressure to start bubbling than other experiments and therefore bubbling started later in the experiment. As a result, the final suspended sediment concentrations were different. This is believed to be the consequence of the random nature by which the ebullition channels formed. The effect of ebullition on suspended sediment concentrations was examined by performing an ebullition experiment in the presence of a low shear stress flow as also performed for other experiments with different air injection rates. The outcome was the same indicating the decreased effectiveness of ebullition once the bubbling channels were formed (Figure 5.20). In addition, the repetitions of the constant low shear stress experiments demonstrated some degree of variability resulting in different resuspension rates each time they were repeated.

As can be seen from a synthesis of all the data, ebullition results in greater sediment resuspension compared to advective flow only experiments. This effect increases with the ebullition rate (Figure 5.21). However, the data also suggest that once bubbling channels are formed in the sediment bed, the contribution of ebullition to the resuspension rates becomes minimal. For the resuspension rate calculations, the data obtained from the 2.4 cm/d ebullition experiments were examined in more detail. It was noted that the computation of resuspension rates was not straightforward and the number of experiments to study was limited. The issue arises from the apparent random nature of ebullition events. As opposed to the hourly resuspension rates computed for seepage and advective flow experiments, it is not possible to compute rates in a time averaged manner for the ebullition experiments. Ebullition events seem to create resuspension on an event-oriented basis. Each event has its own resuspension potential and this potential basically depends on several parameters as explained previously. The data suggest that the amount of pressure build-up between the events affects the resuspension rates significantly. If

somehow bubbling does not occur for an extended period of time, pressure builds up significantly creating very high resuspension rates when the pressure is released. However, the relationship between the pressure build-up and the resuspension rates does not seem to follow a well-defined trend. In the 2.4 cm/d ebullition experiments, the initial bubbling event lasted 40-50 min and an average resuspension rate associated with it was calculated as approximately 0.85-1.85 mg s^{-1} m^{-2}. In general, the magnitude of water head required to initiate the ebullition process by overcoming the hydrostatic pressure, pressure of the sediment layer and the surface tension of the hoses varied from 1.1 m to 1.2 m. There is no direct relationship between the duration of the event and the pressure build-up to start the event. In one of the three experiments, the ebullition event was continuous. In the two other experiments, for the five hour duration of the experiments, 3-4 more events occurred lasting 20-60 min each. The amount of pressure build-up for these additional events ranged from 0.09-0.52 m with the resuspension rates ranging between 1.05-3.86 mg s^{-1} m^{-2} and the highest resuspension rate generally corresponds to the highest amount of pressure build-up, but not all the time. As the advective flow was also quite effective in increasing the suspended sediment concentrations during the last three hours of the experiments, some of the rates calculated include the effect of erosion due to shear. If the two 2.4 cm/d ebullition experiments in the presence of a low shear stress are examined, they correspond to one initial high resuspension rate due to continuous bubbling. Rates from these experiments varied between 0.96-1.27 mg s^{-1} m^{-2}. The average standard deviation calculated for advective flow only experiments with respect to the quadratic curve fit relationship is 0.25 mg s^{-1} m^{-2} therefore; the uncertainty involved in some of the ebullition experiments is significantly higher, for example 2.4 cm/d ebullition experiments giving a range of 1.05-3.86 mg s^{-1} m^{-2} for the resuspension rates.

In an effort to determine the contribution of ebullition to resuspension rates, the amount of sediments in suspension was calculated. For the three 2.4 cm/d ebullition experiments, the amount of sediment suspended due to the advective flow induced shear stresses was calculated using the quadratic equation determined previously as

$$R = 96.7(\tau - 0.194)^2 \quad (5.3)$$

It was determined that 40 g of sediment on average was suspended due to the effect of advective flow in each experiment. The contribution of the ebullition to the total was calculated from the concentration measurements made in the experiments with 2.4 cm/d ebullition in the presence of low shear stress as 50 g on average. Although the amount of suspended sediment in a 2.4 cm/d ebullition experiment would be expected as 90 g, two of the ebullition experiments resulted in 140 g on average. These ones involved discrete ebullition events throughout the duration of the experiments. The one with the continuous bubbling, on the other hand, resulted in approximately 80 g of sediment resuspension. It was concluded that the final sediment concentrations in water are highly depended on how the ebullition progresses and apparently, calculating the resuspension rates related to the contribution of the ebullition is highly dependent on the specific nature of the ebullition process.

5.3.2. Sand Cap

The sand cap with d_{50}=340 μm was examined for its effectiveness in minimizing the resuspension rates under the influence of ebullition. None of the air injection fluxes (1.2 cm/d, 2.4 cm/d, and 12 cm/d) caused any detectable suspended sediment concentration in the flume within the duration of the experiments. This result indicates that the cap material filtered all the contaminated sediment transported by bubbles from the sediment layer beneath it. However, it is unknown if any resuspension would be detected over extended periods of time, but the qualitative observations reported in Chapter 3 admit this possibility. In addition, observations in the flume did not show any indication of bed destabilization on the cap due to air injection. A low flow rate was used to re-circulate the flow in the flume without creating any destabilization on the surface of the bed due to the shear stress applied.

5.4. Results and Discussion for the Combined Effect of Pore Water and Ebullition Fluxes

5.4.1. The Anacostia River Sediment Bed

It would be reasonable to expect seepage and ebullition occurring at the same time in nature. In fact, pore water movement could potentially decrease the bulk density of the sediment facilitating the release of gas pressure or alternatively, bubbling events could facilitate the movement of the pore water by creating channels in the bed. Therefore, in this part of the investigation, the combined effect of water and air injection on resuspension rates was examined. The effect of pore water fluxes of 1.2 cm/d and 12 cm/d together with 2.4 cm/d ebullition flux was examined. The reasoning behind the decision of focusing on 2.4 cm/d ebullition flux were explained in the previous section. The observations made in separate pore water and ebullition experiments were still valid for these experiments. The resuspension rates, on the other hand, showed some differences. Figure 5.22 shows the suspended sediment concentration measurements from two repetitions of the 1.2 cm/d pore water - 2.4 cm/d ebullition experiments. The results seem very consistent and in comparison to the 1.2 cm/d pore water or 2.4 cm/d ebullition experiments, the combined effect of the processes creates higher suspended sediment concentrations. The same behavior is observed with 12 cm/d pore water - 2.4 cm/d ebullition experiments with much higher concentration values (Figure 5.23). The results of the two repetitions give consistent results similar to the previous case. If all the results are compared to each other, the 12 cm/d pore water - 2.4 cm/d ebullition experiments create the highest resuspension rates and followed by the 12 cm/d pore water experiment (see Figure 5.24). The complex influence of ebullition on resuspension processes raises the same issues related to the resuspension rate calculations as were discussed above for ebullition only experiments

5.4.2. Sand Cap

The sand cap with d_{50}=340 μm was examined for its effectiveness in minimizing resuspension rates under the combined influence of ebullition and pore water flux. Although no contribution to suspended sediment concentrations was observed in the

experiments considering the individual effects of ebullition and seepage, the possibility of resuspension when these factors act together was investigated. Observations from the experiments involving the application of the highest pore water flux (12 cm/d) and ebullition flux (12 cm/d) on the sand cap indicated no sediment resuspension into the flow. The sand cap was still effective in filtering the sediment. No indications of bed destabilization were observed on the sand cap surface.

After analyzing the data collected from different types of experiments conducted within the content of this study, it is concluded that pore water movement and gas ebullition through the beds are in fact significantly effective in increasing the resuspension rates if the rates are large enough. In typical bed stability investigations, both processes need to be considered in addition to the advective flow induced shear stresses. The degree of impact of ebullition and seepage depends on the rates of fluxes and therefore in-situ measurements of these fluxes are required. Although additional investigations may be required to include the effect of consolidation degree in a way that is more representative of the field conditions, quadratic relationships provided in the previous sections are useful to predict the erosion rates especially for newly deposited surficial sediment beds. For the derivation of the quadratic excess shear stress-resuspension rate formula, average resuspension rates computed for each shear stress increment were used as this was determined to be a reasonable approach in predicting general trends. It is noted that the data also demonstrated that there is a significant variation in resuspension rates during one hour shear stress increments. The rates tend to decrease towards the end of one hour increment.

Pore water experiments showed that with the increased rate of injection, resuspension rates are increased. It is believed that the sediment is entrained into the water column by vertical pore water flow which creates channels in the bed. No significant change in critical shear stresses was observed. Only a limited number of experiments were performed and this fact should be considered in making generalizations. Within the range of pore water fluxes tested, a linear function relating resuspension rate constant to pore water fluxes was also provided in the previous sections. Contrary to advective flow and

pore water experiments, it was not possible to derive a relationship between resuspension rates and ebullition fluxes. Two extreme cases with low and high ebullition rates were observed. In a case with a relatively low ebullition flux, it was not possible to generate multiple bubbling events which would have been necessary in order to derive some conclusions regarding the effect of ebullition. On the other hand, in a case with a high ebullition flux, bubbling was continuous; it seems doubtful that this occurrence is consistent with what occurs in natural systems. Therefore, the experiments were restricted to a very narrow range of ebullition fluxes. Resuspension rates were determined to be event-oriented and there was no direct or consistent relationship between duration of the events or the pressure build-up leading to the formation of the events and resuspension rates. However, data showed that higher ebullition fluxes resulted in higher suspended sediment concentrations. When the effects of ebullition and pore water fluxes were combined, the resuspension rates were increased even more. It is important to note that for a given ebullition flux, a continuous bubbling event tends to end up with lower resuspension rates when compared to an ebullition event consisting of distinct bubbling events. This is attributed to the formation of well-defined channels in case of continuous bubbling. For two repetitions of the same experiment, it is possible to observe either a continuous ebullition or a set of distinct bubbling events unless the ebullition flux is very high causing continuous bubbling. This variability in behavior indicated the random nature of the ebullition events.

AquaBlok® stability tests revealed that this material is highly stable under even very high bed shear stresses. Critical shear stress of the sand cap has been determined to be quite close to the critical shear stress of the Anacostia sediment. If a consolidated state of the Anacostia sediment is considered, the sand cap could be even less stable. Therefore, careful consideration is required in selection of the appropriate sand cap material which is expected to be more resistant to erosion when compared to the native sediment. Although there might be some questions related to stability of the selected sand cap material placed in the Anacostia River, it has been demonstrated by the resuspension data that the sand cap filters the sediment carried from the sediment layer beneath it by either ebullition or seepage or a combination of the two processes. It is important to note that these

experiments were run for a limited period of time and if the duration of the experiments is increased, there might be a possibility to get some resuspension into the water column. The flux chamber experiments described in Chapter 3 showed indications of this possible behavior.

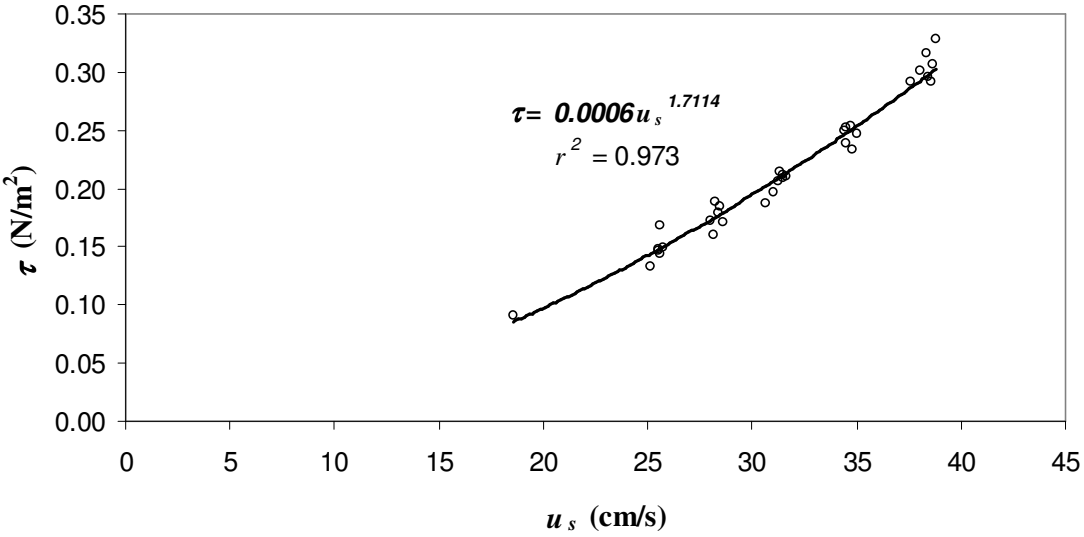

Figure 5.1: The relationship defining the correlation between free stream velocity, u_s and bed shear stress, τ.

Q (m^3/s)	u_s (cm/s)	τ (N/m^2)
0.033	25.511	0.153
0.036	27.996	0.180
0.041	31.027	0.214
0.046	34.513	0.257
0.051	38.454	0.309

Table 5.1: Average discharge, free stream velocity and bed shear stresses applied to the test section for the resuspension experiments.

Figure 5.2: Eroded sediment bed surface with lighter colored oxidized sediment layer and the underlying darker layer at the eroded locations of the bed.

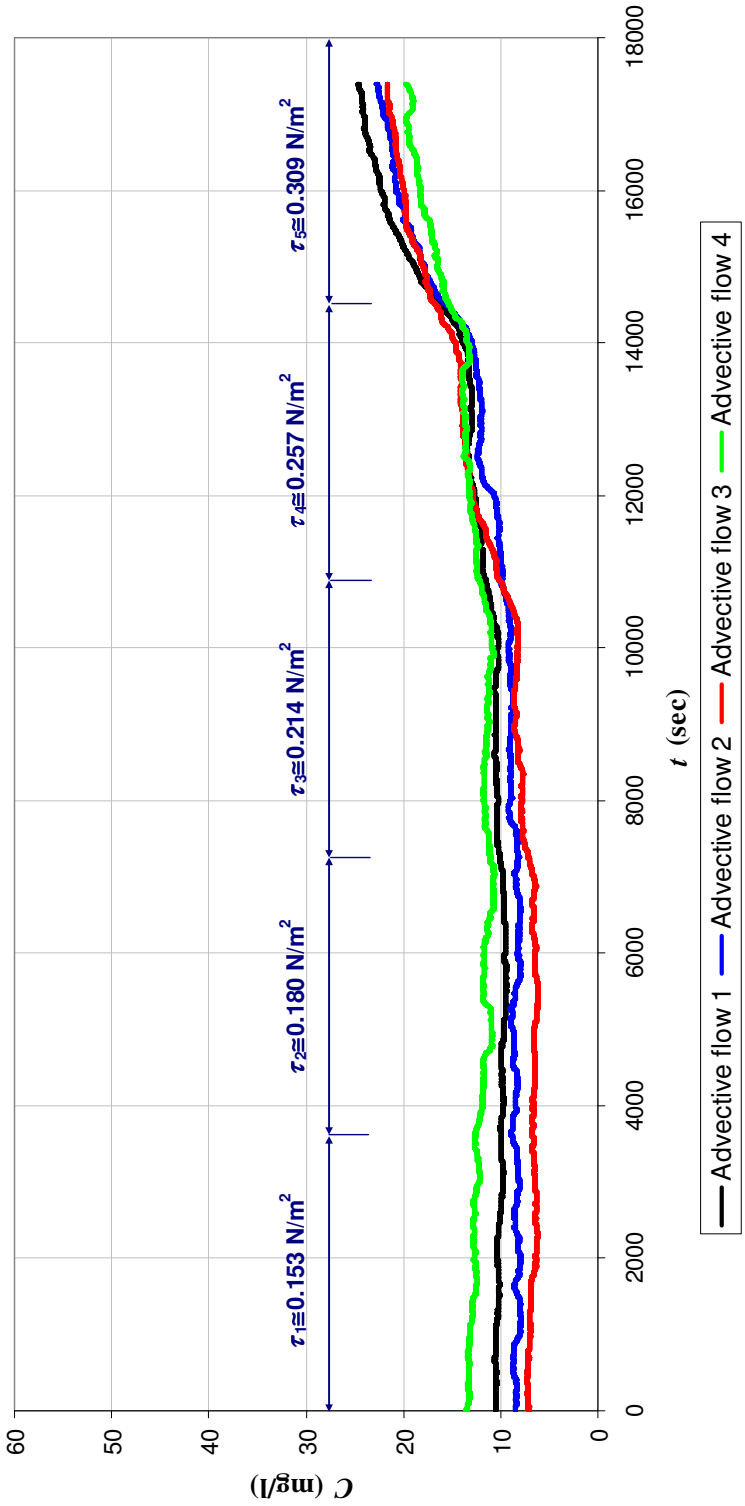

Figure 5.3: Sediment concentration versus time graphs for four advective flow experiments together with the applied bed shear stresses.

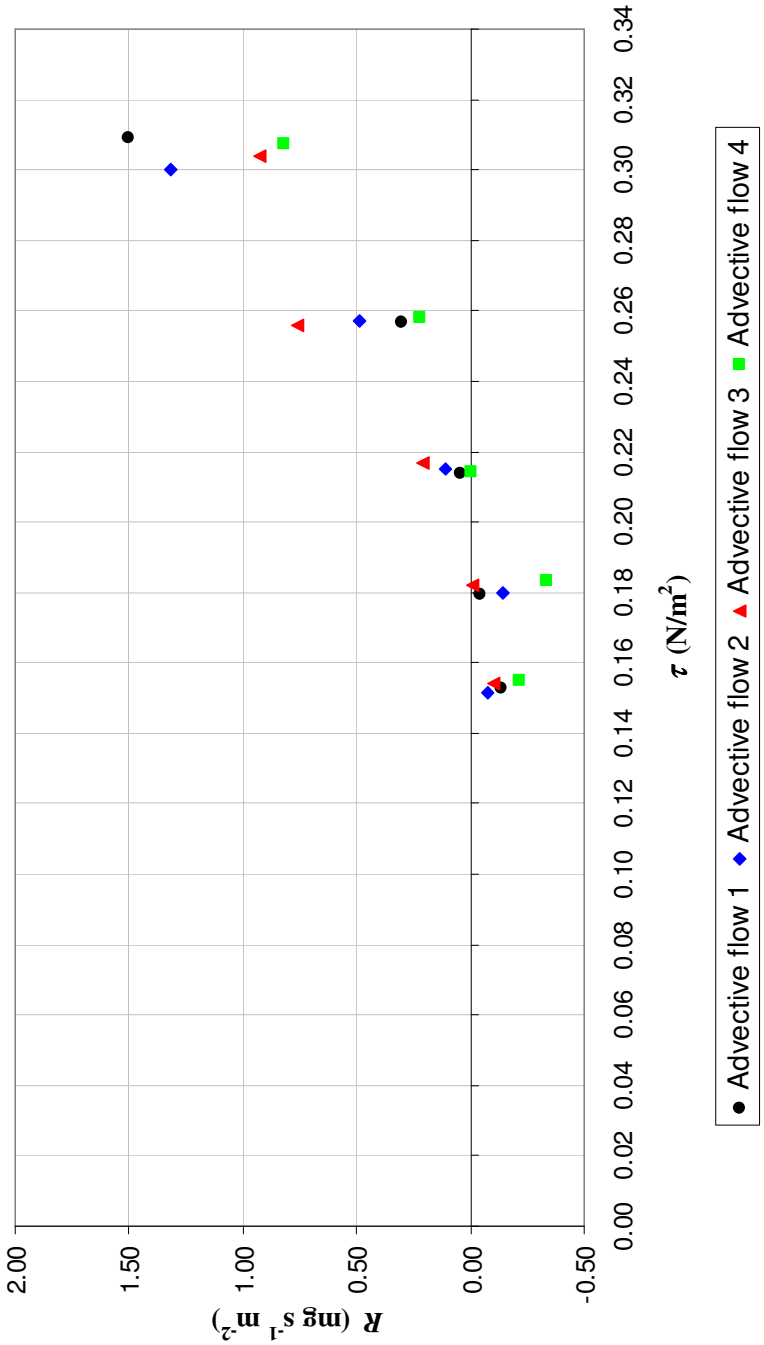

Figure 5.4: Hourly averaged resuspension rates (*R*) versus applied shear stresses (τ) for four advective flow experiments.

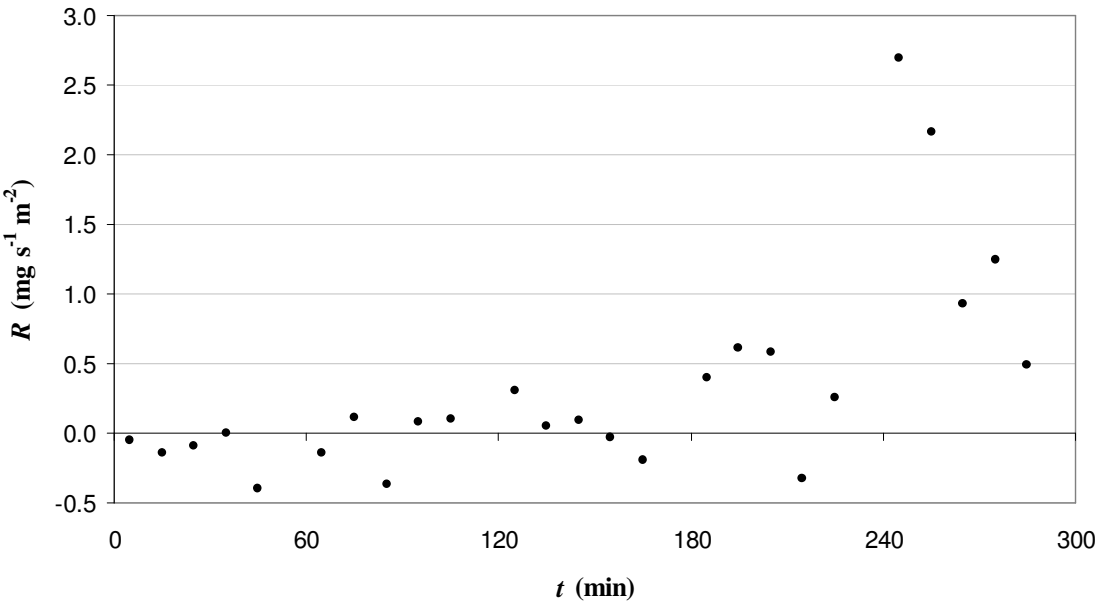

(a)

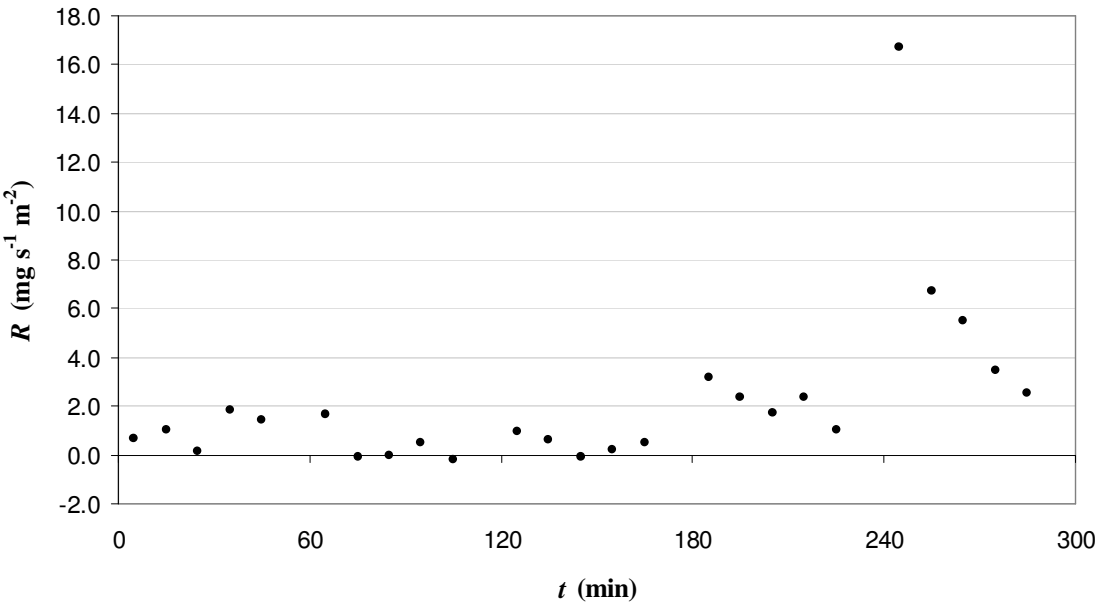

(b)

Figure 5.5: Sample resuspension rate versus time graphs showing the variation of the rates during each hour of the five hour long experiments: (a) "Advective flow 1" experiment, (b) "12 cm/d pore water 1" experiment.

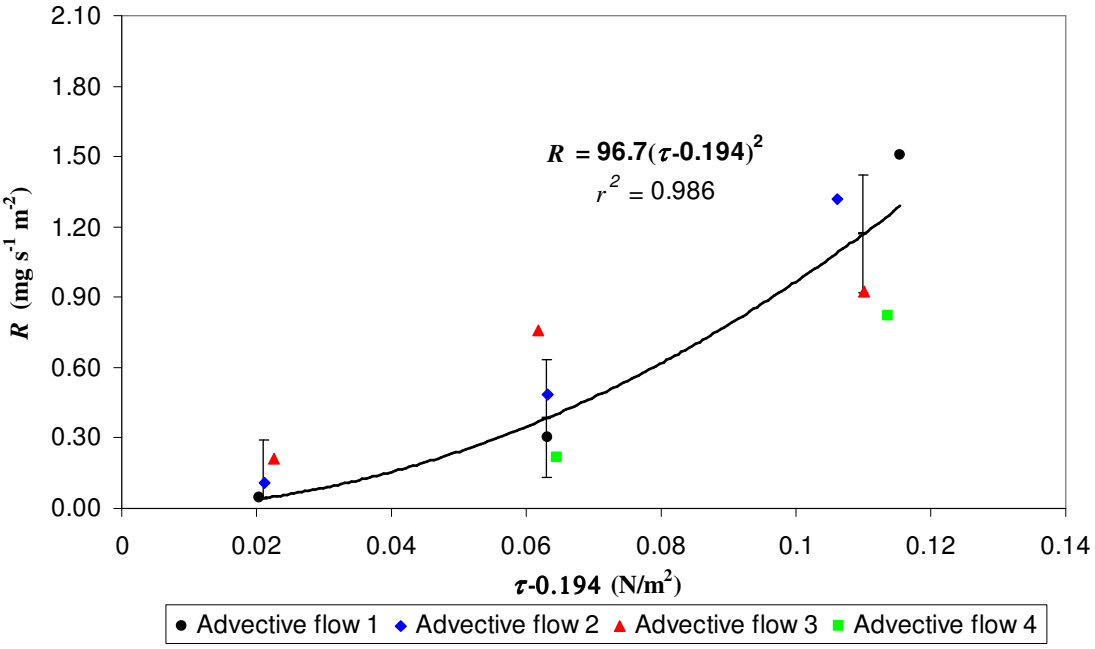

Figure 5.6: Curve fit according to the "Advective flow 1" experiment and the results of all the advective flow experiments with respect to the curve fit.

d_{50} (μm)	τ_c (N/m^2)	Ratio to τ_c of Cohesive Anacostia River Sediment
160	0.174	0.90
340	0.260	1.34
500	0.234	1.21
1200	0.492	2.53

Table 5.2: Critical shear stresses for different size sand beds and their ratios to the critical shear stress of the Anacostia River sediment (0.194 N/m^2).

Q (m^3/s)	u_s (cm/s)	τ (N/m^2)
0.033	26.494	0.164
0.035	29.538	0.197
0.041	32.374	0.231
0.046	35.883	0.275
0.051	39.515	0.324
0.056	42.685	0.370
0.058	45.220	0.408
0.069	53.921	0.552
0.078	60.454	0.671
0.101	79.276	1.067
0.126	108.935	1.839
0.142	115.488	2.032
0.143	132.324	2.565

Table 5.3: Average discharge, free stream velocity and bed shear stresses applied to test section for AquaBlok® experiments.

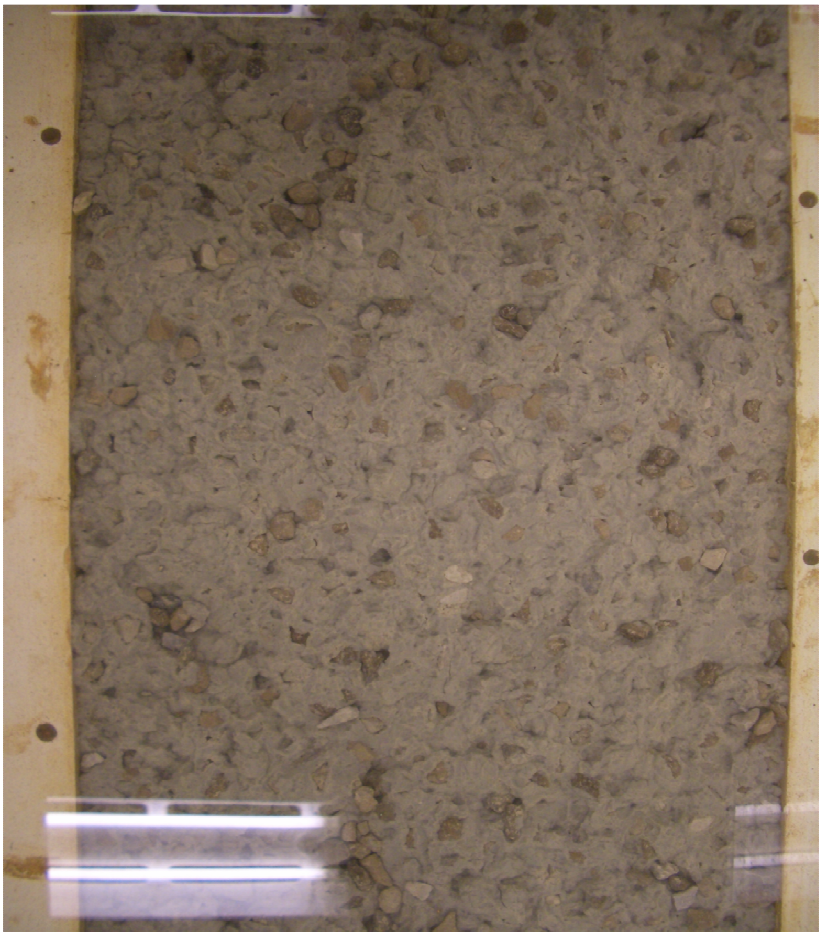

Figure 5.7: AquaBlok® bed surface after an experiment (aggregate adhering to the bentonite layer underneath creating an armoring layer).

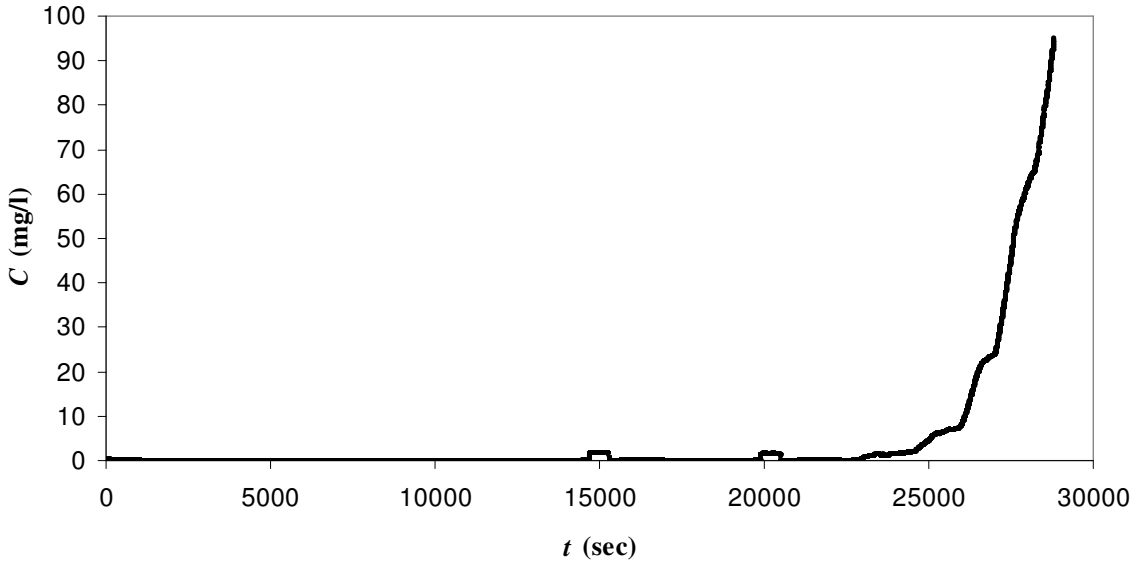

Figure 5.8: Concentration measurements from an AquaBlok® bed stability experiment (turbulence next to the pump entrance further downstream of the test section created resuspension of previously eroded bentonite material which was not related to the bed stability).

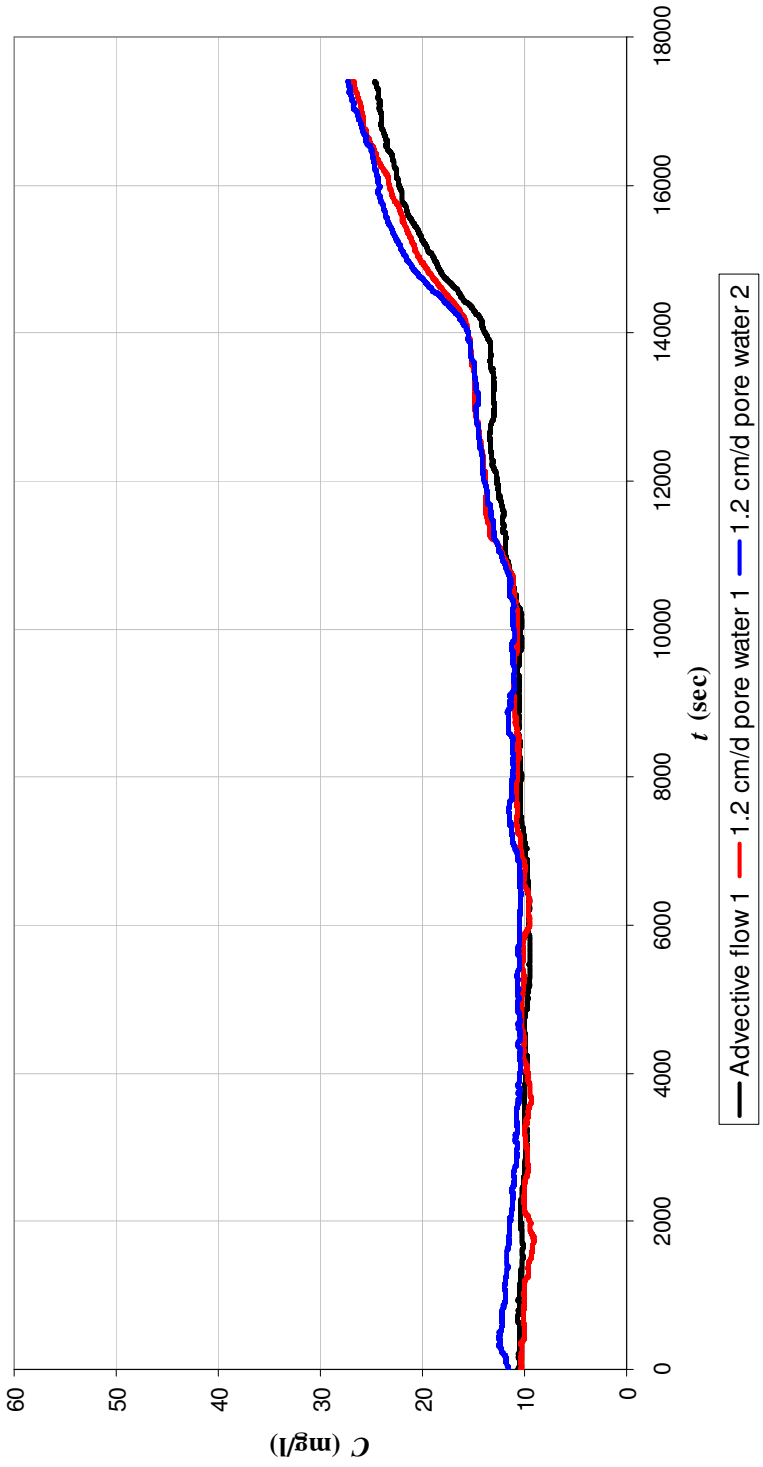

Figure 5.9: Suspended sediment concentration measurements from two 1.2 cm/d pore water experiments in comparison to the suspended sediment concentration measurements from an advective flow experiment.

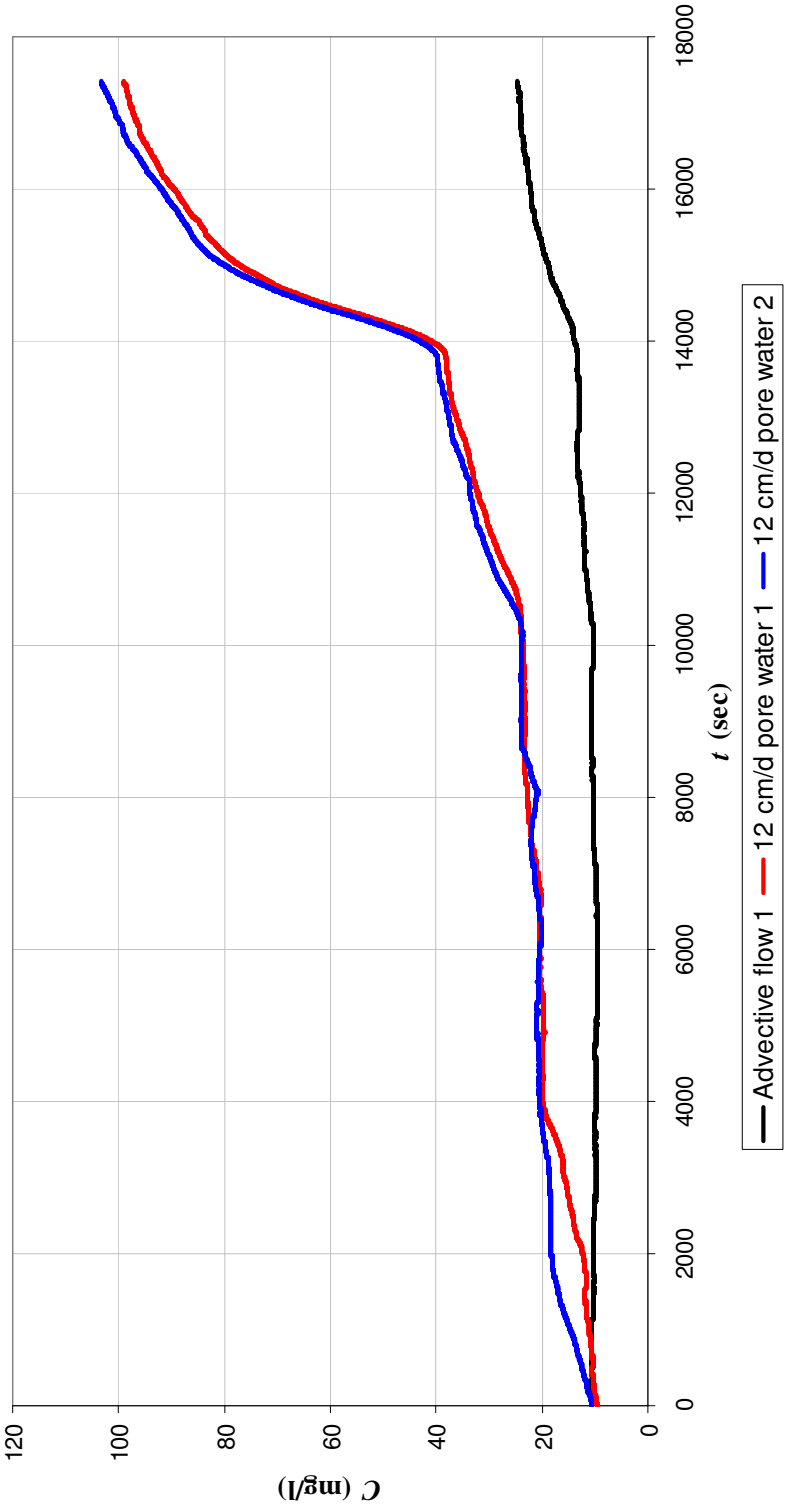

Figure 5.10: Suspended sediment concentration measurements from two 12 cm/d pore water experiments in comparison to the suspended sediment concentration measurements from an advective flow experiment.

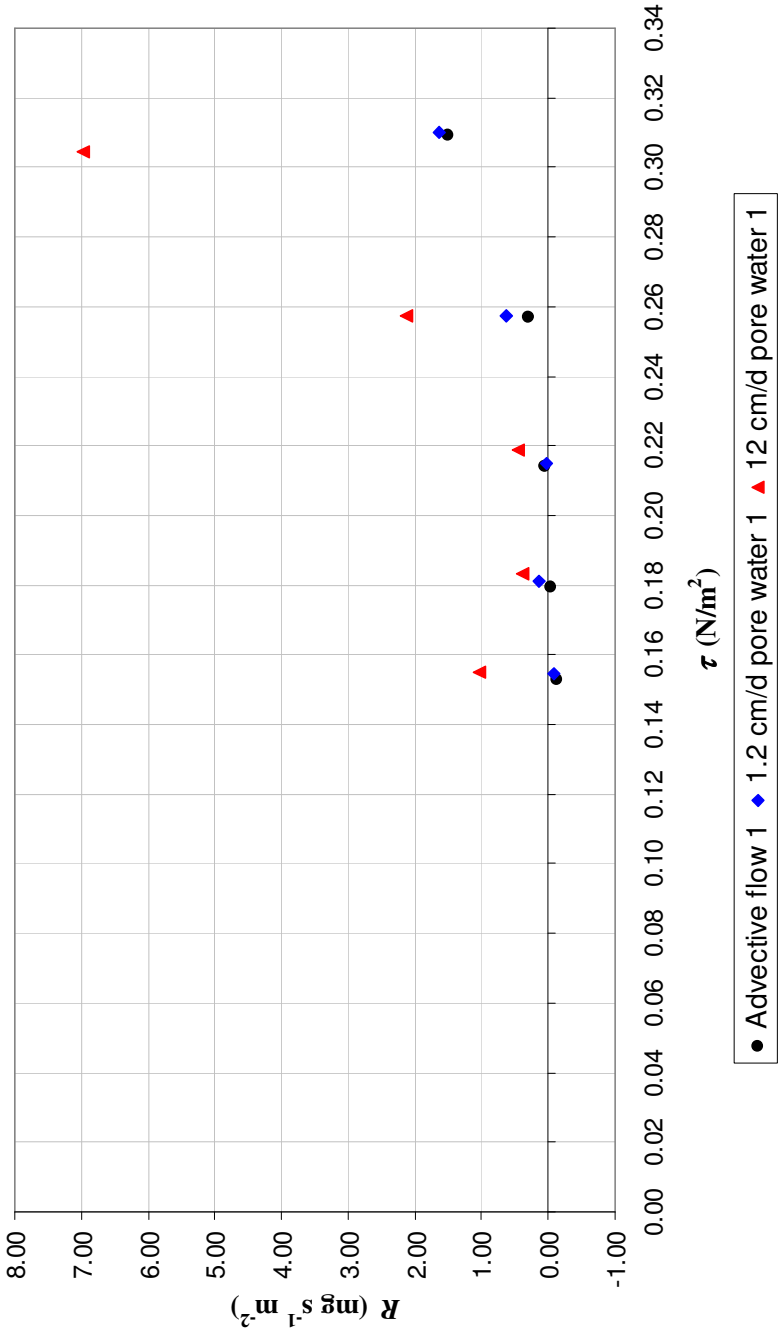

Figure 5.11: A comparison of the resuspension rates calculated for an advective flow experiment, a 1.2 cm/d pore water experiment and a 12 cm/d pore water experiment.

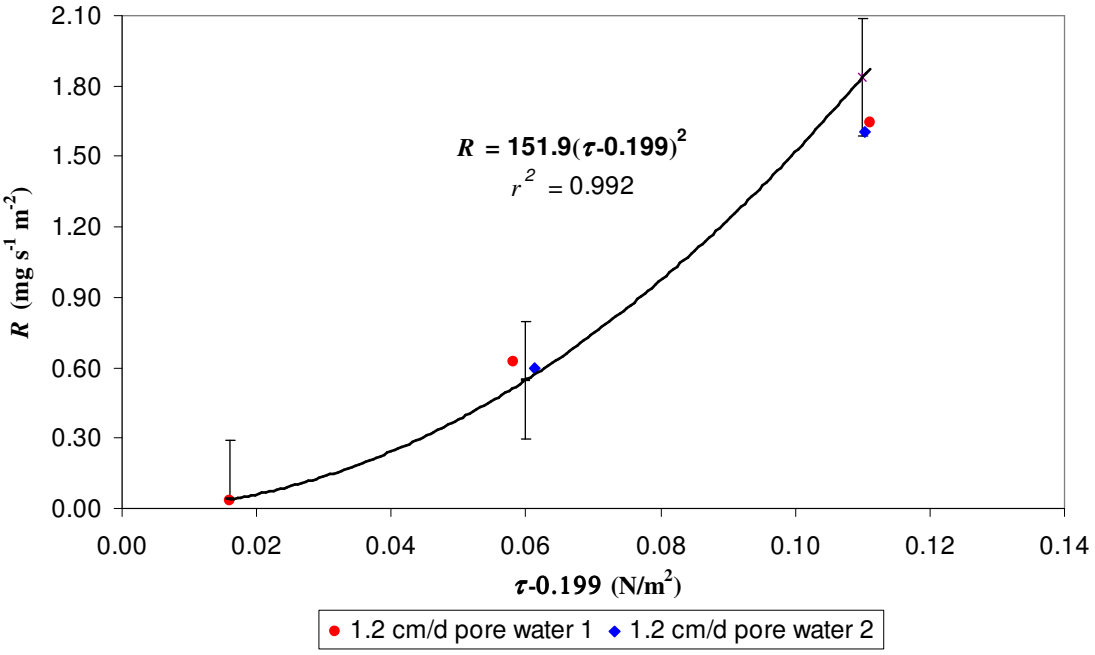

Figure 5.12: Curve fit according to the "1.2 cm/d pore water 1" experiment and the results of both 1.2 cm/d pore water experiments with respect to the curve fit.

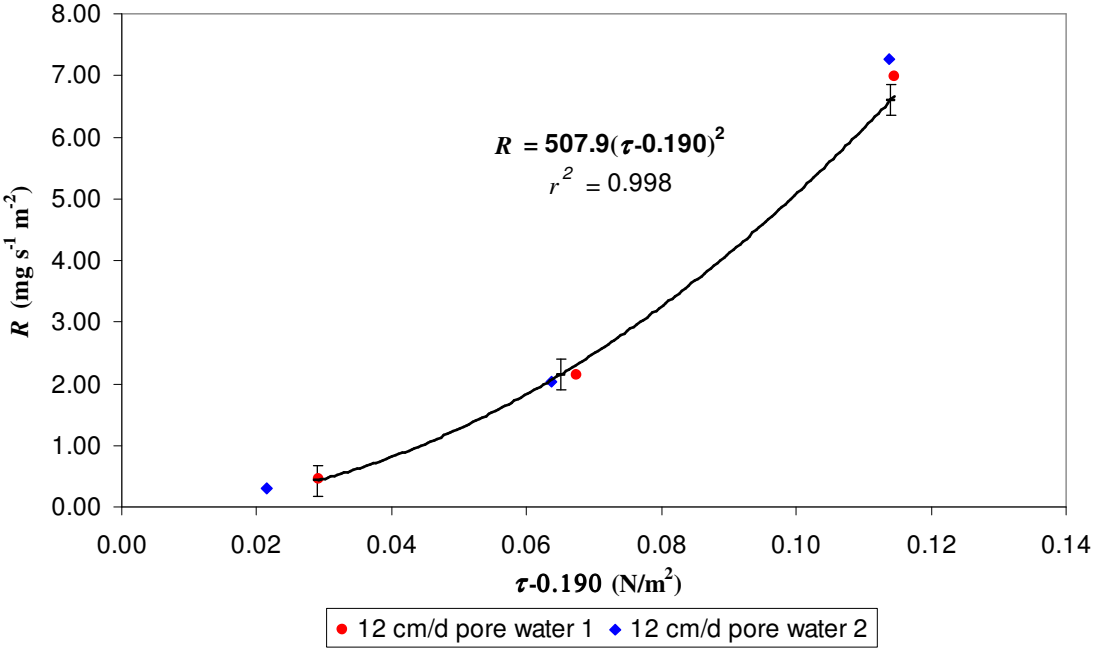

Figure 5.13: Curve fit according to the "12 cm/d pore water 1" experiment and the results of both 12 cm/d pore water experiments with respect to the curve fit.

I (cm/d)	Seepage rate (ml/min)	M (mg s^{-1} m^{-2} Pa^{-2})	τ_c (N/m^2)
0	0	96.7	0.194
1.2	5	151.9	0.199
12	50	507.9	0.190

Table 5.4: The values for parameters in $R = M(\tau - \tau_c)^2$ with respect to different pore water fluxes (I).

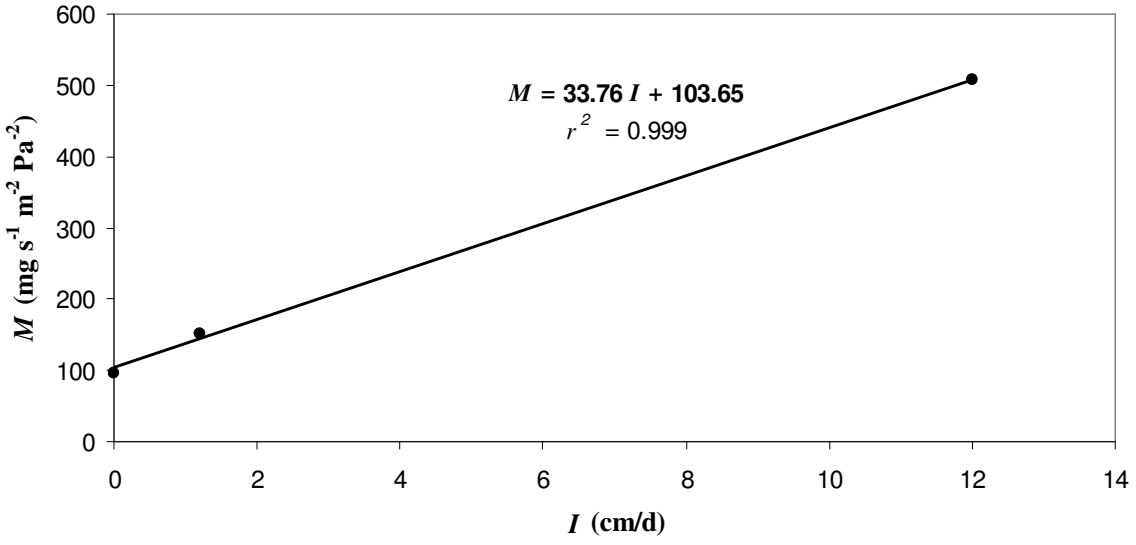

Figure 5.14: The relationship between the pore water flux (I) and the resuspension rate constant (M).

Figure 5.15: A view from the surface of a well-established channel formation in the cohesive sediment bed as a result of continuous air bubbling and local erosion created at close proximity of the channel (flow direction is from right to left and the channel is located towards the middle of the test section, the smooth surface is downstream from the bubble channel).

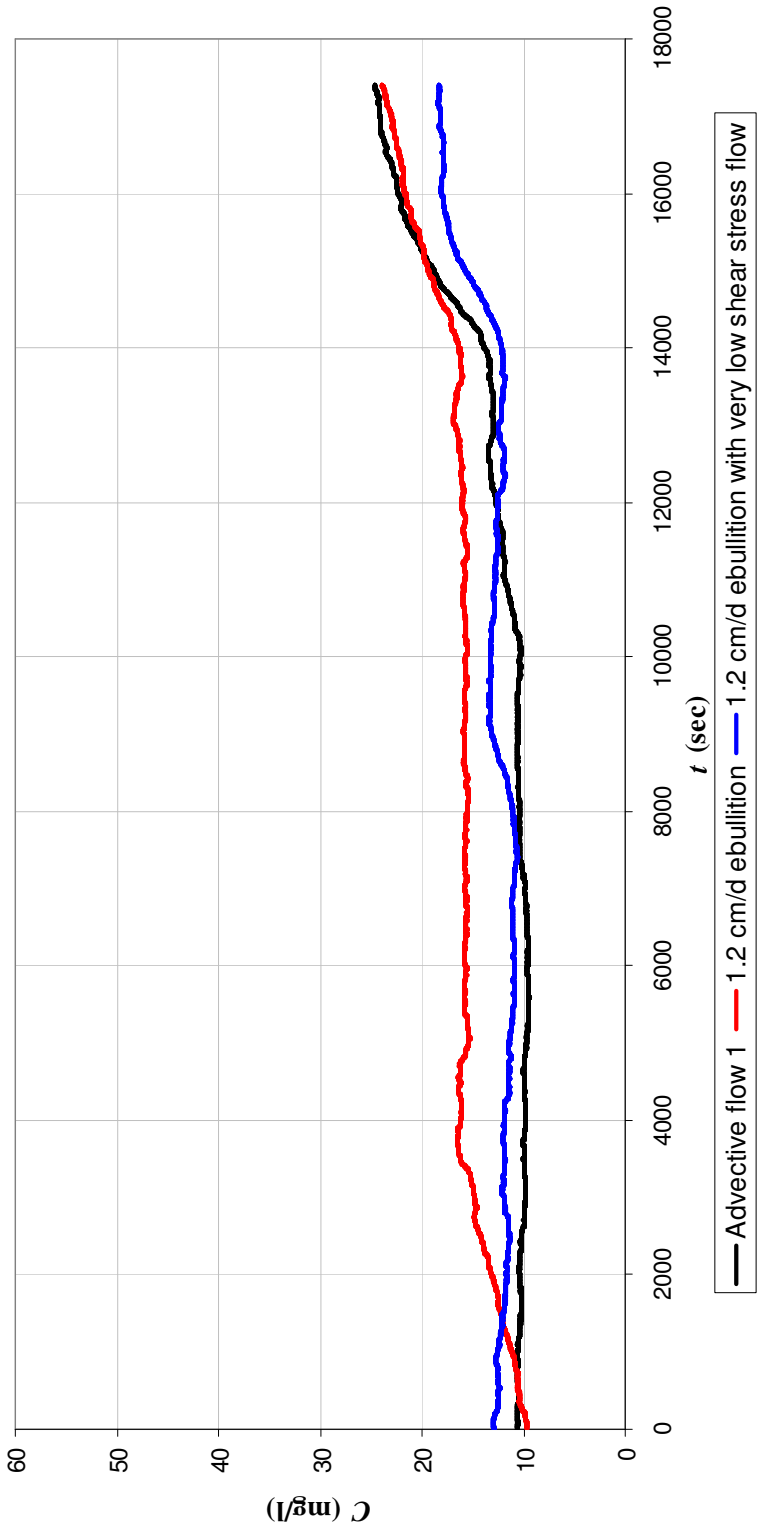

Figure 5.16: A comparison of the suspended sediment concentration measurements from an advective flow experiment, a 1.2 cm/d ebullition experiment and a 1.2 cm/d ebullition with very low shear stress flow experiment.

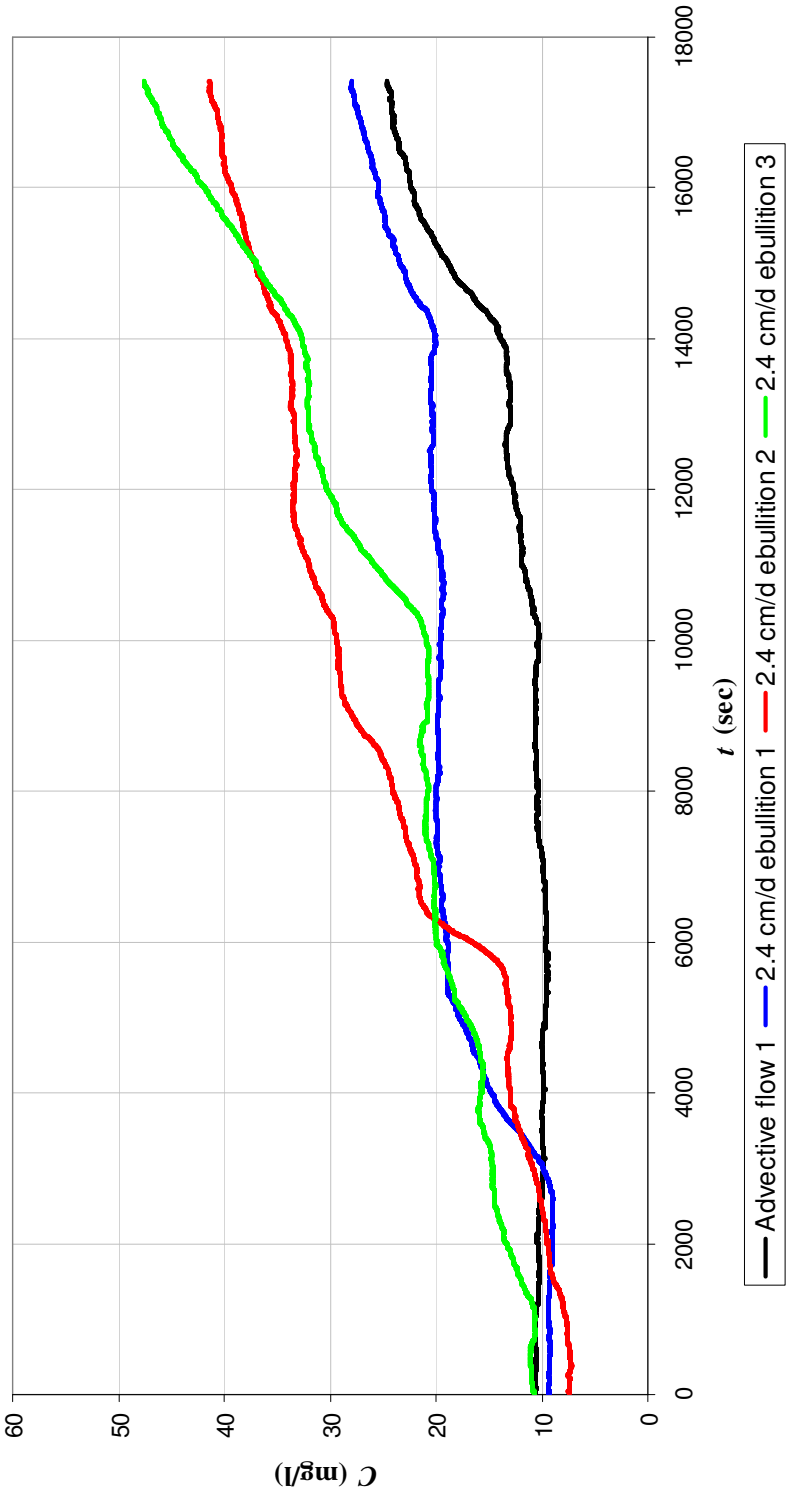

Figure 5.17: Suspended sediment concentration measurements from three 2.4 cm/d ebullition experiments in comparison to the suspended sediment concentration measurements from an advective flow experiment.

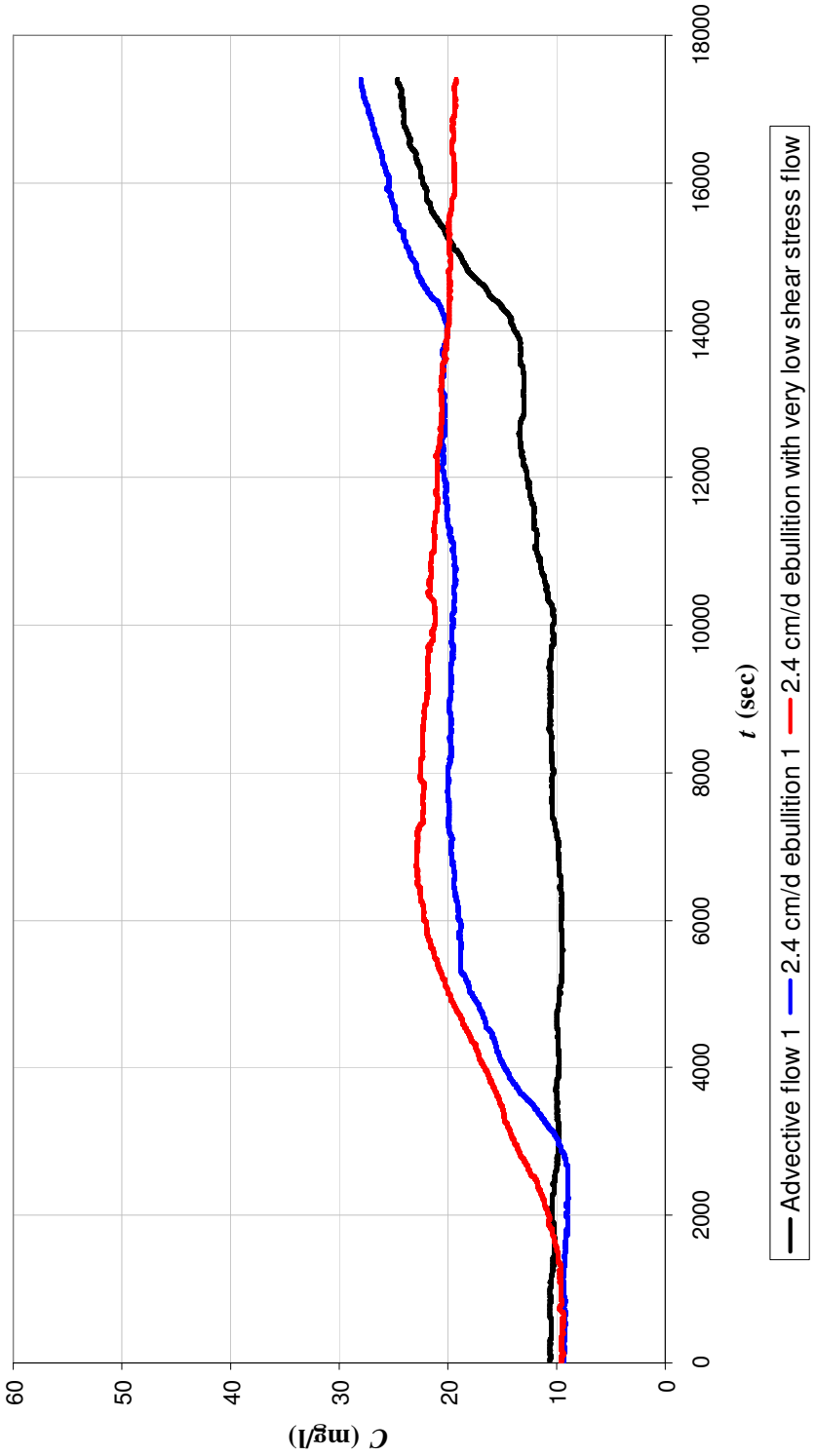

Figure 5.18: Suspended sediment concentration measurements from a 2.4 cm/d ebullition experiment in comparison to the suspended sediment concentration measurements from an advective flow experiment and a 2.4 cm/d ebullition with very low shear stress flow experiment.

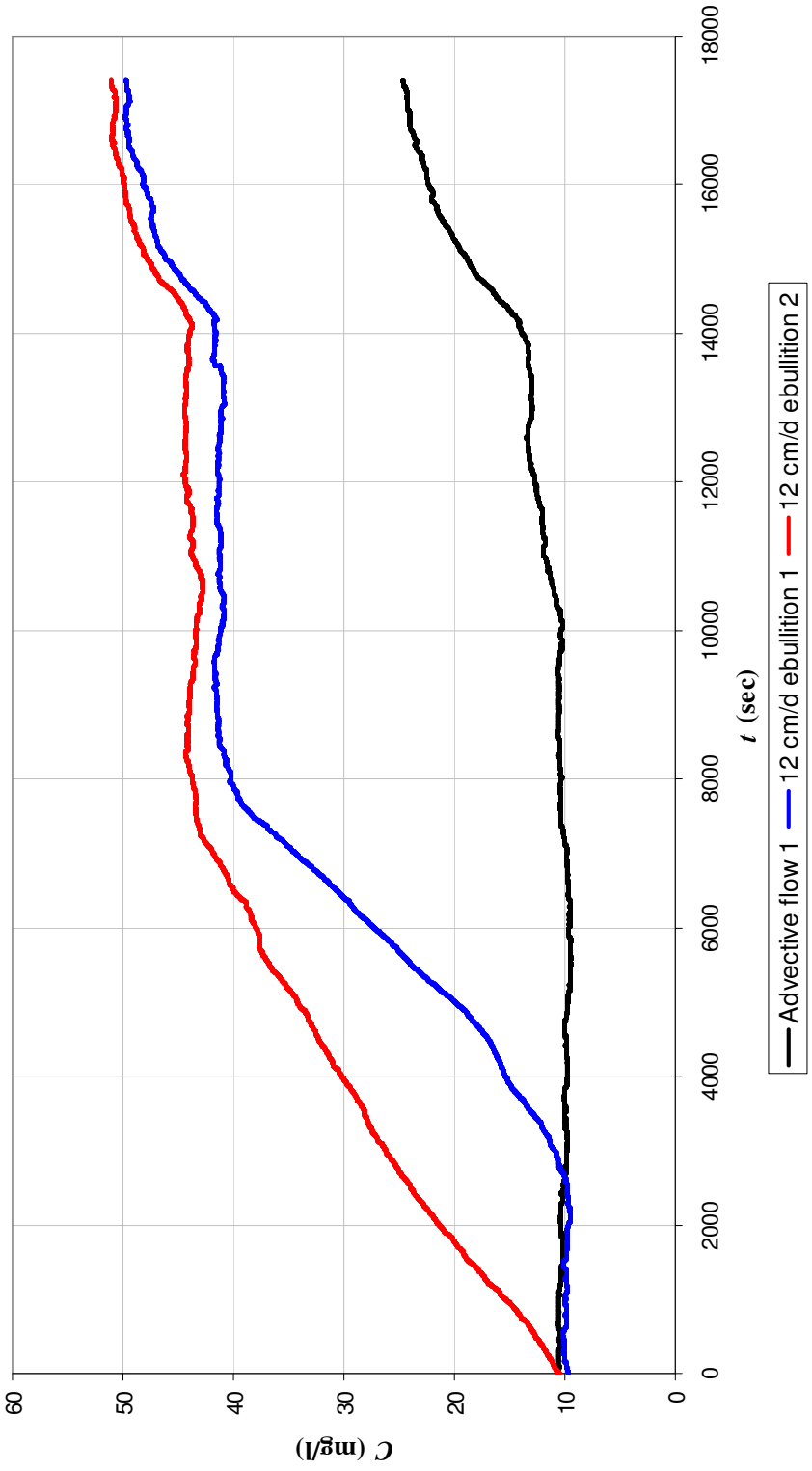

Figure 5.19: Suspended sediment concentration measurements from two 12 cm/d ebullition experiments in comparison to the suspended sediment concentration measurements from an advective flow experiment.

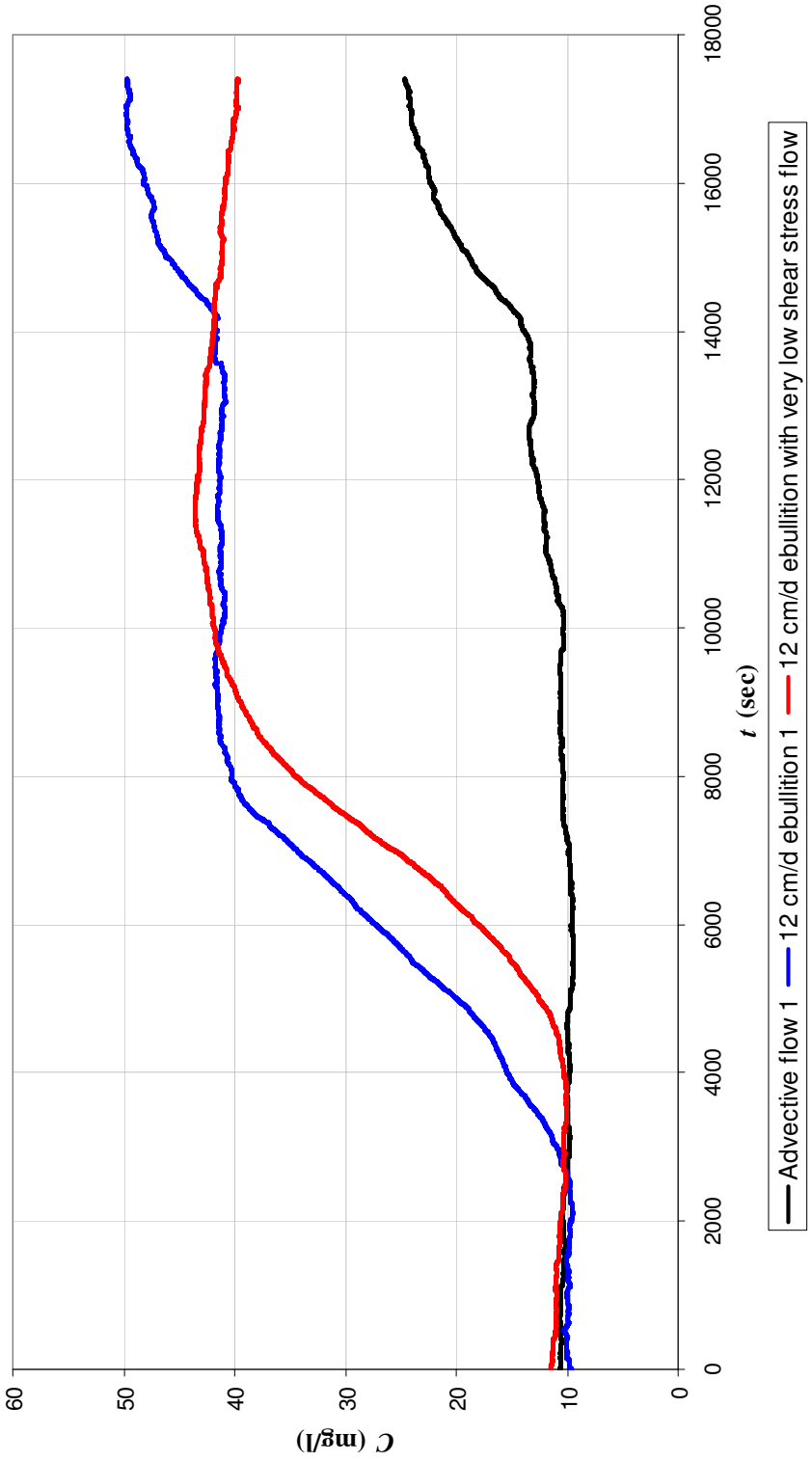

Figure 5.20: Suspended sediment concentration measurements from 12 cm/d ebullition experiment in comparison to the suspended sediment concentration measurements from an advective flow experiment and a 12 cm/d ebullition with very low shear stress flow experiment.

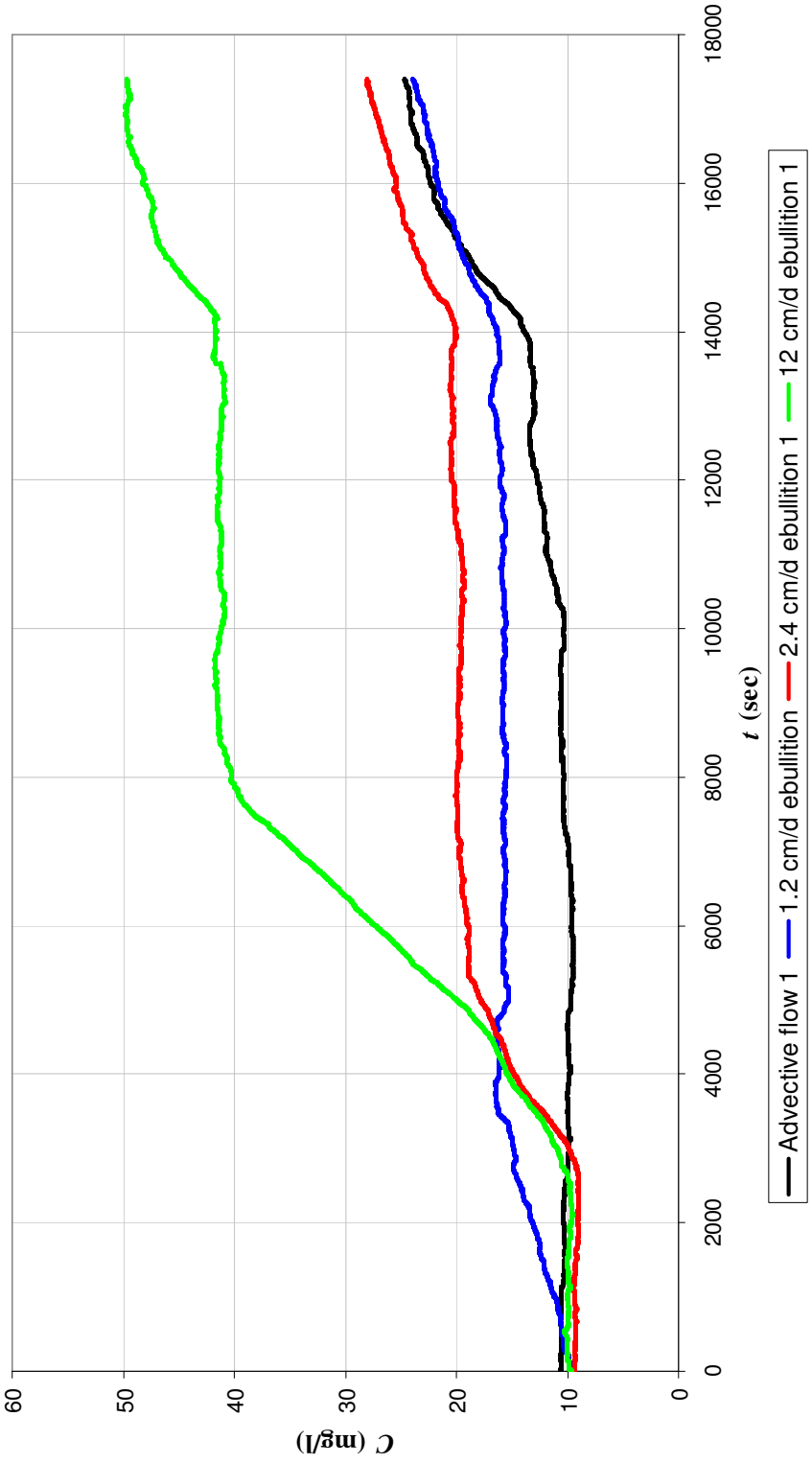

Figure 5.21: A comparison of suspended sediment concentration measurements among ebullition experiments with different ebullition fluxes and an advective flow experiment.

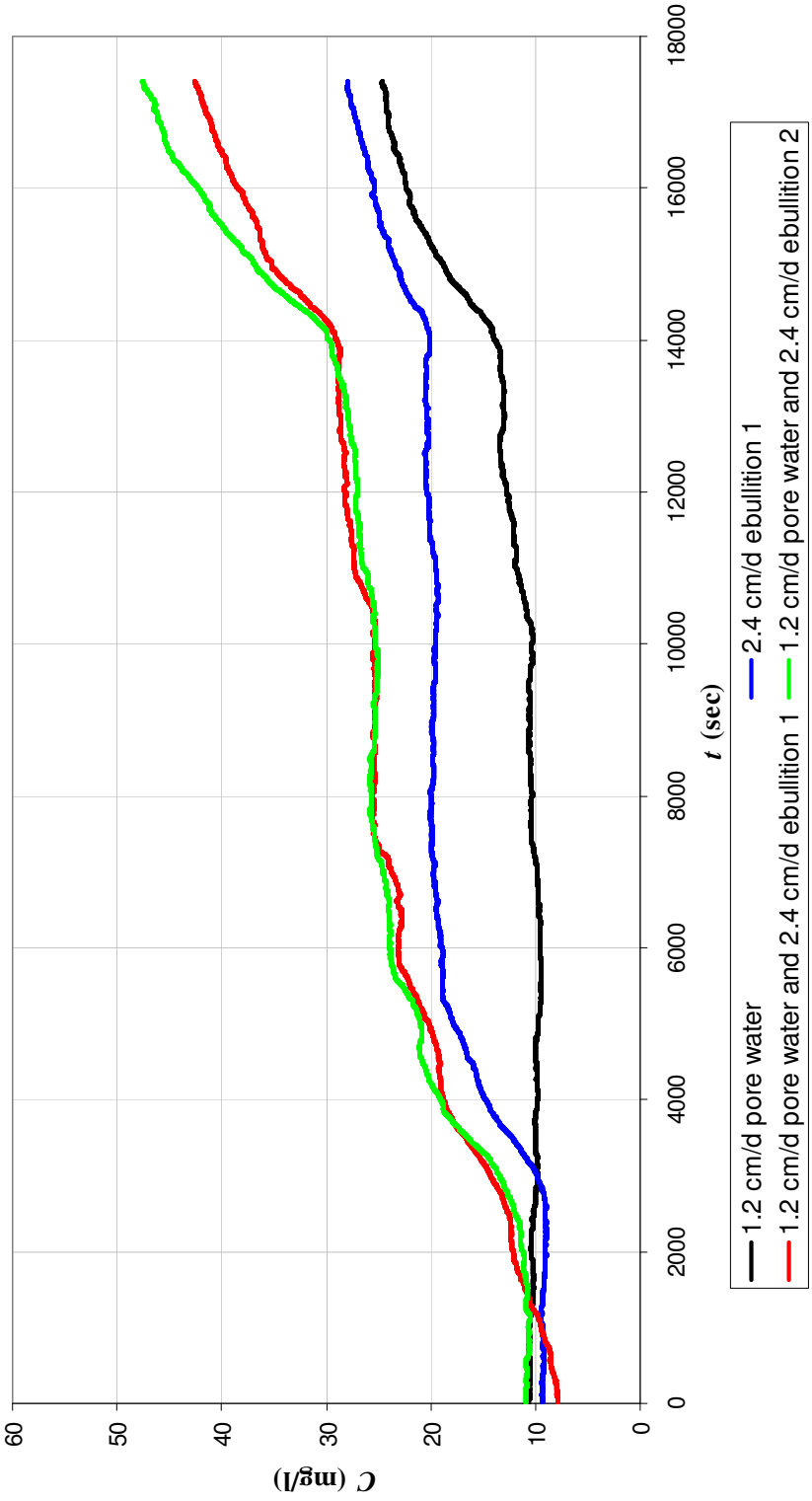

Figure 5.22: Suspended sediment concentration measurements from two 1.2 cm/d pore water-2.4 cm/d ebullition experiments in comparison to the experiments performed for their individual effects.

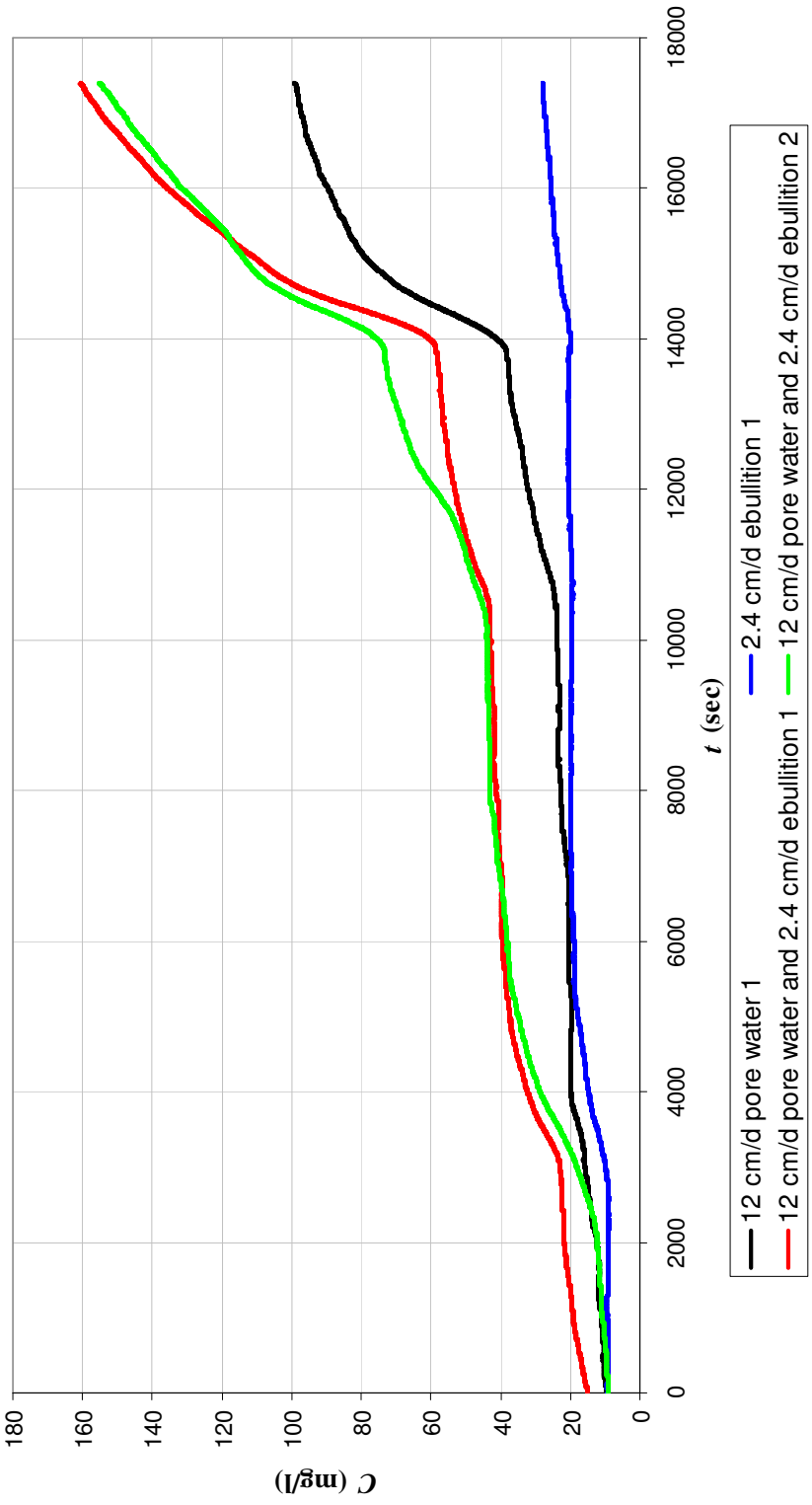

Figure 5.23: Suspended sediment concentration measurements from two 12 cm/d pore water-2.4 cm/d ebullition experiments in comparison to the experiments performed for their individual effects.

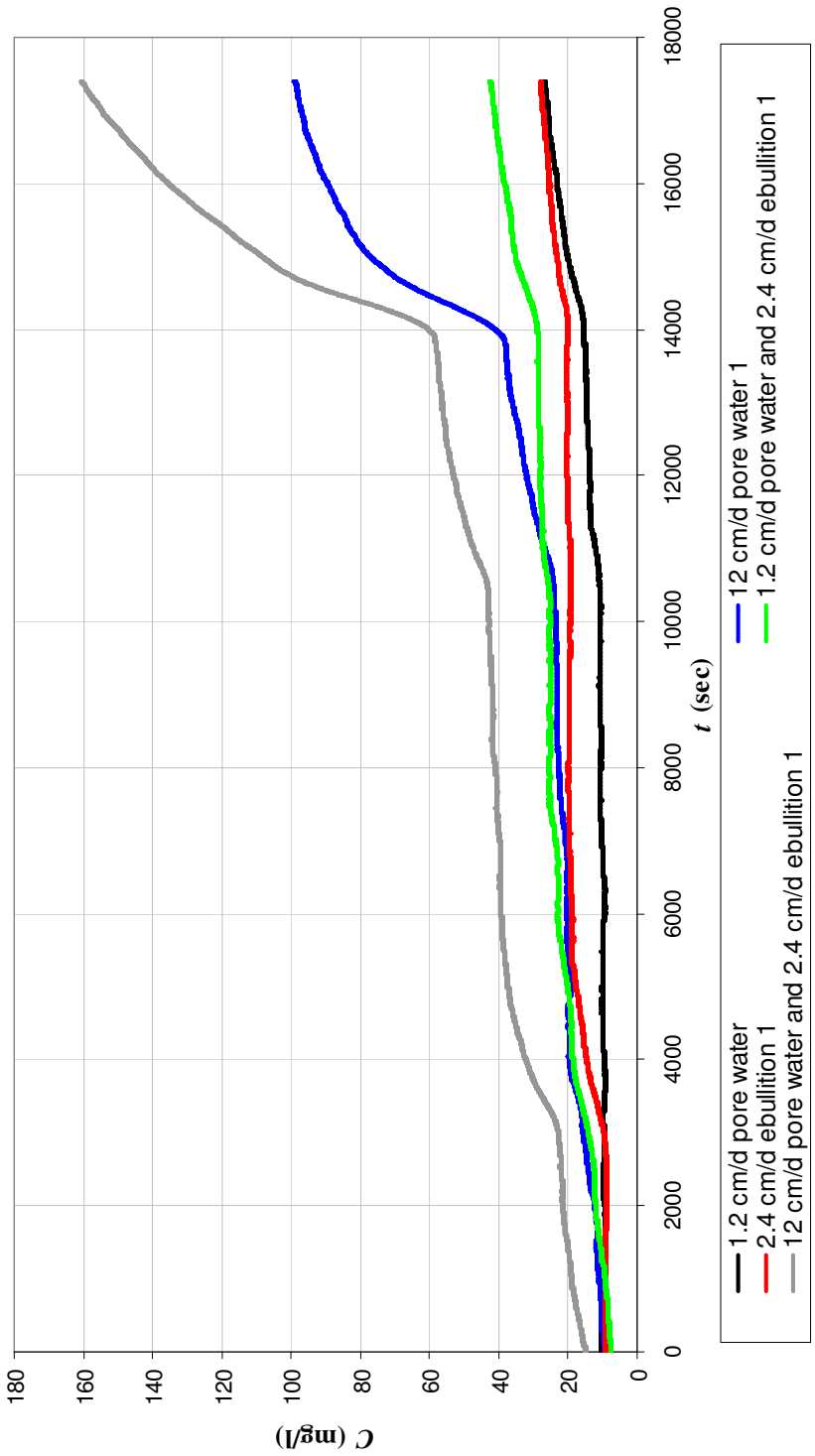

Figure 5.24: A general comparison to demonstrate the influence of the combined effects of pore water and ebullition fluxes on the suspended sediment concentrations (measurements from 1.2 cm/d pore water, 12 cm/d pore water, 2.4 cm/d ebullition, 1.2 cm/d pore water-2.4 cm/d ebullition and 12 cm/d pore water-2.4 cm/d ebullition experiments).

CHAPTER 6

CONCLUSIONS AND RECOMMENDATIONS

In recent years, capping has been considered as an alternative sediment remediation technique which may be successful if the processes influencing the effectiveness of the cap layers are well-understood and the long-term effectiveness can be assured. The main function of a cap is accepted as the capability to minimize the contaminant fluxes into the water column due to the resuspension of the contaminated sediments while staying intact for extended periods of time under different destabilizing environmental occurrences. The conditions leading to sediment resuspension may be critical to concentrations of contaminants within the water column where they can be more readily available to human or aquatic organism exposure. In this research study, the primary objective was to gain a better understanding of the fundamental processes affecting the stability of capped and uncapped sediments and effectiveness of the selected caps in reducing resuspension rates of covered sediments. Establishing a better understanding of processes that are not currently well understood will reduce the uncertainties in the application of capping technologies and provide a better basis for the selection of appropriate capping technologies. The selected parameters of focus were advective flow induced shear stresses, pore water flux (groundwater seepage) and gas ebullition due to microbial activity. The experimental investigations were performed using cohesive Anacostia River sediment, either alone or in conjunction with sand and AquaBlok® caps.

This study has provided significant contributions to the above stated objectives in three major areas. These are in the following general areas:

- The effect of pore water seepage on the stability of non-cohesive sediments such as sand caps;

- The role of pore water seepage and/or gas ebullition on the resuspension from fine-grained cohesive sediment beds, from the standpoint of observed fundamental processes as well as the measurement of resuspension rates under a range of applied fluxes;
- Observations on the performance of selected capping alternatives in reducing resuspension rates.

The following paragraphs discuss these contributions in more detail as well as the specific conclusions resulting from this study.

An investigation on the influence of bed seepage was conducted after a review of the available literature indicated inconsistent and inconclusive results. For example, many studies considered the bed seepage velocity to be a controlling parameter while others consider the hydraulic gradient to be most relevant. Even more significantly, some studies suggest that seepage from the bed into the overlying flow destabilizes the sediment bed while other studies suggest the opposite conclusion. Analysis of these previous studies suggests that a key issue is the means by which the bed shear stress is estimated since it is not a quantity that can be measured directly. This study addressed these concerns by a number of key approaches. A methodology to determine bed shear stress from turbulence measurements in the vicinity of the bed surface was developed. A framework for including bed seepage rates into traditional approaches characterizing bed stability in the absence of seepage was proposed. Finally, experiments were devised to validate this analysis that incorporated a sufficient range of sediment size and bed hydraulic gradients so that clear conclusions on the effects of certain parameters were afforded.

Previous studies documenting the effects of pore water seepage and gas ebullition on resuspension rates from cohesive sediment beds in a systematic way are not available. This study required the development of a complete protocol for performing such an investigation. In the process, many useful observations on the nature of gas release and pore water flow through fine-grained cohesive sediment beds were made. These observations are relevant to approaches used to model sediment processes in fate and

transport models. A baseline study was conducted in order to be able to determine the increase in sediment resuspension due to pore water flow and ebullition. A comparison of the results indicates that under pore water and ebullition fluxes that have been suggested from various field site observations, relevant increases in sediment resuspension rates are possible. This suggests that sediment fate and transport models may need to include one or both of these processes in certain applications.

The final segment of the study considered the effectiveness of two capping technologies in reducing sediment resuspension, providing useful insight for practical applications. Findings from the experimental investigations on caps provide some guidance for remedial strategy decision making as two limiting cases were studied: a permeable sand cap and nearly impermeable AquaBlok® cap.

6.1. Conclusions

Investigations with regards to non-cohesive sediment bed stability were performed aiming to validate a proposed framework to modify the conventional Shields parameters to account for the effects of bed seepage on stability. It is derived by considering an elementary force balance on a particle resting on the bed surface. This framework suggests that hydraulic gradient through the bed is a key parameter while many previous studies suggest that the velocity through the bed surface is the key parameter. Experiments were conducted on sand beds subject to pore water flux and visual incipient motion observations were made to determine the threshold for movement. Experiments were performed with relatively high suction and injection hydraulic gradients ranging from -0.84-0.71. Even though these may not always be representative of field conditions, the framework suggests that gradients this high will clearly show the effect of seepage on bed stability and illustrate the validity of the formulation. Since estimation of bed shear stress for the beds subject to seepage appears to be a major issue influencing the interpretation of the findings leading to contradictory results such as reported in the literature, detailed studies were performed for the determination of the critical bed shear stresses from turbulence measurements in the vicinity of the bed surface. The bed stability was examined by evaluating the critical bed shear stress (resultant bed shear

stress experienced by the individual grains at the threshold condition) in a way that all the different effects of seepage either on the flow or on the sediment bed particles were considered together. For example, injection reduces the effective weight of the individual grains while decreasing the local velocity and increasing the thickness of the boundary layer; at the same time, the Reynolds shear stress increases near a bed subject to injection relative to a condition without injection at the same free stream velocity. After including all the possible different effects of injection and suction in the data analysis framework, it was concluded by the interpretation of the findings from the sand beds studied (d_{50}=160 μm, d_{50}=500 μm and d_{50}=1200 μm) that injection destabilizes the bed and suction does the reverse (see Figure 4.12). Although a number of assumptions were made for the determination of the bed shear stress used in the determination of the modified dimensionless shear stress and the grain Reynolds number used in the modified Shields curve, the data agree fairly well with the modified Shields curve. Computation of the modified Shields parameters eliminates much of the scatter in the data but even more importantly, the data for individual grain sizes tend to follow the general trends of the Shields curve much better than the un-modified data especially for the 160 and 1200 μm. Furthermore, a methodology has been developed to start with data or predictions that would be commonly available (e.g. from models of sediment beds without seepage) and extend that information to apply for application with higher rates of suction or injection. When the data by Rao and Sitaram (1999) were transformed into a comparable data format using the methodology developed, they were found to be in reasonable agreement with the results of the current study even though the original study reached the opposite conclusions regarding the influence of injection or suction on bed stability.

There are no standard methods described in the literature to guide the experimental methodology with regards to the cohesive sediment experiments especially the ones conducted to investigate the effect of pore water and gas ebullition fluxes. Thus, it was necessary to develop experimental procedures to be consistently followed in both this study and in a companion one (flux chamber experiments) that investigated the transport of contaminants bound to the sediments into the overlying water column. Preliminary tests and observations that were performed on the sediment (as a part of flux chamber

experiments), primarily with respect to pore water flux and ebullition processes or related to cap behavior dictated the subsequent decisions on laboratory procedures. Channels through which the pore water or gas migrated were observed in the sediment during the ebullition and seepage tests were recognized to be an important mechanism. In order to generate pore water flow or gas ebullition without the influence of wall effects, special injection systems were developed: soaker hoses for the flume experiments and bubble bars for the flux chamber experiments. A setup was developed to provide a constant air flux for the ebullition experiments as this was identified as an issue to resolve in preliminary experiments. The Anacostia River sediment was already disturbed during transportation and therefore it was not possible to conduct experiments with undisturbed sediments. As a result of additional practical issues faced during preliminary experiments, sediment beds were prepared by applying the sediment in a slurry form without letting it consolidate. This allowed the consistent preparation of test beds as well as the ability to conduct all the planned experiments in a reasonable time frame. Observations in the preliminary experiments showed that air bubbles formed in the ebullition tests can carry significant amounts of sediment into the water column when there is no cap to restrict the resuspension. Further preliminary experiments showed various AquaBlok® failure modes (e.g., mound formation at the center of the tank, uplift at a corner of the tank) due to water or air pressure build-up beneath. It was demonstrated that once the AquaBlok® is ruptured, there is nothing to stop resuspension from the cohesive sediment layer underneath it. Flux chamber experiments also showed that the formation of the rupture was apparently quite random in time and space, thus obtaining reproducible results in a laboratory flume experiment even with the relatively significant test bed surface area seemed to be difficult and side wall effects would dominate the behavior of the experiment. Further regarding the flume experiments, a rupture formation would make the flow dynamics over the cap very complicated and strongly dependent on the geometry of the ruptured surface.

Suspended sediment concentrations were measured during the uncapped and capped cohesive sediment experiments in order to investigate the individual and combined effects of advective flow induced shear stress, pore water and gas ebullition fluxes on

resuspension rates. A five-step discharge increase was taken as the experimental protocol, starting from a low shear stress level and incrementally increasing the shear stress. When the shear stress levels are increased step-wise, the erosion rate is initially relatively high at the beginning of each shear stress level and then decreases with time for the cohesive sediment beds. This time dependency was observed in previous studies and it has resulted in different interpretations of resuspension data and rate calculations in the literature. Although different schemes were considered, the final approach that was followed in this study involved computation of moving averaged concentration measurements followed by the computation of average resuspension rates for each shear stress step. The results of advective flow experiments performed on the Anacostia River sediment showed a critical shear stress value of approximately 0.19 N/m^2 which is larger than the critical shear stress determined for the smallest non-cohesive grain size bed (d_{50}=160 μm) indicating that cohesiveness of the sediment plays an important role in bed stability. Dependence of resuspension rates to the excess shear stress was determined to follow a quadratic relationship (Equation 5.1). Similar power law relationships were reported in previous studies (e.g., Jepsen et al., 1997). Advective flow experiments provided the data for a reference state without a cap and without the effects of ebullition and pore water fluxes. Contribution of ebullition and pore water fluxes to resuspension rates and the impact of presence of a cap on resuspension rates were identified in comparison to the results of the advective flow experiments.

With regards to the pore water and ebullition experiments, although initially wider ranges were considered as reported in literature (0.01-48 cm/d for ebullition, 0.01-124 cm/d for seepage) in order to see the effect of the applied fluxes on resuspension rates within the duration of the experiments, some of the lowest rates were eliminated from the experimental investigations. Then, after some initial trials, some of the ebullition rates were found to be too high to consider as it was felt that in nature these rates indicating continuous bubbling would not be commonly observed. The ranges of fluxes that were focused on varied from 1.2 cm/d to 12 cm/d for both ebullition and seepage experiments. A narrower range when compared to the range reported in literature was considered from the start of the investigations for seepage fluxes as lower rates were reported in the

literature for fine-grained low permeability sediments. The reported high-end seepage rates for the Anacostia River due to tidal fluctuations range from 2.7 cm/d to 5 cm/d. During the investigations, the lower applied pore water flux caused only minimal amount of additional resuspension when compared to advective flow experiments but the 12 cm/d flux increased the resuspension rates significantly. It is speculated that the density was lowered near the soaker hose injection and then the upwards flow through channels left the bulk of the bed surface basically unchanged except in the location of the exit channels. Data analysis did not show any apparent change in critical shear stresses when compared to advective flow experiments. A similar quadratic relationship was found to be valid for the results of both 1.2 cm/d and 12 cm/d pore water experiments. A linear relationship (Equation 5.2) was determined relating the erosion rate constant, M to the pore water flux, I.

In both the flux chamber experiments and the flume experiments it was observed that air migration tend to occur as a series of discrete "bubbling events" associated with a cyclical buildup of gas pressure within the sediment and a decrease of that pressure following bubble release. The lowest air injection flux (1.2 cm/d) experiments mostly ended up with a situation where no air bubbling events occurred during some one hour measurements periods. On the other hand, 12 cm/d was a very high rate creating continuous air bubbling which would be difficult to visualize occurring in many natural systems. Therefore, an additional ebullition flux of 2.4 cm/d was investigated which also generally created fairly sustained bubbling in some of the experiments. Although bubbling events increased the resuspension rates significantly, it was also observed that once a bubbling channel in the sediment was well-established, the contribution of the ebullition events to the resuspension rates was negligible. The random nature of ebullition events as well as the time dependent entrainment of sediment within the ebullition channels made it impossible to determine a direct and consistent relationship between air injection fluxes and resuspension rates. This problem remained for the experiments conducted to investigate the combined effect of ebullition and pore water fluxes.

Stability tests performed on AquaBlok® has showed that this material is extremely stable without failure under even very high shear stresses and it is much more stable than any sand bed considered in this investigation. However a limitation under practical applications may be that the buildup of pressure beneath the cap causes the AquaBlok® to deform and rupture under fairly low differential pressures. If the water or gas accumulated under this relatively impermeable barrier can not be released in a way that is not destructive, the pressure build-up would lead to the failure of the cap. For the permeable cap material which is the Anacostia sand cap (d_{50}=340 μm), there was not such an issue observed. Observations also showed that the sand cap filters the contaminated sediment transported from the sediment layer underneath it either by bubbles or by the pore water flux during the limited time that the experiments were conducted. Turbidity measurements confirmed this observation registering no change in concentrations. This was consistently observed even during the experiments conducted to investigate the combined effects of pore water and gas ebullition fluxes at their highest rates. As a result of the stability experiments, the critical shear stress for the sand cap was determined to be 0.26 N/m^2 which is relatively close to the critical shear stress of the Anacostia River sediment which was tested in its unconsolidated state. This raises the question about whether this sand cap is stable enough for a practical application or not.

Given the above observations from this research, the following conclusions in the form of a summary are made:

- The proposed framework to modify the conventional Shields parameters to account for the effects of bed seepage on stability was validated by the performed investigations. The framework used for determining the modified Shields parameters suggests that hydraulic gradient through the bed is a key parameter and is supported by the experimental data.
- The bed shear stress needs to be estimated appropriately in the presence of high seepage gradients and a methodology to estimate this bed shear stress starting with commonly available site-specific data is suggested and validated by comparison with available data.

- Relatively high injection gradients destabilize non-cohesive sediment beds while suction does the reverse.
- Gas and pore water fluxes may be effective in increasing resuspension rates of cohesive sediments. As gas or pore water fluxes are increased, resuspension rates are also increased.
- Gas flux as well as high rates of pore water flow occur through distinct channels formed in the sediment bed. It is reasonable to expect flow with both processes will occur through the same channels.
- Resuspension rates as a result of the applied advective flow induced shear stresses can be related to excess shear stresses by a quadratic relationship with a critical shear stress required to initiate resuspension. Similar relationships are valid when seepage is applied through the bed with the resuspension rate increasing with the pore water seepage rate.
- Critical bed shear stresses do not change significantly among advective flow only experiments and pore water experiments.
- Ebullition increases the resuspension rates significantly; however, once a bubbling channel in the sediment is well-established due to continuous bubbling, the contribution of the ebullition events to the resuspension rates is negligible. This time dependency as well as the apparently random nature of the gas release process made it difficult to quantify resuspension rates as a function of gas flux.
- The sand cap implemented at the Anacostia River demonstration site was found to be quite effective in filtering the contaminated sediment transported from the sediment layer underneath it by the gas flow, by the pore water flux, or by the combined effect of them during the limited duration of the experiments (five hours).
- AquaBlok® is very stable without failure under even very high shear stresses. However the build-up of pressure beneath the cap due to water or air flow causes the AquaBlok® to rupture at relatively modest pressure differentials.

6.2. Recommendations for Future Research

Many aspects of the present investigation were somewhat exploratory in nature although every attempt was made to obtain quantitative results. The overall research objectives were sufficiently broad that every issue that arose could not be investigated in minute detail. Considerable effort has been made in the presentation of results to document both the issues encountered in the conduct of the experiments as well as the choices made to resolve them. It is probable that an objection could be raised to the particular decisions made in the development of each experimental procedure. The lack of standard procedures for conducting experiments on cohesive sediment transport in particular makes it impossible to respond to such objections except with the argument that the protocols developed seemed reasonable to meet the experimental constraints and objectives for repeatable results. Therefore, there are many different paths for further research to complement and to extend the present investigation.

Many elements of the investigations performed within the content of this research study involved development of experimental methodologies and setup designs to ensure consistent and repeatable results and to be representative of field conditions insofar as feasible. The experiments related to the cohesive sediments were especially challenging with many decisions required at almost every step of the study. Tests were carried out trying to maintain consistency in the procedures while aiming to complete the target number of experiments that would provide a better insight with regards to the processes studied. However, some improvements to the procedures may be performed. For example, more appropriate methods for bed preparation procedures would be developed in order to be more representative of field conditions. In natural systems, the sediment beds are in a consolidated state which was not considered in this study. It would be worthwhile to conduct experiments on sediments which are left to consolidate over extended periods of time in the presence of pore water and/or ebullition flux. This type of application would present some practical issues related to how to create such an experimental procedure while allowing the conduct of multiple experiments in order to derive important conclusions.

Several other different aspects of site-specific conditions could be incorporated into the experimental investigations. For example, tidal fluctuations influence the bottom pressure experienced by the sediment bed. The pressure variations could affect the seepage fluxes (see Chapter 2 for further discussion) and timing of ebullition events which would in turn affect the bed stability. Although cyclical events were observed in this investigation as a result of the nature of the ebullition events, a tidal variation in pressure head on the sediment bed could serve to provide a strong control on the gas release and ultimately influence resuspension rates. An experimental scheme to simulate tidal effects could be revealing.

There are some limitations to experimental investigations, especially with regards to ebullition. In-situ testing and observations would be very beneficial to gain a much better insight related to ebullition processes in natural systems and this would also help to understand if the laboratory observations are consistent with the field. In this study, when the range of ebullition rates reported in the literature was applied to the test bed, continuous bubble release was observed for a significant range of the upper end of ebullition fluxes suggested in the literature. Intuitively, this occurrence does not seem reasonable. Some in-situ observations and tests would clarify this specific issue. Further laboratory investigations on native sediment that has potential to produce significant amounts of gas would also be helpful to study. Under controlled laboratory conditions, it would be possible to compare the microbially-generated gas release process to what was observed during the air injection experiments. Examination of the bubble release process in particular would be useful since the resuspension rates that were observed in the flume experiments seem to critically depend on it. Resuspension experiments on this sediment could also be run for extended periods of time in a smaller scale setup compared to the flume experiments conducted in this study without the need of a recirculating flow in order to investigate the effect of ebullition. For this kind of setup, it would only be required to mix the surface water that would simulate the mixing processes in natural surface water systems.

As presented in Chapter 2, stability of cohesive sediment beds is influenced by many factors. While it may not be possible to investigate all of them in a single study, the number of variables could be increased if they can be controlled successfully. In the experimental scheme followed in this study, a procedure involving a five-step discharge increase was utilized. Each shear stress level was applied to the bed for an hour. It was observed during this and other investigations (e.g., Sanford and Maa, 2001) that there is a time dependency to the resuspension rates when a bed is subjected to advective flow induced shear stresses. This aspect could be very interesting to examine further, possibly in conjunction with the effects of seepage and ebullition. Tests with an extended duration in a recirculating flume setup with a pump result in an increase in the water temperature over time and this aspect should be carefully examined. If the temperature increase is significantly high, this would decrease the viscosity of the water decreasing the bed shear stress while more importantly potentially affecting other stability characteristics of the cohesive sediment.

Additional experiments involving the parameters investigated in this study can be conducted in order to determine the significance of bed load transport in erosion rates. As also presented in Chapter 2 the erosion rate is usually assumed to be approximately equal to resuspension rate although the potential importance of bed load transport was indicated by several researchers (e.g., Debnath et al., 2007). An additional objective of such a study could be to determine the relative effectiveness of mass transfer from the smaller relative surface area associated with the sediment chunks carried as bed load compared to the smaller particle sizes (and therefore larger relative surface area) carried in suspension.

Sand caps have been identified as very effective in mitigating resuspension rates. However, if the experiments are conducted for longer durations, it is possible that there is a capacity to the amount of sediment that can be filtered by a sand cap. Therefore, experiments could be conducted to determine whether a breakthrough of sediment through the sand cap occurs in time with either pore water flux or ebullition. If sediment starts to escape through the sand cap, then next question would be related to the significance of the cap thickness in reduction of the resuspension rates. Time dependency

can also be related to the issues with AquaBlok® caps. This material is advertised to be self-healing if time is allowed and this aspect of it was not investigated in this research study. If a consistent procedure could be developed to conduct resuspension experiments with AquaBlok® caps by rupturing it in a controllable manner, first resuspension experiments could be conducted to determine effective resuspension rates for ruptured AquaBlok® caps. This could be followed by an investigation of the self-healing property with regards to resuspension rate reduction. For this type of experiment, a large test bed surface would be necessary to obtain meaningful rupture patterns. Several repetitions of the experiments would appear to be required in order to obtain statistically useful results. In addition, performance of AquaBlok® caps in a simulated tidal system where pressure head variations are significant enough (tidal fluctuations greater than about 30 cm) would be examined to see if this effect causes stability problems for the AquaBlok®.

Finally, with regards to the data analysis procedures followed in this study, some decisions and assumptions were made along the way which were found to be reasonable and satisfactory. There is always the possibility to develop more rigorous procedures to be followed. One of the major issues faced was the determination of the bed shear stress in the presence of seepage. This was overcome by the methodology developed as presented in Chapter 4 but the procedure involved some specific assumptions that were not rigorously verified. The development of an accurate and straightforward method for determination of bed shear stress would improve the conduct of experiments for stability of both cohesive and non-cohesive sediments. A second major issue related to data analysis was in regards to the determination of resuspension rates in cohesive sediment beds since these are not constant with time even with a constant applied shear stress. Hourly averages were used at the end for further data analysis after trying different schemes and details of this procedure was presented in Chapter 5. The relationship between this approach and others described in the literature should be investigated.

APPENDICES

APPENDIX A

A.1. TURBIDITY-SUSPENDED SEDIMENT CONCENTRATION CALIBRATION

Turbidity (water clarity) data were collected using a flow-through Orbeco-Hellige 965-10AR turbidimeter covering a wide range of turbidity values and recorded in terms of voltages using a data acquisition system. At the discharge end of the flow-through cell, 100 ml samples were collected simultaneously. The voltage readings were averaged for the duration of the sampling for each sample. Samples were analyzed for total suspended sediments following the 2540D standard test procedure provided in "Standard Methods for the Examination of Water and Wastewater Manual". Millipore Type HA, 0.45 μm glass-fiber filters were used for filtering the samples. A calibration curve relating the voltage readings, ω to the suspended sediment concentrations, C is presented in Figure A.1. Another calibration curve is presented in Figure A.2 for the AquaBlok® tests.

Recording the data through a computerized system increased the precision of the measurements. However, turbidity is commonly measured in Nephelometric Turbidity Units (NTU). The range of voltages recorded for 100 ml sediment-water mixture samples corresponds to 5-90 NTU.

A.2. HYDROMETER ANALYSIS

Hydrometer analysis is performed if the grain sizes of a sediment blend are too small for a sieve analysis. It is an application of Stokes Law which states that larger particles fall more quickly in a suspending fluid, while finer particles remain in suspension longer. The function of the hydrometer is based on Archimedes principle that a solid suspended in a container filled with fluid will be buoyed up by a force equal to the weight of the liquid displaced. Hence, the lower the density or the specific gravity of the soil-water

mixture, the lower the hydrometer will sink. During the application of the test, the time at which the hydrometer readings are taken determines the size of particle remaining in suspension, while the reading on the hydrometer determines the amount of that size. Several assumptions may be required to be made about particles shape and other test conditions, so the results are somewhat approximate. The particle specific gravity of the Anacostia sediment was determined to be 2.71 which was used in the computations of the hydrometer analysis.

Hydrometer analysis following the ASTM D422 standard test procedure was preformed on two samples of the Anacostia River sediment to determine the median sedimentation diameter using ASTM Soil Hydrometer 152H. Two samples from different drums of sediment were tested to ensure that the results are representative of the total amount of sediment as much as possible. The median grain size was determined approximately to be 10μm for both samples.

A.3. ATTERBERG LIMITS TEST

A fine-grained soil may exist in four states depending on the water content: solid, semi-solid, plastic and liquid. In each state the behavior of the soil is different. Atterberg limits are the boundaries between these states. Plastic limit is the water content where soil starts to exhibit plastic behavior and in terms of the applied test, it means that the soil begins to crumble when rolled into threads of specified size. Liquid limit is the water content where a soil changes from plastic to liquid and in terms of the applied test, it means that the soil has such a small shear strength that it flows to close a groove of standard width when treated in a specified manner. Some properties of the soil such as the mineral and chemical composition, size and shape of the soil particles influence the amount of water that could be adsorbed on the particles.

Atterberg limits tests following the ASTM D4318 standard test procedure were preformed on two samples of the Anacostia River sediment to determine the plastic and liquid limits of the sediment. The plastic limit was determined to be 43.4% and the liquid limit was determined to be 77.7% on average.

A.4. SHIELDS CURVE RELATIONSHIPS

In 1963, Bonnefille used piece-wise relationships relating grain Reynolds number, Re_* to dimensionless grain size, D_* in order to define an approximation to the Shields curve given as

$$D_* = 2.33\,\mathrm{Re}_*^{0.79}, \quad \mathrm{Re}_* < 1 \tag{A.1}$$

$$D_* = 2.33\,\mathrm{Re}_*^{0.85}, \quad 1 < \mathrm{Re}_* < 5 \tag{A.2}$$

$$D_* = 2.78\,\mathrm{Re}_*^{0.74}, \quad 5 < \mathrm{Re}_* < 10 \tag{A.3}$$

$$D_* = 3.96\,\mathrm{Re}_*^{0..584}, \quad 10 < \mathrm{Re}_* < 100 \tag{A.4}$$

where $D_* = \left(\frac{\rho_s - \rho}{\rho} \frac{g d^3}{\upsilon^2} \right)^{1/3}$ and $\mathrm{Re}_* = \frac{u_* d}{\upsilon}$. These relations can be solved to determine the dimensionless shear stress $\tau_* = \frac{\tau}{(\gamma_s - \gamma) d}$ required to produce the Shields curve (Raudkivi, 1998).

Later in 1984, van Rijn presented another approximation to the Shields curve defined as

$$\tau_* = 0.24(D_*)^{-1}, \quad D_* \le 4 \tag{A.5}$$

$$\tau_* = 0.14(D_*)^{-0.64}, \quad 4 < D_* \le 10 \tag{A.6}$$

$$\tau_* = 0.04(D_*)^{-0.10}, \quad 10 < D_* \le 20 \tag{A.7}$$

$$\tau_* = 0.013(D_*)^{0.29}, \quad 20 < D_* \le 150 \tag{A.8}$$

$$\tau_* = 0.055, \quad D_* > 150 \tag{A.9}$$

where $\tau_* = \frac{\tau}{(\gamma_s - \gamma) d}$.

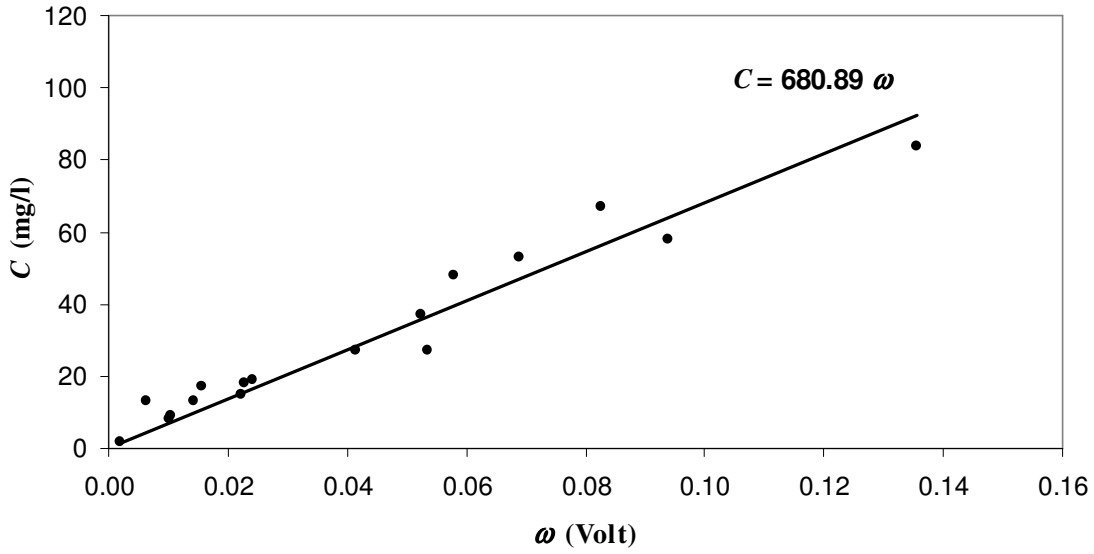

Figure A.1: Calibration curve relating the suspended sediment concentrations to the voltage readings.

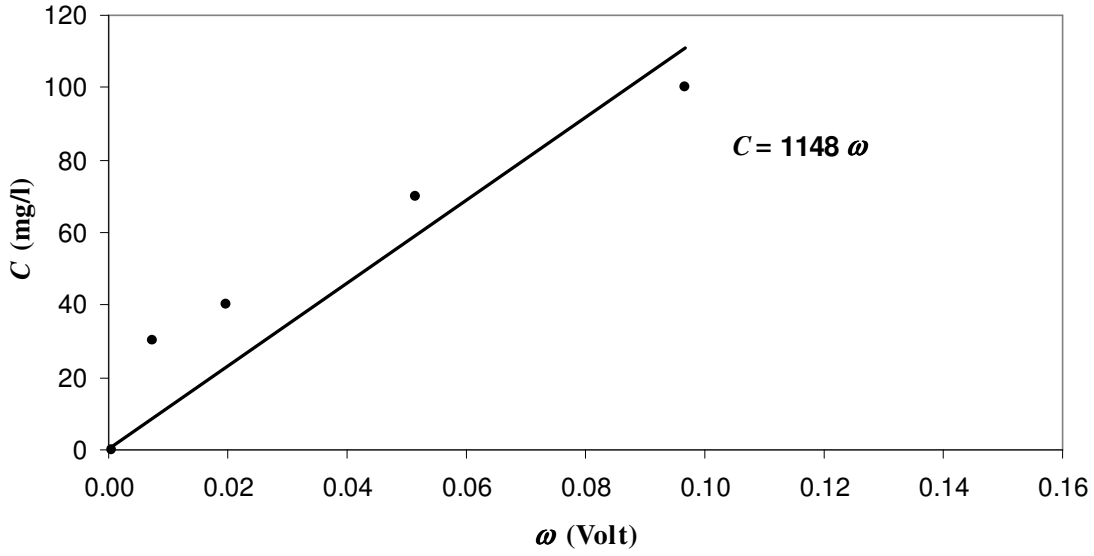

Figure A.2: Calibration curve relating the suspended AquaBlok® material to the voltage readings.

APPENDIX B

NOTATION

A	bed surface area
A_0	cross sectional flow area
C_D	drag coefficient
C_L	lift coefficient
C	resuspended sediment concentration
$Cov(XZ)$	covariance of the velocity fluctuations in the longitudinal and vertical directions $\left(\equiv \overline{u'v'}\right)$
d	effective sediment diameter ($d = d_{50}$ for the purposes of this study, median grain size)
d_{65}	grain size at which 65% is finer
d_{90}	grain size at which 90% is finer
D_*	dimensionless grain size $\left(\equiv \left(\frac{\rho_s - \rho}{\rho} \frac{g d^3}{\upsilon^2} \right)^{1/3} \right)$
F_D	drag force
F_W	submerged weight of a particle
F_L	lift force
g	gravitational acceleration
h	water depth
i	hydraulic gradient
I	seepage flux (velocity)

k_s equivalent roughness height

k hydraulic conductivity

M resuspension rate coefficient

n bed porosity

P wetted perimeter

Q flume discharge

q_i metered injection or suction rate

R resuspension rate

R_0 hydraulic radius $\left(\equiv A_0 / P\right)$

Re_* grain Reynolds number $\left(\equiv \frac{u_* d}{\upsilon}\right)$

Re_t transition Reynolds number (from laminar to turbulent boundary layer and $\equiv \frac{u_s x_t}{\upsilon}$)

S adjustment factor for the hydraulic gradient at the sediment/water interface

S_W water surface slope

t time

u_s free stream velocity

u local average stream-wise velocity

U some characteristic velocity describing the free stream flow

u_* shear velocity $\left(\equiv \sqrt{\frac{\tau}{\rho}}\right)$

u' velocity fluctuation in the longitudinal direction

v' velocity fluctuation in the vertical direction

x distance along the flume

x_t distance from the inlet of the flume to the transition location (laminar to turbulent boundary layer)

z vertical distance from the boundary

γ unit weight of water

γ_s unit weight of sediment

δ boundary layer thickness

δ_t boundary layer thickness at the transition from laminar to turbulent boundary layer

κ von Karman constant $(\equiv 0.4)$

υ kinematic viscosity of fluid

ω voltage corresponding to suspended sediment concentration

ρ density of fluid

ρ_s density of sediment

τ bed shear stress when $i = 0$

τ_i bed shear stress when $i \neq 0$

$\tau_{\exp}$ shear stress calculated using maximum covariance

τ_0 bed shear stress calculated from the Blasius equation

τ_c critical bed shear stress

τ_* Shields parameter $\left(\equiv \dfrac{\tau}{(\gamma_s - \gamma)d} \right)$

τ_{*m} modified Shields parameter $\left(\equiv \dfrac{\tau}{(\gamma_s - \gamma(1 + Si))\, d} \right)$

BIBLIOGRAPHY

BIBLIOGRAPHY

Aberle, J., Nikora, V., McLean, S., Doscher, C., McEwan, I., Green, M., Goring, D., and Walsh, J. (2003). "Straight Benthic Flow-Through Flume for In Situ Measurement of Cohesive Sediment Dynamics." *Journal of Hydraulic Engineering*, ASCE, 129(1), 63-67.

Aberle, J., Nikora, V., and Walters, R. (2004). "Effects of Bed Material Properties on Cohesive Sediment Erosion." *International Journal of Marine Geology, Geochemistry and Geophysics*, 207, 83-93.

Aberle, J., Nikora, V., and Walters, R. (2006). "Data Interpretation for In Situ Measurements of Cohesive Sediment Erosion." *Journal of Hydraulic Engineering*, ASCE, 132(6), 581-588.

Achman, D. R., Brownawell, B. J., and Zhang, L. (1996). "Exchange of Polychlorinated Biphenyls between Sediment and Water in Hudson River Estuary." *Estuaries*, 19, 950-965.

Amos, C. L., Sutherland, T. F., and Zevenhuizen, J. (1996). "The Stability of Sublittoral, Fine-Grained Sediments in a Subarctic Estuary." *Sedimentology*, International Association of Sedimentologists, 43, 1-19.

Amos, C. L., Droppo, I. G., Gomez, E. A., and Murphy, T. P. (2003). "The Stability of a Remediated Bend in Hamilton Harbour, Lake Ontario, Canada." *Sedimentology*, International Association of Sedimentologists, 50, 149-168.

Bear, J. (1979). *Hydraulics of Groundwater*, McGraw-Hill, New York.

Berlamont, J., Ockenden, M., Toorman, E., and Winterwero, J. (1993). "The Characterisation of Cohesive Sediment Properties." *Coastal Engineering*, 21, 105-128.

Buffington, J. M. (1999). "The Legend of A. F. Shields." *Journal of Hydraulic Engineering*, ASCE, 125(4), 376-387.

Burnett, W. C., Taniguchi, M., and Oberdorfer, J. (2001). "Measurement and Significance of the Direct Discharge of Groundwater into the Discharge Zone." *Journal of Sea Research*, 46, 109-116.

Cable, J. E., Burnett, W.C., Chanton, J. P., Corbett, D. R., and Cable, P. H. (1997). "Field Evaluation of Seepage Meters in the Coastal Marine Environment." *Estuarine, Costal, and Shelf Science,* 45, 367-375.

Chadwick, D. B. (2002). "Coastal Contamination Migration Monitoring." *Proceedings of Remediation Technologies Development Forum Workshop on Groundwater-Surface Water Interaction*, Seattle, WA, October.

Chanton, J. P., and Martens, C. S. (1988). "Seasonal Variations in Ebullitive Flux and Carbon Isotropic Composition of Methane in a Tidal Freshwater Estuary." *Global Biogeochemical Cycling*, 2(3), 289-298.

Charbeneau, R. J. (2000). *Groundwater Hydraulics and Pollutant Transport*, Prentice Hill, Upper Saddle River, NJ.

Cheng, N. S., and Chiew, Y.-M. (1998a). "Turbulent Open-Channel Flow with Upward Seepage." *Journal of Hydraulic Research*, 36(3), 415-430.

Cheng, N. S., and Chiew, Y.-M. (1998b). "Modified Logarithmic Law for Velocity Distribution Subjected to Upward Seepage." *Journal of Hydraulic Engineering,* 124(12), 1235-1241.

Cheng, N. S. and Chiew, Y.-M. (1999). "Incipient Sediment Motion with Upward Seepage." *Journal of Hydraulic Research*, 37(5), 665-681.

Debnath, K., Nikora, V., Aberle, J., Westrich, B., and Muste, M. (2007). "Erosion of Cohesive Sediments: Resuspension, Bed Load, and Erosion Patterns from Field Experiments." *Journal of Hydraulic Engineering*, ASCE, 133(5), 508-520.

Dey, S. and Cheng, N.-S. (2005). "Reynolds Stress in Open Channel Flow with Upward Seepage." *Journal of Engineering Mechanics*, 131(4), 451-457.

Eganhouse, R. P., Pontonillo, J., and Leiker, T. J. (2000). "Diagenetic Fate of Organic Contaminants on the Palos Verdes Shelf, California." *Marine Chemistry*, 70, 289-315.

Fendinger, N.J., Adams, D.D., and Glotfelty, D.E. (1992) "The Role of Gas Ebullition in the Transport of Organic Contaminants from Sediments." *The Science of the Total Environment*, 112, 189-201.

Fukuda, M. K., and Lick, W. (1980). "The Entrainment of Cohesive Sediments in Freshwater." *Journal of Geophysical Research*, 85(C5), 2813-2824.

Harrison, S. S., and Clayton, L. (1970). "Effects of Groundwater Seepage on Fluvial Processes." *Bulletin of the Geological Society of America*, 811, 1217-1225.

Horne Engineering Services, Inc. (2003). "Revised Draft – Site Characterization Report for Comparative Validation of Innovative "Active Capping" Technologies, Anacostia River, Washington, DC." *Prepared for: South and Southwest Hazardous Substance Research Centers, Louisiana State University*.

Houwing, E. J. (1999). "Determination of the Critical Erosion Threshold of Cohesive Sediments on Intertidal Mudflats along the Dutch Wadden Sea Coast." *Estuarine, Coastal and Shelf Science*, 49, 545-555.

Huls, H., Costello, M. (Service Engineering Group), and Sheets, R. (Soil Technology, Inc.) (2003a). "Gas, NAPL, and PAH Flux Assesment in Sediments." *Proceedings of the Second International Conference on Remediation of Contaminated Sediments*, Venice, Italy.

Huls, H., Costello, M. (Service Engineering Group), and Sheets, R. (Soil Technology, Inc.) (2003b). "Bench Test Design Evaluation of a Remedial Wetland Cap (with Regard to Ebullition and Its Control)." *Presented at: In-Situ Contaminated Sediment Capping Workshop*, Cincinnati, OH.

Hunt, S. D., and Mehta, A. J. (1985). "An Evaluation of Laboratory Data on Erosion of Fine Sediment Beds." *Proceedings of the International Symposium Workshop on Particulate and Multiphase Processes and the 16th Annual Meeting of the Fine Particle Society*, 503-518.

Jepsen, R., Roberts, J., and Lick, W., (1997). "Effects of Bulk Density on Sediment Erosion Rates." *Water, Air and Soil Pollution*, 99, 21-31.

Jepsen, R., McNeil, J., and Lick, W. (2000). "Effects of gas generation on the density and erosion of sediments from the Grand River." *Journal of Great Lakes Research*, 26(2), 209-219.

Joyce, J., and Jewell, P.W. (2003). "Physical Controls on Methane Ebullition from Reservoirs and Lake." *Environmental and Engineering Geoscience*, IX(2), 167-178.

Kelly, W.E., and Gularte, R.C. (1981). "Erosion Resistance of Cohesive Soils." *Journal of Hydraulics Division*, ASCE, 107(HY10), 1211-1224.

Kramer, H. (1935). "Sand mixtures and sand movement in fluvial models." *Trans. ASCE*, 100, 798-838.

Lau, Y. L., and Droppo, I. G. (2000). "Influence of Antecedent Conditions on Critical Shear Stress of Bed Sediments." *Water Research*, 34, 663–667.

Lau, Y.L., Droppo, I.G., and Krishnappan, B.G. (2001). "Sequential Erosion/Deposition Experiments- Demonstrating the Effects of Depositional History on Sediment Erosion." *Water Res*earch, 35(11), 2767-2773.

Lick, W., Xu, Y., and McNeil, J. (1995). "Resuspension Properties of Sediments from the Fox, Saginaw, and Buffalo Rivers." *Journal of Great Lakes Research*, 21(2), 257-274.

Liikanen, A., Tanskanen, H., Murtoniemi, T., and Martikainen, P. J. (2002). "A Laboratory Microcosm for Simultaneous Gas and Nutrient Flux Measurements in Sediments." *Boreal Environment Research*, **7**, 151-160.

Maa, J. P.-Y, Sanford, L., and Halka, J. P. (1998). "Sediment Resuspension Characteristics in Baltimore Harbor, Maryland." *International Journal of Marine Geology, Geochemistry and Geophysics*, 146, 137-145.

Maclean, A. G. (1991). "Open Channel Velocity Profiles Over a Zone of Rapid Infiltration." *Journal of Hydraulic Research*, 29(1), 15-27.

Martens, C. S., and Klump, J. V. (1980). "Biogeochemical Cycling in an Organic-rich Coastal Marine Basin – I. Methane Sediment-Water Exchange Processes." *Geochimica et Cosmochimica Acta*, 44, 471-490.

Martin, C.S. (1970). "The Effect of a Porous Sand Bed on Incipient Sediment Motion." *Water Resources Research*, 6(4), 1162-1173.

Martin, C. S., and Aral, M. M. (1971). "Seepage Force on Interfacial Bed Particles." *Journal of the Hydraulics Division*, ASCE, 101(7), 1081-1100.

McNeil, J., Taylor, C., and Lick, W. (1996). "Measurements of Erosion of Undisturbed Bottom Sediments with Depth." *Journal of Hydraulic Engineering*, ASCE, 122(6), 316-324.

Mehta, A. J. (1991). "Review Notes on Cohesive Sediment Erosion." *Coastal Sediments*, 40-53.

Mehta, A. J., Hayter, E. J., Parker, W. R., Krone, R. B., and Teeter, A. M. (1989). "Cohesive Sediment Transport I: Process Description." *Journal of Hydraulic Engineering*, ASCE, 115(8), 1076-1093.

Nikora, V., and Goring, D. (2000). "Flow Turbulence Over Fixed and Weakly Mobile Gravel Beds." *Journal of Hydraulic Engineering,* ASCE, 126(9), 679-690.

Oldenziel, D. M., and Brink, W. E. (1974). "Influence of Suction and Blowing on Entrainment of Sand Particles." *Journal of the Hydraulics Division*, ASCE, 100(7), 935-949.

Olson, R. M., and Wright, S. J. (1990). *Essentials of Engineering Fluid Mechanics,* Harper & Row, New York.

Palermo, M. R., Thompson, T. A., and Swed, F. (2002). "White Paper No. 6B – In-Situ Capping As a Remedy Component for the Lower Fox River – Ecosystem-Based Rehabilitation Plan – An Integrated Plan for Habitat Enhancement and Expedited Exposure Reduction in the Lower Fox River and Green Bay" *Response to a Document by the Johnson Company*.

Parchure, T. M., and Mehta, A. J. (1985). "Erosion of Soft Cohesive Sediment Deposits." *Journal of Hydraulic Engineering*, ASCE, 111(10), 1308-1326.

Piedra-Cueva, I., and Mory, M. (2001). "Erosion of a Deposited Layer of Cohesive Sediment." In: McAnally, W. H., and Mehta, A. J. (Eds.), Coastal and Estuarine Fine Sediment Processes, Elsevier, Amsterdam, 45-51.

Prinos, P. (1995). "Bed-Suction Effects on Structure of Turbulent Open-Channel Flow." *Journal of Hydraulic Engineering,* ASCE, 121(5), 404-412.

Rao, A. R., Subrahmanyam, V., Thayumanavan, S., and Damodaran, N. (1994). "Seepage Effects on Sand-Bed Channels." *Journal of Irrigation and Drainage Engineering*, ASCE, 120(1), 60-79.

Rao, A.R., and Sitaram, N. (1999). "Stability and Mobility of Sand-Bed Channels Affected by Seepage." *Journal of Irrigation and Drainage Engineering*, ASCE, (125)6, 370-379.

Raudkivi, A. J. (1998). *Loose Boundary Hydraulics*, A. A. Balkema, Rotterdam.

Ravens, T. M., and Gschwend, P. M. (1999). "Flume Measurements of Sediment Erodibility in Boston Harbor." *Journal of Hydraulic Engineering*, ASCE, 125(10), 998-1005.

Ravens, T. M. (2007). "Comparison of Two Techniques to Measure Sediment Erodibility in the Fox River, Wisconsin." *Journal of Hydraulic Engineering*, ASCE, 133(1), 111-115.

Richardson, M. D. (1998). "Coastal Benthic Boundary Layer: A Final Review of the Program." *NRL Memorandum Report*, Marine Geosciences Division – Naval Research Laboratory.

Rijn, L. C. van (1984). "Sediment Transport, Part I: Bed Load Transport." *Journal of Hydraulic Engineering,* ASCE, 110(10), 1431-1455.

Roberts, J., Jepsen, R., Gotthard, D., and Lick, W. (1998). "Effects of Particle Size and Bulk Density on Erosion of Quartz Particles." *Journal of Hydraulic Engineering*, ASCE, 124(12), 1261-1301.

Sanford, L. P., and Maa, J. P.-Y. (2001). "A Unified Formulation for Fine Sediments." *International Journal of Marine Geology, Geochemistry and Geophysics*, 179, 9-23.

Schlichting, H. (1979). *Boundary-Layer Theory*, McGraw-Hill, New York.

Simon, A., and Collison, A. J. C. (2001). "Pore-Water Pressure Effects on the Detachment of Cohesive Streambeds: Seepage Forces and Matric Suction." *Earth Surface Processes and Landforms*, 26, 1421-1442.

Simons, D. B., and Richardson, E.V. (1966). "Resistance to Flow in Alluvial Channels." *U.S. Geological Survey Professional Paper 422-J.*

Taylor, B. D., and Vanoni, V. A. (1972). "Temperature Effects in Low Transport, Flat Bed Flows." *Journal of Hydraulics Division*, ASCE, 98(HY8), 1427-1445.

Tolhurst, T. J., Black, K. S., Paterson, D. M., Mitchener, H. J., Termaat, G. R., and Shayler, S. A. (2000). "A Comparison and Measurement Standardization of Four In Situ Devices for Determining the Erosion Shear Stress of Intertidal Sediments." *Continental Shelf Research*, 20, 1397-1418.

Turcotte, D.L. (1960), "A Sublayer Theory for Fluid Injection into the Incompressible Turbulent Layer." *Journal of Aerospace Sciences*, 27(9), 675-678.

U.S. EPA (2004, November). "The Incidence and Severity of Sediment Contamination in Surface Waters of the United States – National Sediment Quality Survey, Second Edition." U.S. Environmental Protection Agency, Office of Science and Technology, Washington, DC, EPA-823-R-04-007.

U.S. EPA (2005, December). "Contaminated Sediment Remediation Guidance for Hazardous Waste Sites." U.S. Environmental Protection Agency, Office of Solid Waste and Emergency Response, Washington, DC, EPA-540-R-05-012.

U.S. EPA (2007, September). "Demonstration of the AquaBlok® Sediment Capping Technology – Innovative Technology Evaluation Report." U.S. Environmental Protection Agency, Office of Research and Development, Washington, DC, EPA-540-R-07-008.

Taniguchi, M., Burnett, W. C., and Cable, J. E., and Turner, J. V. (2002). "Investigation of Submarine Groundwater Discharge." *Hydrological Processes*, 16, 2115-2129.

Vanoni, V.A. (1975). *Sedimentation Engineering*, ASCE Manual, No.54.

Watters, G. Z., and Rao, M. V. P. (1971), "Hydrodynamic Effects of Seepage on Bed Particles." *Journal of the Hydraulics Division*, ASCE, 101(3), 421-439.

Wolfe, J. R. (2004). "In-Situ Sediment Treatment: Technologies, Findings, and Research Issues." *Presented at: SERDP/ESTCO Contaminated Sediments Workshop*.

Wright, S. J., Mohan, R. K., Brown, M. P., and Kim, C. C. (2001). "Filter Design Criteria for Sediment Caps in Rivers and Harbors." *Journal of Coastal Research*, 17(2), 353-362.

Yalin, M. S. and Karahan, E. (1979). “Inception of Sediment Transport.” *Journal of the Hydraulics Division*, ASCE, 105(HY11), 1433-1443.

Yalin, S. M. (1976). *Mechanics of sediment transport*, Pergamon, Tarytown, N.Y.